

ABSTRACT

Title of Document: THE PHARMACOLOGY AND DYNAMICS OF
THE LIGHT-INDUCED CALCIUM SIGNAL IN
LIMULUS VENTRAL PHOTORECEPTORS

Youjun Wang, Doctor of Philosophy, 2007

Directed By: Professor Richard Payne, Neuroscience and
Cognitive Neuroscience program

The *Limulus* ventral photoreceptor is a model system for understanding inositol (1,4,5) trisphosphate (IP₃) induced calcium (Ca²⁺) release and the light response of invertebrate photoreceptors. Light-induced Ca²⁺ release via the phosphoinositide cascade is thought to activate the photocurrent in *Limulus*. The pharmacology and dynamics of the light-induced Ca²⁺ signal was investigated. Application of 1-100 μM 2 - aminoethoxydiphenyl borate (2-APB), a non-specific IP₃ receptor inhibitor, reversibly inhibited the photocurrent in a concentration-dependent manner, acting on at least two processes thought to mediate the visual cascade. 2-APB reversibly inhibited both light and IP₃-induced calcium release, consistent with its role as an inhibitor of the IP₃ receptor. 2-APB also reversibly inhibited the activation of depolarizing current flow through the plasma membrane by released calcium ions. In addition, 100 μM 2-APB reversibly inhibited voltage-activated potassium currents. This lack of specificity of 2-APB's action in *Limulus* suggests that the effects of 2-

APB need to be interpreted with caution. Dynamics: The light-induced Ca^{2+} release begins at the light sensitive plasma membrane of the R lobe. Consistent with its role in mediating light responses, this Ca^{2+} signal rises to its peak with a similar time course to that of the electrical signals. Then the Ca^{2+} signal spreads into the interior of the cell with two phases. The initial fast phase is a diffusion driven process that needs both the diffusion of IP_3 and of Ca^{2+} released by IP_3 , since both manipulations that alter the apparent diffusion coefficient (D) of Ca^{2+} ions or those that change the life span of IP_3 molecules can change the spread of the fast phase. A model of simple diffusion of IP_3 molecules (or Ca^{2+} ions) and a diffusion model for IP_3 and Ca^{2+} released by IP_3 were constructed using estimated D values of Ca^{2+} and IP_3 inside cells obtained through the Graham's Law. Simulation results indicate that diffusion of IP_3 and released Ca^{2+} is both necessary and sufficient to determine the initial fast phase. The expected spread of excitation following absorption of one photon can be predicted by this model.

THE PHARMACOLOGY AND DYNAMICS OF THE LIGHT-INDUCED
CALCIUM SIGNAL IN *LIMULUS* VENTRAL PHOTORECEPTORS

By

Youjun Wang

Dissertation submitted to the Faculty of the Graduate School of the
University of Maryland, College Park, in partial fulfillment
of the requirements for the degree of
Doctor of Philosophy
2007

Advisory Committee:

Professor Richard Payne, Chair
Professor Steven Brauth
Professor Hey-kyoung Lee
Professor Sergei Sukharev
Professor David Yager

© Copyright by
Youjun Wang
2007

ACKNOWLEDGMENTS

I would like to dedicate this thesis to my parents, Xiaochun Wang and Yanfen Lei, to my wife, Xiaosong Hu, and to my sister, Youling Wang. Without them, I wouldn't have made such achievements.

It has been a great pleasure to work with Dr. Richard Payne. As an advisor, he has really solid and insightful understanding of electronics, science, and life. He was always there when I needed help. And his suggestions and opinions, both for daily life and academic issues, always hit the main point and turned out to be very helpful. Over these years of step by step training, I learned a lot and I wish I could have learned more.

I would like to thank Dr. Steven Brauth for serving as the dean's representative of my defense committee. I thank Drs. Hey-Kyoung Lee, Sergei Sukharev, David Yager, and Contreras-Vidal Jose for serving as my committee members and giving me great advices.

I especially thank Dr. Ian Mather for letting us use his Confocal microscope. I also would like to thank Dr. Amy Beaven for helping me with the Confocal microscope. I especially thank Feiquan Luo, Yadong Wang, Feng Rong, Huan Luo for their help on the usage of Matlab. I thank Dr. Monika Desponde and Alan Dabdoub from my lab for their help and support.

I also extend my gratitude to Lois Reid, Sandy Davis, Lillian Rollins and Pam Komarek for their logistic support during this entire period of my study here.

TABLE OF CONTENTS

Acknowledgements	ii
Table of Contents	iii-iv
Chapter 1: General Introduction	1-21
The photo-transduction cascade in <i>Limulus</i> ventral photoreceptors	1-5
Ca ²⁺ is a necessary link for understanding the photo-transduction	
Cascade: it mediates both the excitation and the adaptation of the	
light response in <i>Limulus</i> ventral photoreceptor.....	6-10
How does the Ca ²⁺ signal perform its multiple functional roles:	
the dynamics of Ca ²⁺ signals in <i>Limulus</i> ventral photoreceptors?.....	10-21
Chapter 2: 2-Aminoethoxydiphenyl Borate Inhibits Phototransduction	
and blocks Voltage-gated Potassium Channels in <i>Limulus</i> Ventral	
Photoreceptors.....	22-57
Abstract	22-23
Introduction.....	24-26
Material and Methods.....	27-31
Results	32-50
Discussion	51-57
Chapter 3: Estimating the diffusion coefficients of substances with	
known molecular weights.....	58-77
Abstract	58-59
Introduction.....	60-61

Material and Methods.....	62-64
Results and discussion.....	66-77
Chapter 4: Investigation of the mechanisms that define the spatial-temporal profile of Ca ²⁺ signal and estimation of the peak calcium signal inside <i>Limulus</i> ventral photoreceptors.....	
	78-123
Abstract	78-79
Introduction.....	80-82
Material and Methods.....	83-92
Results.....	93-118
Discussion.....	119-123
Chapter 5: General discussion.....	124-131
Reference.....	132-144

General Introduction

Abstract

Photo-transduction in *Limulus* ventral photoreceptors starts as a G-protein-coupled signaling cascade. The G protein then activates the phosphoinositide (PI) pathway which is shared in most invertebrate photoreceptors. The products of the PI pathway, inositol trisphosphate and perhaps diacylglycerol are then thought to mediate the activation of “light-activated” ion channels. The events downstream of the Ca^{2+} signal, particularly the identity of the light-activated channels, are still unknown. Some experimental data supports a role for cGMP gated channels, while other data suggest that the light-sensitive channels might be some type of canonical TRP channel. New pharmacological and genetic approaches are needed to clarify this issue.

Consistent with the idea that light-induced Ca^{2+} release is essential to the excitation and adaptation of the phototransduction cascade, light-induced Ca^{2+} release originates within 4 μm distance of the light sensitive membrane of the R lobe. Moreover, the timing and the peak of the Ca^{2+} induced fluorescence at its origin are tightly correlated to those of the electrical signal-induced by light at all intensities examined so far. The spread of light-induced Ca^{2+} signal has been shown to have two phases. However, the spatial relationship between the phototransducing membrane and the origin of light-induced Ca^{2+} release as well as the mechanism by which the Ca^{2+} signal spreads are still unknown and need to be clarified.

Following the first description (Millecchia and Mauro, et al., 1966), the mechanism that drives the light response of the *Limulus* ventral photoreceptor has been intensely investigated. Experimental evidence shows that its phototransduction cascade shares some elements common to the pathways of other photoreceptors, especially those of invertebrates, but that it may also have unique components as well (Dorlochter and Stieve, 1997).

The photo-transduction cascade in *Limulus* ventral photoreceptors (Fig. 1)

The photo-transduction in Limulus ventral photoreceptors starts with the universal G-protein-coupled signaling cascade. The early components of the phototransduction cascade in ventral photoreceptors are shared by all photoreceptors (Pugh and Lamb, 2000). Briefly, photons are absorbed by a membrane bound pigment, rhodopsin (Rh). Rh then undergoes a conformational change which allows it to catalyze the activation of GTP-binding proteins (G proteins). The α subunit of the G protein (G_α) then activates different targets in different photoreceptors, which will lead to the opening or closing of ion channels on the plasma membrane. The type of G protein found in *Limulus* ventral photoreceptors is G_q (Contzen and Nagy, 1995), whose target is phospholipase C (Brown et al., 1984). The use of phospholipase C as a target is common to other microvillar photoreceptors in invertebrate species. By

contrast, in the cones and rods of vertebrates, the target of the G_{α} subunit is phosphodiesterase (PDE). PDE hydrolyzes the small messenger molecule, cGMP, leading to the closing of cGMP-activated channels (Pugh and Lamb, 2000).

The G protein activated phosphoinositide (PI) pathway is utilized for the next step of the light response in Limulus ventral photoreceptors. Phospholipase C (PLC) breaks phosphatidylinositol (4,5) bisphosphate (PIP_2) down into water-soluble D-myoinositol 1,4,5 trisphosphate (IP_3) and lipid-soluble diacylglycerol (DAG). IP_3 and/or DAG is then thought to lead to the opening of cation channels on the plasma membrane of the photoreceptor (Nasi E, et al., 2000; Lisman, Richard et al., 2002). This process is shared by most invertebrate photoreceptors.

Downstream events of the PI pathway in Limulus ventral photoreceptors: the IP_3 and perhaps the DAG branch participate in photo-transduction events. IP_3 -induced Ca^{2+} release has been shown to mediate the light response of *Limulus* ventral photoreceptors. Briefly, IP_3 diffuses to the endoplasmic reticulum (ER) and releases calcium (Ca) by opening IP_3 receptors. Ca^{2+} then excites and adapts the cell through a complex mechanism (discussed in detail below).

The target of Ca^{2+} or DAG is unknown. The depolarizing light response of *Limulus* ventral photoreceptors is driven by a conductance that is largely permeable to sodium ions (Brown and Mote, 1974). Experiments on excised patches of rhabdomeral membrane indicate the presence of cGMP-gated channels, and a novel cGMP-gated

channel has been cloned from ventral eye mRNA (Bacigalupo et al., 1991; Chen et al., 2001). Mediation of the light response by cGMP-activated channels would require a calcium-activated guanylate cyclase to generate cGMP. There is some pharmacological evidence for this (Garger, et al., 2001, 2004). Another possibility is the activation of TRPC channels by DAG and Ca^{2+} . There is also pharmacological evidence for this linkage, and a potential target channel has been cloned from ventral eye mRNA (Bandyopadhyay and Payne, 2004). This latter proposal would be similar to the proposed pathway linking calcium influx and a DAG metabolite to the activation of TRP channels in *Drosophila* photoreceptors (Hardie, 2001). Whether these two branches exist and what their relative contributions to the photo-transduction cascade are in *Limulus* ventral photoreceptors remains unknown. Specific pharmacological agent or genetic manipulations that inhibit or delete one of the two possible components are needed for this purpose.

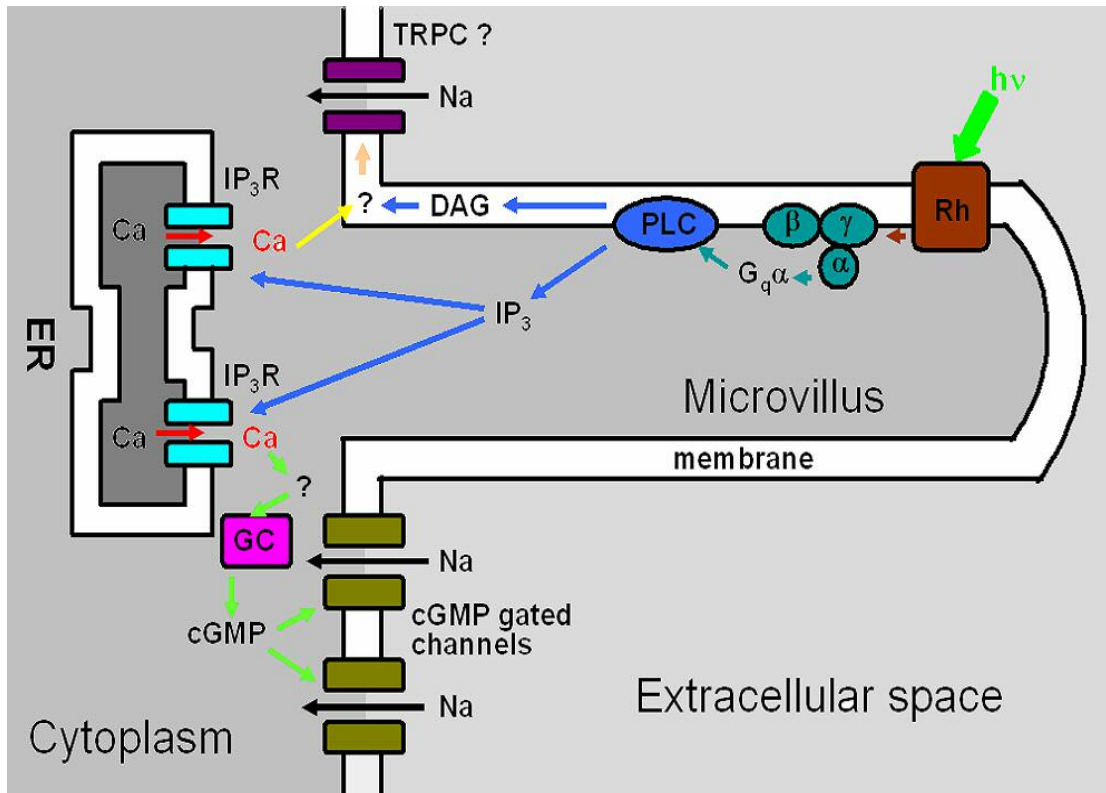


Figure 1. The signal transduction pathway mediating the light response of *Limulus* ventral photoreceptors. See text for abbreviations and descriptions (modified from Nasi, et al., 2000)

In summary, the photo-transduction cascade of *Limulus* ventral photoreceptors shares some common features with other photoreceptors. Therefore, the knowledge of the mechanisms of the photo-transduction is helpful for understanding the light response of other photoreceptors. Moreover, IP₃-induced Ca²⁺ release is commonly used for many cellular responses (Berridge, 1995), thus the study of the behavior of IP₃-induced Ca²⁺ release in *Limulus* ventral photoreceptors may be relevant to many cell types.

Ca²⁺ is a necessary link for understanding the photo-transduction cascade: it mediates both excitation and the adaptation of the light response in *Limulus* ventral photoreceptors

1) Evidence that transient a Ca²⁺ release excites ventral photoreceptors.

As described above, light induces a transient Ca²⁺ release from ER (Brown, Blinks, 1974). The onset of this Ca²⁺ release highly correlates with the onset of the light-induced current (Ukhanov & Payne, 1995; Payne & Demas, 2000).

Intracellular pressure injection of either IP₃ or Ca²⁺ into the light sensitive lobe mimics the electrical response to light. Injection of IP₃ induces a transient intracellular Ca²⁺ concentration ([Ca]_i) increase (Brown et al., 1984; Payne et al., 1986) with a latency that is 20-45 ms shorter than light-induced Ca²⁺ release (Ukhanov and Payne, 1997). In either case, depolarization results due to the activation of an inward current. Subsequent responses to light are desensitized (adapted). The injection-induced current has a similar reversal potential and sodium dependence to those of light-induced current (Brown et al., 1984; Fein et al., 1984; Payne et al., 1986a and b).

Manipulations that inhibit the light-induced increase in [Ca]_i also greatly reduce the amplitude of the light-induced current. Those manipulations include depletion of Ca²⁺ stores by a Ca²⁺ pump inhibitor, cyclopiazonic acid (CPA) (Seidler et al., 1989;

Ukhanov & Payne, 1995); inhibition of Ca^{2+} release by the IP_3 receptor inhibitor heparin (Frank et al., 1991; Nagy, 1993; Faddis & Brown, 1993; Contzen et al., 1995) and injection of the Ca^{2+} buffer BAPTA (Frank et al., 1991; Contzen et al., 1995).

The above lines of evidence support the idea that the light-induced transient increase in $[\text{Ca}]_i$ excites the cell. Ca^{2+} accomplishes this by activating some downstream pathway. One candidate for such a pathway is through the indirect activation of cGMP-gated channels (Bacigalupo et al., 1991; Chen et al., 2001; Garger et al., 2001, 2004), and the other candidate is the activation of canonical TRP channels (Bandyopadhyay and Payne, 2004).

It is also still controversial whether light-induced Ca^{2+} release is the only pathway for excitation or whether another parallel pathway exists (Nasi E, et al., 2000; Lisman, Richard et al., 2002). One strong argument against the obligatory role of Ca^{2+} in excitation is the finding that the pharmacological abolition of any detectable $[\text{Ca}]_i$ increase cannot prevent intense light from activating the photocurrent (Ukhanov & Payne, 1995). Others, however, have argued that this might be caused by some undetectable local residual Ca^{2+} release (Ukhanov and Payne, 1995; Payne and Demas, 2000; Fein, 2003).

2) Evidence that elevated intracellular calcium ($[\text{Ca}]_i$) mediates light adaptation:

$[\text{Ca}]_i$ increase produces light adaptation through delayed negative feedback (Lisman et al., 2002). This results in a transition of the light response from a peak initial

response to a smaller plateau during prolonged, intense illumination. Responses to subsequent light flashes are subsequently desensitized.

When $[Ca]_i$ is increased slowly through iontophoretic injections, the light response desensitizes progressively (Lisman and Brown, 1972) and speeds up both characteristics of light adaptation. When Ca^{2+} is transiently introduced into cells by light or by rapid pressure injection of Ca^{2+} or IP_3 , cells also adapt after the initial excitation (Payne R et al., 1990; Lisman and Brown, 1972, 1975). Clamping $[Ca]_i$ at different levels through injection of Ca-EGTA will desensitize the cell. The higher the free calcium concentration, the stronger the desensitization associated with adaptation (Lisman and Brown, 1975). Clamping $[Ca]_i$ near its resting level abolishes light adaptation (Lisman and Brown, 1975). Using a Ca-sensitive electrode to monitor $[Ca]_i$, it was found that a roughly two fold decrease in light sensitivity was accompanied by only a 0.2 – 0.4 μM steady $[Ca]_i$ increase (Levy and Fein, 1985)

The above evidence indicates that a Ca^{2+} increase is necessary and sufficient for light adaptation as well as excitation.

3) Ca^{2+} ions are a minor component of the light-induced current in *Limulus* ventral photoreceptors.

By substituting external ions for less- or non- permeable substances and measuring the light-induced current and reversal potential, the light-induced current was

determined to be mainly carried by sodium ions (Millecchia and Mauro, 1972). Potassium is mainly responsible for the remaining part of the conductance (Brown and mote, 1974).

Because of the huge Ca^{2+} release from ER, the light-induced Ca^{2+} influx is difficult to measure. Using Mn^{2+} as a Ca^{2+} substitute, Hsiao and Payne's estimate of the calcium influx rate under continuous saturating light stimulus is below $0.1 \mu\text{M s}^{-1}$, which is much less than the initial light-induced Ca^{2+} release rate from intracellular stores (350 or $1640 \mu\text{M s}^{-1}$, measured with calcium green 5N and Fluo-5N respectively). This indicates that calcium influx contributes very little to the initial light-induced calcium transient.

Possible roles of Ca^{2+} influx: Although this tiny Ca^{2+} influx hardly has any impact during ongoing Ca^{2+} release from the ER, its role after ER Ca^{2+} release has terminated or slowed down could be important. One indicator of this is that under steady strong light stimulus, after the cell is desensitized by adaptation, the reduced Ca^{2+} influx rate is comparable to Ca^{2+} extrusion rate through Ca^{2+} exchanger (maximum around $1\mu\text{M s}^{-1}$, as estimated by O'Day and Gray Keller, 1989). Therefore, then Ca^{2+} influx under these conditions may be important for maintaining an elevated $[\text{Ca}]_i$ level during sustained illumination, after the initial, massive release from stores is over.

In summary, Ca^{2+} mediates every aspect of *Limulus* ventral photoreceptor light responses, both excitation and adaptation. To understand its multiple roles, it is therefore important to determine the dynamics of the light-induced Ca^{2+} signal.

The dynamics of Ca^{2+} signals in *Limulus* ventral photoreceptors: how does the Ca^{2+} signal perform its multiple functional roles?

Calcium (Ca) is a very important intracellular messenger that controls many cellular processes occurring over different time scales, such as visual transduction (milliseconds to hundreds of milliseconds), exocytosis (hundreds of microseconds), gene transcription (minutes), and muscle contraction (milliseconds and above). This vital, multifunctional role of Ca^{2+} is accomplished by modulating its amplitude, as well as its temporal and spatial features through combinations of Ca^{2+} release, termination and effector machineries (Berridge, et al., 2001). Therefore, accurate estimate of the timing, amplitude, temporal and spatial properties of the Ca^{2+} signal is important to understand the role of Ca^{2+} in cellular responses.

- 1) The location of the light-induced Ca^{2+} release: Is excitation confined within the R lobe?

If Ca^{2+} mediates the light response of the photoreceptor, then there should be a co-localization of Ca^{2+} release and the other machinery of the light response.

Limulus ventral photoreceptors have two distinct lobes. The cell body of *Limulus* ventral photoreceptors has a diameter around 60 μm and is about 200 μm long. It is divided into two distinct lobes: the rhabdomeral lobe (the R lobe) and arhabdomeral lobe (the A lobe) (Fig. 2A) (Stern et al., 1982; Calman & Chamberlain, 1982). The R lobe is covered by microvilli (Fig 2B). The axon originates from the A lobe, which contains the nucleus and other structures that are vital to the cell. Although the R and the A lobe are structurally and functionally different, there is no physical barrier between them (Feng et al., 1994). Since all of the microvilli containing the machinery which has so far been shown to be required for the response to light, are localized within the R lobe (Battelle et al., 2001; Stern et al., 1982), then if Ca^{2+} mediates the light response, most of the light-induced Ca^{2+} release should be confined within the R lobe.

Light-induced Ca^{2+} release is mostly confined with the R lobe. Ca^{2+} was found to be released within the photoreceptor non-uniformly, and localized mostly to the R lobe (Harary & Brown, 1984; Levy & Fein, 1985, Ukhanov & Payne, 1995). It was also shown that Ca^{2+} release due to intracellular injection of IP_3 was also confined mainly within the R lobe (Payne & Fein, 1987; Ukhanov and Payne, 1997). However, the detailed spatial relationship of the light-induced Ca^{2+} signal and the microvillar membrane of the R lobe has not been demonstrated.

The A lobe is also capable of Ca^{2+} release. There might also be light-induced Ca^{2+} release in the A lobe (Stern et al., 1982). There are IP_3 receptors in the cytoplasm of

the A lobe (Ukhanov et al., 1998), and IP₃-induced Ca²⁺ has been observed there with a much smaller amplitude than in the R-lobe (Ukhanov and Payne, 1997). But whether the A lobe participates in the light response remains unknown.

These results are consistent with the essential role of Ca²⁺ in the photo-transduction cascade. However, detailed information on the timing, amplitude and spreading of the Ca²⁺ signals in these two lobes is needed to get a better understanding of how Ca²⁺ mediates the light response.

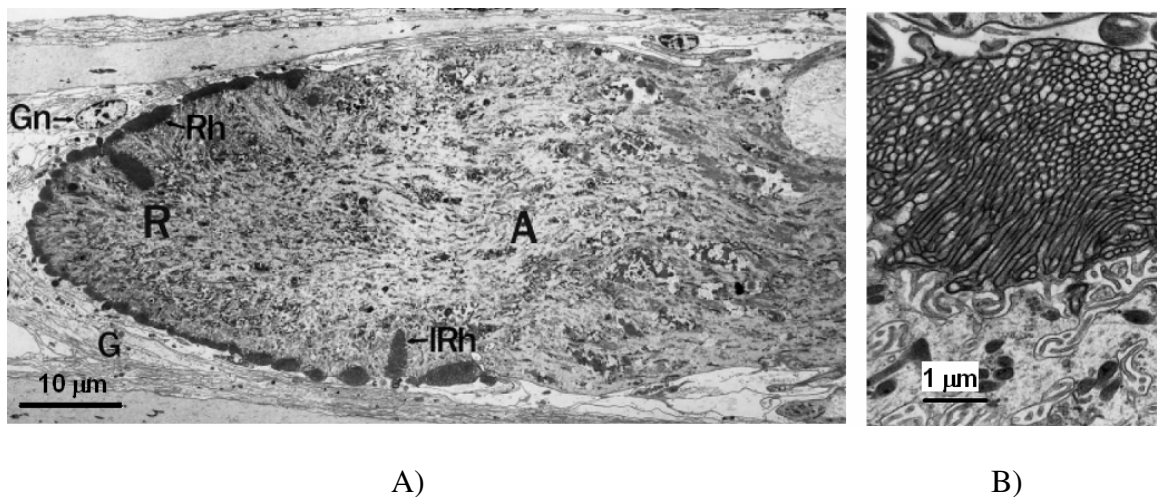


Figure 2. The anatomy of *Limulus* ventral photoreceptor cells (Modified from Dabdoub et al., 2002). A) Photoreceptors have two distinct lobes. A rhabdomeral lobe (R), specialized for phototransduction, and a nontransducing arhabdomeral lobe (A). Other abbreviations: Rh, microvillar rhabdomere; IRh, internal rhabdomere; G, glial cells; Gn, nucleus of glial cells. B) Tightly packed microvilli in dark adapted cells. The rhabdomere of the photoreceptor is composed of microvilli.

2) The timing of Ca^{2+} release at its site of origin spots: How fast is the excitation?

If transient Ca^{2+} release is essential to excite ventral photoreceptors, then the light-induced Ca^{2+} release must precede that of the electrical responses. Due to technical difficulties, this question has not been fully resolved yet.

Early measurements: Before the invention of the confocal imaging method, several attempts to reveal the timing of the light or IP_3 injection-induced Ca^{2+} release across the entire receptor or in the R lobe resulted in some unexpected results (Brown & Blinks, 1974; Payne & Flores, 1992; Stieve & Benner, 1992): Ca^{2+} release began 10-25 ms later than that of the light-induced current and reached its peak much later. These observations did not support the idea that Ca^{2+} mediates the light-induced current.

Confocal measurements: The above results could have been due to slow Ca^{2+} diffusion, limited resolution and spatial averaging of the Ca^{2+} signal across the entire cell. Using confocal imaging method to measure Ca^{2+} release in a spot, Ukhanov and Payne showed that the onset of the light-induced Ca^{2+} release was highly correlated with that of the electrical response (Ukhanov et al., 1995, 1997; Payne et al., 2000). In response to an intense light stimulus, the latency of both Ca^{2+} and electrical response is around 20-40 ms. Ca^{2+} release in about one third of their measurements preceded that of the electrical response by up to 5 ms. For the remaining 2/3 cells in which

detectable Ca^{2+} release appeared several milliseconds after the onset of the electrical response, they argued that a displacement of the measuring spot from the microvilli by a few microns could delay detection of the Ca^{2+} signal. The relationship between the misplacement of the measuring spot and the measured Ca^{2+} release latency was not studied.

In a subsequent study (Payne & Demas, 2000), the time to peak and decline of Ca^{2+} release-induced by dim flashes (50-5000 effective photons per sec) was compared to that of the electrical response. For dim flashes, the onsets of Ca^{2+} signals were found to be well correlated with those of receptor potentials. However, for intense flashes the time-to-peak of Ca^{2+} release still lagged that of the electrical responses.

Therefore, these rather incomplete results are consistent with the idea that Ca^{2+} release in the R lobe mediates the excitation of the photo-transduction cascade.

If light-induced Ca^{2+} release mediates the light response, then its amplitude and the area over which it spreads should reflect the intensity of the stimulus. Moreover, by examining the relationship between the amplitudes of Ca^{2+} signals and those of light-induced currents, some information about the mechanism of how Ca^{2+} mediates downstream events might be obtained.

3) The peak amplitude of the Ca^{2+} signal at the phototransducing membrane

The peak amplitude is an important property of the Ca²⁺ signal

The peak amplitude of the Ca²⁺ signal indicates the extent of excitation and thus reflects the intensity of a stimulus. Generally, according to their amplitude and localizations, Ca²⁺ signals can be divided into two classes: highly localized elementary events and global Ca²⁺ waves. Elementary Ca²⁺ signals are either spontaneous or induced by weak stimuli. A stronger stimulus enables the cooperation of the local Ca²⁺ signals to generate bigger global Ca²⁺ waves. Elementary Ca²⁺ events usually have a diameter around several micrometers. Their durations range from 0.5 to 500 ms and the peak [Ca]_i rise is usually in the sub-micro molar range. These elementary events, caused by opening of multiple Ca-permeable channels provide highly localized Ca²⁺ pulses to regulate cell responses, or if many occur synchronously, they could generate global Ca²⁺ signals to trigger a larger response. (Berridge MJ, 1997; Bootman et al., 2001). Ca²⁺ signals of different amplitude might induce different functions. In pancreatic acinar cells, for example, a large Ca²⁺ (>10 μM) in the trigger zone leads to exocytosis, while a submicromolar [Ca]_i only activates the secretion or uptake of chloride ions. (Ito et al., 1997). The peak amplitude of the Ca²⁺ signal is also an indicator of the speed of spread of the Ca²⁺ signal. The effective Ca²⁺ diffusion rate increases as the [Ca]_i goes up because of the saturation of Ca²⁺ buffering proteins (Allbritton et al., 1992), so [Ca]_i affects the speed of Ca²⁺ diffusion.

Since Ca^{2+} signals are generally not evenly distributed across the cell, the measurement position and the measurement volume across which the $[\text{Ca}]_i$ is measured is important. Simulation results show that Ca^{2+} peak amplitudes and durations are highly dependent on their distances from open Ca^{2+} channels. Ca^{2+} signals adjacent to open Ca^{2+} channels (within 20 nm) can reach amplitudes as high as 100 μM , rising and falling within microseconds. Ca^{2+} signals 200 nm away from the channel might peak at 5-10 μM , changing at a slower rate (milliseconds) (Neher, 1998).

*There are uncertainties about the current estimations of the high peak $[\text{Ca}]_i$ in
Limulus ventral photoreceptors*

As discussed in the above section, early studies of *Limulus* ventral photoreceptors measured the average peak Ca^{2+} signal as being within the range of 30-100 μM . Later, with the help of the confocal technique, the averaged Ca^{2+} signal in a 5 μm^3 spot close to the microvillar membrane could be measured (Ukhanov and Payne, 1995; Payne and Demas, 2000). In response to saturating light stimuli, the peak $[\text{Ca}]_i$ was approximately 150 μM , as determined by a medium-affinity dye Calcium Green-5N ($K_d = 67 \mu\text{M}$) (Ukhanov & Payne, 1995). In examining this data, there are concerns with this measurement. The first is that the Ca^{2+} trace shown in the paper has a plateau, which could represent dye saturation. The second problem concerns localization: since the average Ca^{2+} signal measured in a spot is higher than those measured across the cell, it is obvious that, instead of being released evenly across the cell, Ca^{2+} release is quite localized. If calcium is actually released in a space smaller

than $5 \mu\text{m}^3$ and dye saturates in that space then even confocal measurements will not record the true peak $[\text{Ca}]_i$.

Therefore, to obtain a complete relationship between the peak of $[\text{Ca}]_i$ and that of the light-induced currents in response to light stimuli with varied intensities, the peak $[\text{Ca}]_i$ -induced by intense flashes needs to be examined by low affinity dyes. By doing this, a better understanding of how Ca^{2+} excites the cell can be obtained.

Besides amplitude modulations, cells can also respond to a strong stimulus by using a larger area of excitation through the propagation of regenerative second messenger waves (Ca^{2+} waves for example) (Berridge, 1997). Is this mechanism used in *Limulus* ventral photoreceptors?

4) The spatial-temporal distribution of Ca^{2+} signal: How large is the excitation and how does the excitation spread across the cell?

Diffusion and buffering are the main factors that determine the spread of excitation

For elementary events, simulation results show that Ca^{2+} diffusion and Ca^{2+} buffering can explain the localization of elementary Ca^{2+} signals. (Simon SM et al., 1985). In the squid giant synapse, assuming that the spread of such Ca^{2+} signals are determined by diffusion only, the measured effective Ca^{2+} diffusion coefficient is approximately $27 \mu\text{m}^2 \text{s}^{-1}$, which is in good agreement with those measured in cytosolic extracts (Yao Y et al., 1995; Allbritton et al., 1992). In cardiac muscles, there are also suggestions

that physical barriers set by the ER may contribute to low spread of Ca^{2+} signals (Cheng et al., 1993).

For some larger localized events, cellular organelle or Ca^{2+} binding proteins may help to prevent the Ca^{2+} signal from further spreading. It has been shown in chromaffin cells that mitochondria packed between two functionally distinct areas can act as an active barrier to prevent Ca^{2+} diffusion (Tinel et al., 1999). In *Xenopus* oocytes, Parker's group found that buffers and calcium binding proteins can shape the spatial-temporal patterns of global signals. For example, slow buffers tend to shorten Ca^{2+} spikes and Ca^{2+} waves (Dargan, 2003, 2004).

In response to a strong stimulus, global Ca^{2+} signals can be triggered from local Ca^{2+} "hot spots" and then propagate across a cell as a " Ca^{2+} wave (Berridge MJ, 1997; Bootman et al., 2001). In cell types where IP_3 -induced Ca^{2+} release is involved in Ca^{2+} wave generation, the mechanisms that define the spreading of Ca^{2+} waves are still controversial. Some groups believe that Ca^{2+} waves are generated through Ca^{2+} -induced Ca^{2+} release via ryanodine receptors (Atri et al., 1993), while others favor mediation via Ca^{2+} -induced IP_3 production or Ca^{2+} -facilitated IP_3 -induced Ca^{2+} release. No matter the details, all of these mechanisms are regenerative (utilize positive feedback as well as negative feedback) and all Ca^{2+} waves have a steady moving front. In other words, the speed of the spread and the peak amplitude of the Ca^{2+} signal stay approximately constant.

The mechanisms and function of the spread of light-induced Ca²⁺ signal in Limulus ventral photoreceptors are still unclear

After the introduction of confocal microscopy, the spatial-temporal distribution of the light-induced Ca²⁺ signal was investigated in *Limulus* ventral photoreceptors. Ca²⁺ release was observed to start from the edge of the R lobe, and spreads into its center within several hundred milliseconds. Then the Ca²⁺ concentration in the R lobe decreases gradually with time. Throughout the entire process, the Ca²⁺ signal hardly penetrates into the A-lobe, despite the fact that there is no known physical barrier between the R and the A lobe, (Fig. 3) (Ukhanov & Payne, 1995).

Whether Ca²⁺ waves are generated in the photoreceptor is not known. Also, the mechanisms of the initial fast Ca²⁺ spread and later confinement to the R-lobe are not clear. To address this, we initiated a quantitative description and pharmacological manipulation of the spread of light-induced Ca²⁺ signals.

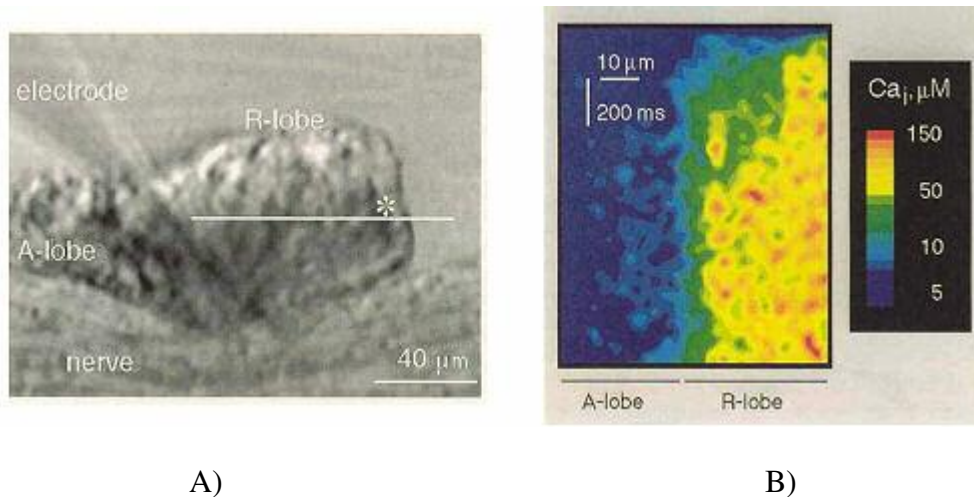


Figure 3. The distribution of Ca^{2+} signal in response to a line scan. A) A conventional image of the photoreceptor cell. The white line shows the position of line scan where fluorescence was measured in B). B) Line scan showing temporal progression of light-induced Ca^{2+} signal. The Ca^{2+} elevation starts from the edge of the R lobe (top right corner), then it spreads to the junction between R and A lobe within the first 200 ms. After that, the Ca^{2+} elevation stays in the R lobe instead of diffusing into the A lobe. $[\text{Ca}]_i$ elevation in the A lobe is low throughout this process. (Modified from Ukhanov & Payne, 1995)

5) The termination of the Ca^{2+} signal in *Limulus* ventral photoreceptors: how fast can the cell regain its sensitivity?

Since Ca^{2+} overload is toxic and may cause cell death (Orrenius & Nicotera, 1994), Ca^{2+} signals need to be transient. The cell also has to be prepared for the next incoming stimulus. There are many mechanisms that remove Ca^{2+} from the cytosol.

For example, Ca/Na exchangers, plasma membrane Ca^{2+} pumps, and Ca^{2+} pumps on the ER membrane. However, their relative roles in this process are not clear. Studies show that, in some cell types like endothelial cells and pancreatic acinar cells, exchangers and plasma membrane Ca^{2+} pumps are used for Ca^{2+} signal termination, whereas ER Ca^{2+} pumps are for the keeping and restoring of ER $[\text{Ca}]_i$ (Moccia F et al., 2002; Mogami H et al., 1998).

It has been shown that the termination of the Ca^{2+} signal across the entire *Limulus* ventral photoreceptor has two phases: one fast phase (seconds) followed by a slower one (tens of seconds). The fast phase has a decay time constant around one sec, and the slow phase has a maximal speed around $1 \mu\text{M}\cdot\text{s}^{-1}$. The slow phase was shown to be mediated by Na/ Ca^{2+} exchangers on the plasma membrane (O'Day & Keller, 1989; Deckert & Stieve, 1991), but the mechanisms that drive the fast phase still remain unknown. The roles of Ca^{2+} diffusion, Ca^{2+} pumps, and Na/ Ca^{2+} exchangers in the termination of the Ca^{2+} signal need to be tested.

2-Aminoethoxydiphenyl Borate Inhibits Photo-transduction and Blocks Voltage-gated Potassium Channels in *Limulus* Ventral Photoreceptors

Abstract

2-aminoethoxydiphenyl borate (2-APB) is a membrane-permeable modulator that inhibits the activation of inositol (1,4,5) trisphosphate (IP₃) receptors, store operated channels (SOCs) and transient receptor potential (TRP) channels in cells that utilize the phosphoinositide cascade for cellular signaling. We investigated the effect of 2-APB on phototransduction in *Limulus* ventral photoreceptors, where light-induced calcium release via the phosphoinositide cascade is thought to activate the photocurrent, which can be mimicked by injection of exogenous Ca²⁺. 1-100 μM 2-APB reversibly inhibited the photocurrent of ventral photoreceptors in a concentration-dependent manner, acting on at least two processes thought to mediate the visual cascade. 2-APB reversibly inhibited both light and IP₃-induced calcium release, consistent with its role as an inhibitor of the IP₃ receptor. In addition, 2-APB reversibly inhibited the activation of depolarizing current flow through the plasma membrane by released calcium ions. We also found that 100 μM 2-APB reversibly

inhibited both transient and sustained voltage-activated potassium current during depolarizing steps. 2-APB has previously been shown to block phototransduction in *Drosophila* photoreceptors.

Introduction

The depolarizing light response of invertebrate microvillar photoreceptors is mediated by the phosphoinositide lipid-signaling pathway (Brown et al., 1984; Bloomquist et al., 1988). The PI pathway has two initial products, inositol (1,4,5) trisphosphate (IP₃) and diacylglycerol (DAG). Current research centers on the role played by each of these products in activating the cation channels in the plasma membrane that carry the photocurrent. Use of a specific IP₃ receptor inhibitor could help resolve the role of IP₃.

2-aminoethoxydiphenyl borate (2-APB) was first introduced and then widely used as a cell-permeable inhibitor of IP₃-induced calcium release (Maruyama et al., 1997, Bootman et al., 2002). Later, it was found that it is also an inhibitor of store operated ion channels (SOCs) (Bootman et al., 2002) and many TRP channels, especially TRPC channels (Clapham et al., 2001; Delmas et al., 2002 ; Trebak et al., 2002; Xu et al., 2005). In addition 2-APB was shown to have many other pharmacological targets, including inhibiting Ca²⁺ pumps at the ER membrane (Bootman et al., 2002) and gap junctions between cells (Harks et al., 2003; Bai, et al., 2006; Tao and Harris, 2006) and exciting TRPV channels (Chung et al., 2004; Hu et al., 2004; Colton and Zhu, 2007). Therefore, although serving as a useful tool, caution is needed to interpret the effects of 2-APB.

2-APB blocks phototransduction in *Drosophila* photoreceptors (Chorna-Ornan 2001; Ma et al., 2001) but since genetic deletion of the IP₃ receptor protein does not affect phototransduction (Acharya et al., 1997; Raghu et al., 2000), 2-APB presumably acts at some other site than on IP₃-induced Ca²⁺ release. Interpretation of the effect of 2-APB is dependent upon its specificity, which is difficult to establish in *Drosophila* photoreceptors.

In contrast to *Drosophila* photoreceptors, a large body of evidence from *Limulus* ventral photoreceptors implicates IP₃ --induced calcium release in the activation of plasma membrane cationic channels during phototransduction (reviews: Dorlochter and Stieve, 1997; Nasi et al., 2000). Pressure injection of IP₃ into ventral photoreceptors mimics excitation by light, in so far as it activates a conductance in the plasma membrane whose permeability to sodium ions and rectification are very similar to that underlying the photocurrent (Brown et al., 1984; Fein et al., 1984). Activation of the plasma membrane conductance by IP₃ appears to result from two sequential processes. First, IP₃ releases calcium from intracellular stores (Brown and Rubin, 1984; Payne et al., 1986b) by a mechanism that is sensitive to the IP₃ receptor-antagonist heparin (Frank and Fein, 1991; Faddis and Brown, 1993). Second, the released calcium ions activate the plasma membrane conductance by a mechanism that is insensitive to heparin (Payne et al., 1986a; Frank and Fein, 1991), but is otherwise little understood. Given the established role of IP₃-induced calcium release in *Limulus* ventral photoreceptors, we thought the preparation useful for establishing whether 2-APB blocks IP₃-induced calcium release in an invertebrate photoreceptor

and whether it has actions on other components of the visual cascade that might offer an explanation of its actions in *Drosophila*. In addition, we felt that an investigation of the specificity of the action of 2-APB on a cell that has proven to be a model system for the investigation of the PI-cascade might be of general interest.

Material and methods:

Preparation of the nerve

The ventral nerves of *Limulus* were taken out of the animal, de-sheathed, and softened with 1 % Pronase (Clark et al., 1969; Fein and DeVoe, 1973). Then they were placed in artificial sea water (ASW), which contains 435 mM NaCl, 10 mM KCl, 10 mM CaCl₂, 20 mM MgCl₂, and 25 mM MgSO₄. In some experiments, the cells were put in 0 Ca²⁺ ASW. This solution is modified ASW which contains no CaCl₂ but 1mM EGTA.

In some experiments, cells were further treated with hydroxylamine so to reduce their sensitivity to light by bleaching rhodopsin. The bleaching solution of hydroxylamine contains (mM) 200 hydroxylamine chloride, 235 NaCl, 10 KCl, 20 MgCl₂, 25 MgSO₄, 10 CaCl₂, 10 HEPES, and was adjusted to pH 6.5 with 10 N NaOH. Nerves were rinsed with 25 ml of bleaching solution cooled to 4°C and then exposed to 10 min of intense white light at 4 °C. Nerves were then washed five times at 10-min intervals with 50 ml of ASW at 4°C. During experiments, along with other substances, GDP-βS was injected into the cells to further reduce the sensitivity of the cells. After these treatments, the sensitivity of the cells to light can be reduced by up to 3 log₁₀ units. (Faddis & Brown, 1992; Payne & Demas, 2000)

Chemicals and solutions

2-APB (Toris Cookson Inc., Ballwin, MO) was dissolved in DMSO to make a 10 mM stock solution and stored at -20°C . The stock was dissolved in DMSO and then ASW to make working solutions with different 2-APB concentration and fixed DMSO concentration (1% v/v). It was applied by superfusion (1ml/min; 5-10 times bath volume). IP_3 (100 μM , Research Biochemicals, Natick, MA), D-myo-inositol 1,4,5-triphosphate, P4(5)-(1-(2-nitrophenyl) ethyl) ester, tris(triethylammonium salt) (NPE-caged IP_3 ; 8mM, Calbiochem, San Diego, CA.), Calcium Aspartate (2 mM), GDP- βS (10mM), and Oregon Green-5N (1 mM, Molecular Probes, Eugene, OR) were dissolved in a carrier solution (100 mM potassium aspartate, 10 mM HEPES, pH 7.0) before injection into cells.

Electrophysiological recording

For current clamp experiments, cells were impaled with a glass micropipette through which membrane potential was measured, containing 3M KCl (thick walled glass; resistance $\sim 30\text{ M}\Omega$) or injection solutions (thin walled glass; resistance $\sim 18\text{ M}\Omega$). Solutions to be injected into the photoreceptors were pulse-pressure injected into the light-sensitive rhabdomeral (R-) lobe of the photoreceptors, as described by Corson and Fein (1983). For voltage clamp experiments, cells were impaled with a second microelectrode for current injection that contained 3M KCl (thick walled glass; resistance $\sim 16\text{ M}\Omega$) and were voltage-clamped at their resting membrane potential in darkness (-45 - -65 mV) using an Axoclamp-2A amplifier (Axon Instruments, Foster City, CA). The voltage-clamped current or the membrane potential was filtered at

300Hz and sampled at 1 KHz using a Digidata 1200 (Axon Instruments) analog-to-digital board installed in a personal computer.

Optics and fluorescence microscopy

White light from a 100W quartz-halogen source (model 6333; Oriel Corporation, Strafford, CT) was used to illuminate the photoreceptors. This light passed through a heat filter (Scott KG3; Ealing Optics, South Natick, MA), neutral density (ND) filters, and a shutter before it reached the preparation. The intensity of light without the ND filters was $80\text{mW}/\text{cm}^2$. Light intensities were measured as \log_{10} units of attenuation relative to this intensity. Attenuation by $-8.5 \log_{10}$ units typically elicited approx. one single photon event (one quantum bump arising from one photoisomerised rhodopsin molecule) per second from the photoreceptors. In order to view the cells with a video camera (Corson and Fein, 1983), the nerve was illuminated by an infrared beam, created by passing a second beam of light through an infrared filter (Schott RG1000).

Confocal imaging was performed as described in Ukhanov and Payne (1995). Briefly, photoreceptors cells loaded with 1 mM Oregon Green-5N, a fluorescent calcium indicator dye, were viewed through an inverted Zeiss LSM 410 microscope. The 488 nm line of an Ar-Kr laser was used to excite the Oregon Green-5N. The laser beam was attenuated to 0.1% to reduce photo-bleaching. After being reflected by a dichroic mirror (IT510) the laser beam was focused onto the cell by a 40x lens (Zeiss, 40x Neofluar, N.A. 0.75). After being passed through a 515 nm long pass filter, the resulting fluorescence emitted by Calcium Green-5N, was collected by a

photomultiplier tube. The fluorescence of Oregon Green-5N was measured within 5 μm of the microvillar membrane of the photoreceptor using the stationary spot recording mode of the microscope.

A double flash protocol (Payne and Demas, 2000) was used to obtain 20ms “snapshots” of the calcium signal that followed dim flashes. Briefly, a 20ms dim flash and a subsequent strong 20 ms flash were used to excite the cell and collect the resulting fluorescence respectively. A ND filter that can reduce the light intensity by 10,000 fold was put into the light path of the 488nm laser beam to obtain the dim flashes. The dim flashes cannot excite sufficient amount dye to enable measurement of fluorescence changes, but they will excite the cell and induce Ca^{2+} release or fluorescence increase after certain latency. A subsequent bright flash from the unattenuated laser was used to elicit the fluorescence either within the latent period, or at the peak, of the receptor potential that followed a 20 ms dim flash. The duration of the strong flash is shorter than its latency to release Ca^{2+} (Payne and Ukhanov, 1996), thus the collected fluorescence is not contaminated by strong flash-induced Ca^{2+} release.

For experiments using caged IP_3 , 8 mM NPE- IP_3 , 10mM GDP- βS and 1mM Oregon Green-5N were dissolved in carrier solution and injected into a chemically bleached cell. The cell was then exposed to a 5s flash of visible (488nm) light so as to record any residual desensitized physiological response to light. Caged IP_3 was then released by a 5ms UV flash (364 nm) delivered from an Ar laser (Innova Technologies) that

was superimposed on the visible light after a 7ms delay (Ukhanov and Payne, 1997). The 364 nm laser beam was reflected by a dichroic mirror (IT510) before it was focused onto the specimen.

Statistical significance and reversal of the effects of 2-APB

All data in the text and figures are given as mean \pm SE. To assess statistical significance, a standard Student's paired t-test was performed. All comparisons of data referred to as significant in the paper met a $P < 0.05$ criterion. Reversal of all of the reported effects of 2-APB required a 40-90 min ASW wash. The effects of 2-APB referred to in the text as “reversible” showed no significant difference between values after washout and control values. Effects referred to as “partially reversible” showed a significant return towards control values following washout of 2-APB, but the mean final values reached were still significantly different from those of the control.

Results

2-APB reversibly inhibits the peak light responses in a light-intensity dependent manner.

Cells were voltage-clamped to their resting potentials in darkness (-45 to -65 mV). The effect of 2-APB on the intensity-response relationship of dark-adapted ventral photoreceptors to brief (20 ms) flashes was investigated.

For dim flashes, 10 min exposure to 100 μ M 2-APB shifted the intensity – peak response curve to the right by about 2.8 log units (Fig. 1), virtually eliminating the response to dim flashes (Fig. 2A). Similar to previous reports (Stieve and Schlösser, 1989), medium intensity flashes (-2.5~-1.0 log₁₀ attenuation) would induce currents that have two peaks. The application of 100 μ M 2-APB abolishes the fast peak (Fig. 2B), whereas the saturated light-induced currents were only reduced by $16 \pm 5\%$. All these effects were partially reversible after washing with ASW (Fig. 1 and Fig. 2).

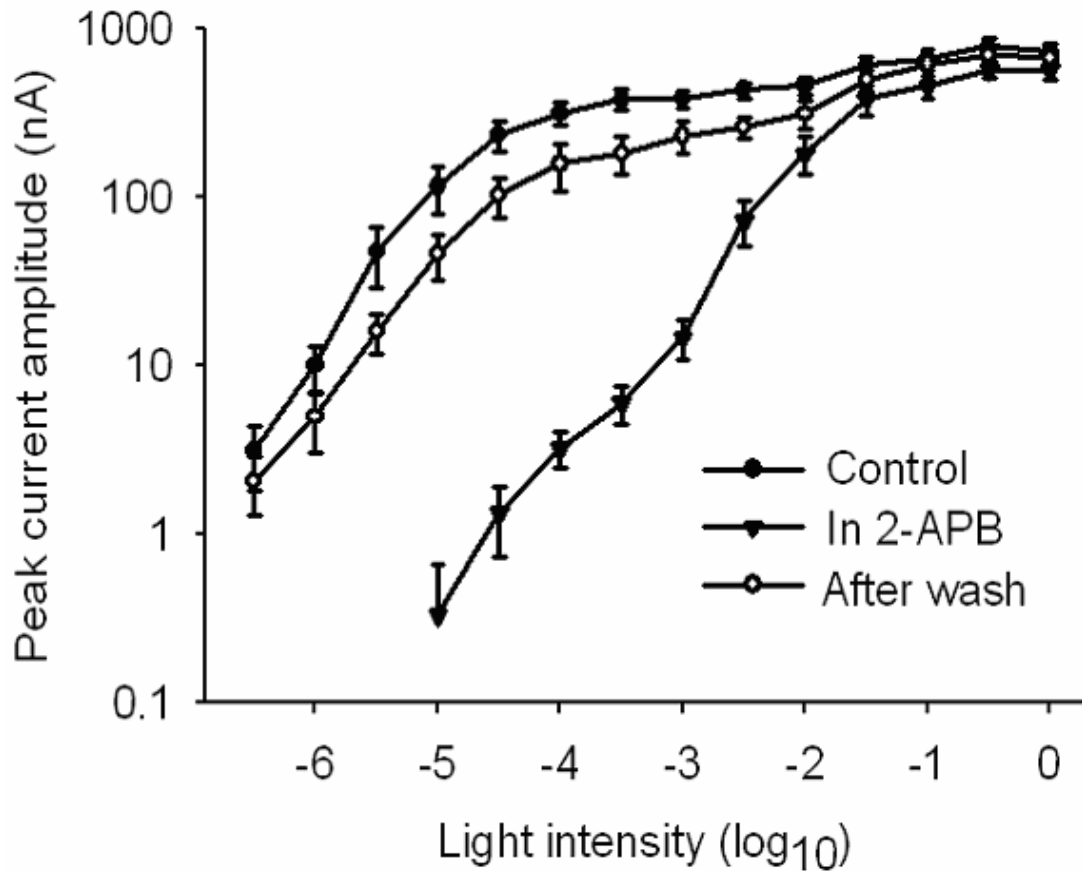


Figure 1. The effect of 2-APB on the peak photocurrent-light intensity curves in voltage clamped *Limulus* ventral photoreceptors. The light stimulus (20 ms flashes) was delivered every minute. Traces of filled circles, triangles, and open circles represent the corresponding peak light-induced-currents obtained before, during the application of 100 μ M 2-APB and after following washouts.

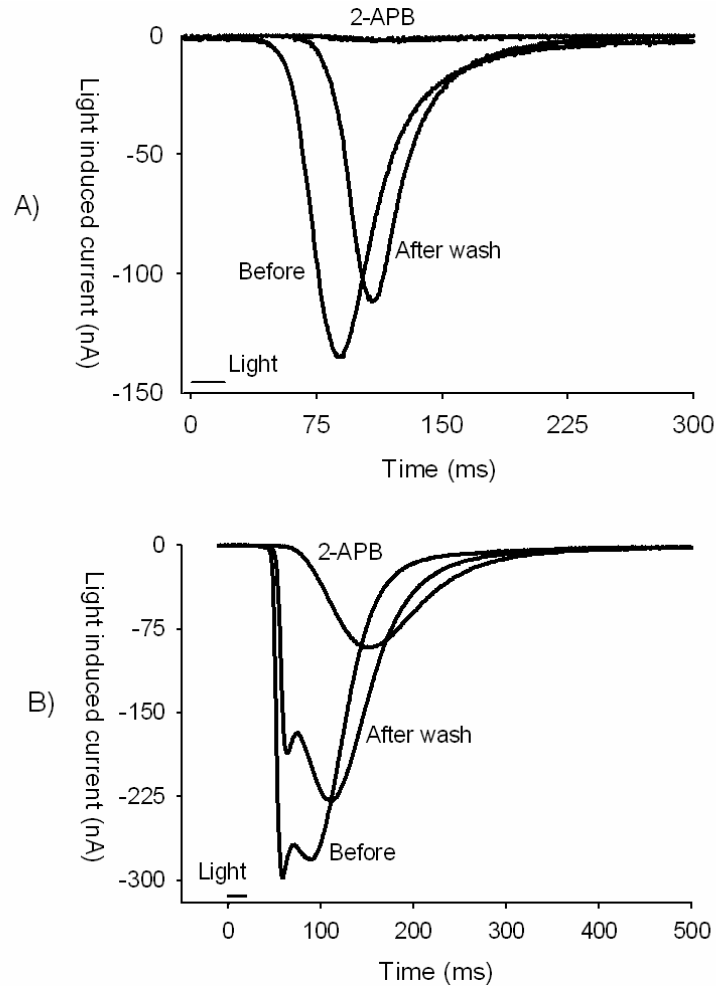


Figure 2. 2-APB reversibly inhibits the light-induced currents in voltage clamped *Limulus* ventral photoreceptors. The light stimulus (20 ms flashes) was delivered every minute. A) The inhibition of 2-APB upon dim flash-induced photocurrent. In this cell, the photocurrent elicited by a dim light flash (intensity $-4.5 \log_{10}$ units) is almost abolished in the presence of 2-APB, partially recovered upon washing with ASW. B) The inhibition of 2-APB on photocurrents elicited by intense light flashes (intensity $-2.0 \log_{10}$ units). In this cell, 2-APB abolished one peak of the light-induced current, and this effect was partially recovered after 2-APB was washed out with ASW.

Application of 100 μM 2-APB also slowed the time-to peak of responses (Fig. 1A), reversibly increasing the time-to-peak of responses to dim ($-4 \log_{10}$ unit) flashes from 101 ± 8 ms to 202 ± 11 ms ($n=7$; Fig. 1A). Partial recovery of the time-to-peak to 127 ± 7 ms was observed following washout of 2-APB.

In contrast to *Drosophila* photoreceptors (Chorna-Ornan et al., 2001), 100 μM 2-APB did not induce any significant current flow in darkness, but in current clamp recordings a small, but significant and reversible, depolarization of 4.4 ± 1.7 mV ($n=19$) was observed during treatment.

The inhibition of 2-APB to light-induced currents is concentration dependent

Dose-response curves of 2-APB (Fig. 3) were constructed using two methods of measuring the sensitivity, either by measuring the peak response to a dim flash of fixed intensity after 10 min exposure to various concentrations of 2-APB or by measuring the increase in the light intensity required to elicit a criterion peak response amplitude of 30 nA. Both methods gave similar results. Significant desensitization began above concentrations of 1 μM . The EC50 was approx 5 μM and the slope of a Hill Plot, 2.8 (inset, Fig. 3), indicates significant co-operativity.

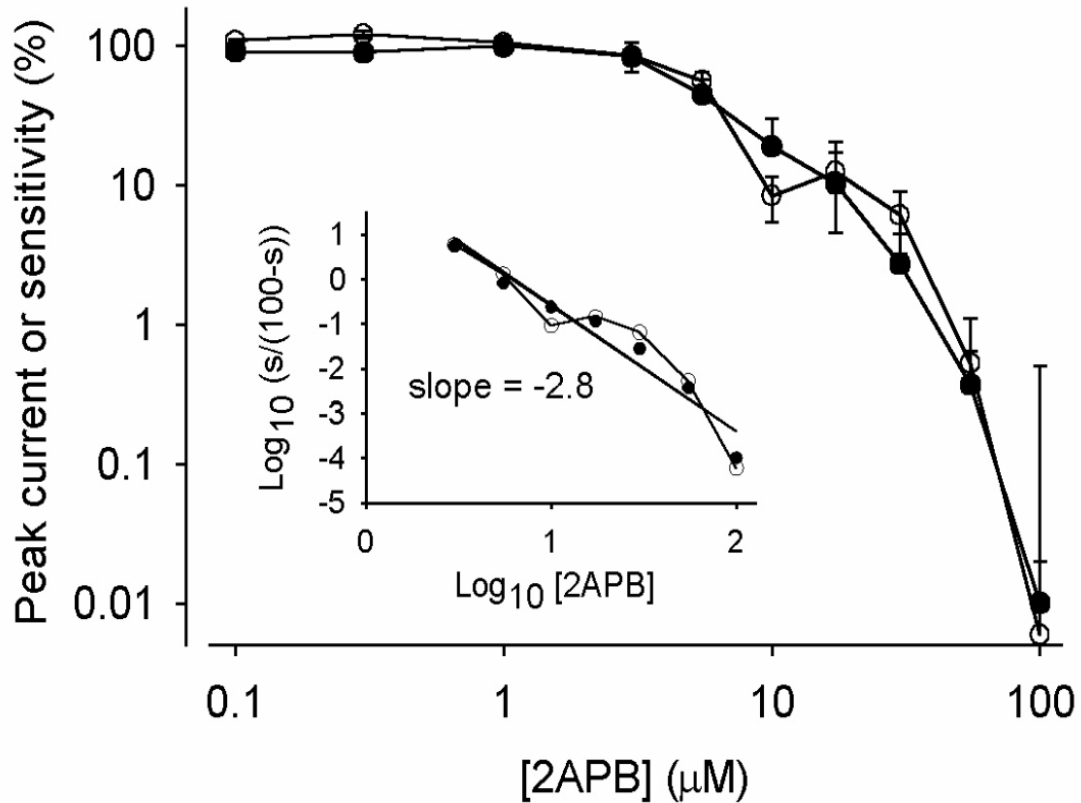


Figure 3: Dose-response curves for 2-APB's inhibition of photoreceptor response. The photoreceptor's sensitivity to light stimulus was determined either by measuring the peak response to a dim flash of fixed intensity (open circles), or by measuring the increase in the light intensity required to elicit a criterion peak response amplitude of 30 nA (Filled circles). In both cases, sensitivity in the presence of 2-APB is shown as a percent of that before. Inset: Hill plot of sensitivity, s , fitted with a linear regression line having a slope of -2.8 .

2-APB reversibly inhibits light-induced calcium release.

The sensitivity and rapidity of the electrical response of ventral photoreceptors to dim flashes is dependent upon light-induced calcium release (Bolsover and Brown, 1985).

Other agents that suppress light-induced calcium elevation, such as high concentrations of heparin, BAPTA or cyclopiazonic acid, also reduce the sensitivity and slow the response of ventral photoreceptors (Frank and Fein, 1991; Faddis and Brown, 1993). We therefore performed confocal fluorescence microscopy experiments to investigate the effect of 2-APB on light-induced calcium release.

As described by Payne and Demas (2000), cells loaded with Oregon Green-5N, a fluorescent calcium-indicator dye, were first stimulated by a 20ms dim flash. Since dim flash cannot elicit sufficient dye fluorescence for $[Ca]_i$ measurements, a subsequent 20 ms intense flash was used to elicit the fluorescence either within the latent period, or at the peak, of the receptor potential that followed a 20 ms dim flash (Fig. 4). Since 20ms are shorter than the latent period for Ca^{2+} release, the fluorescence collected by 20 ms intense flash would only reflect the rest or peak Ca^{2+} release induced by dim flashes (See methods for details). The $\Delta F/F_o$, the increase in dye fluorescence collected at the peak of the receptor potential (ΔF) relative to that recorded during the latent period (F_o) is a measure of the release of calcium ions from intracellular stores by the preceding dim flash (Payne and Demas 2000).

As expected, 10-20 min treatments with 100 μM 2-APB reversibly reduced the receptor potential to 14 ± 5 % of control values ($n=7$), accompanied by a small, reversible, depolarization of 6.9 ± 2.4 mV. $\Delta F/F_o$ was similarly reversibly reduced to 17 ± 9 % of control values (Fig. 4), indicating an inhibition of light-induced calcium release.

F_0 , an indicator of the resting calcium concentration, increased by $17 \pm 8 \%$ during treatment with 2-APB, but did not significantly recover upon washout of 2-APB. Because a small irreversible increase in resting fluorescence could result from leakage of dye from the micropipette used to fill the cell, we were unable to conclude that 2-APB caused any small increase in resting calcium concentration. Neither were we able to verify any increase in F_0 in a second set of experiments performed on cells filled with caged IP_3 (see below).

Overall, these results demonstrate that desensitization of the electrical response to light by 2-APB is accompanied by an inhibition of light-induced calcium release.

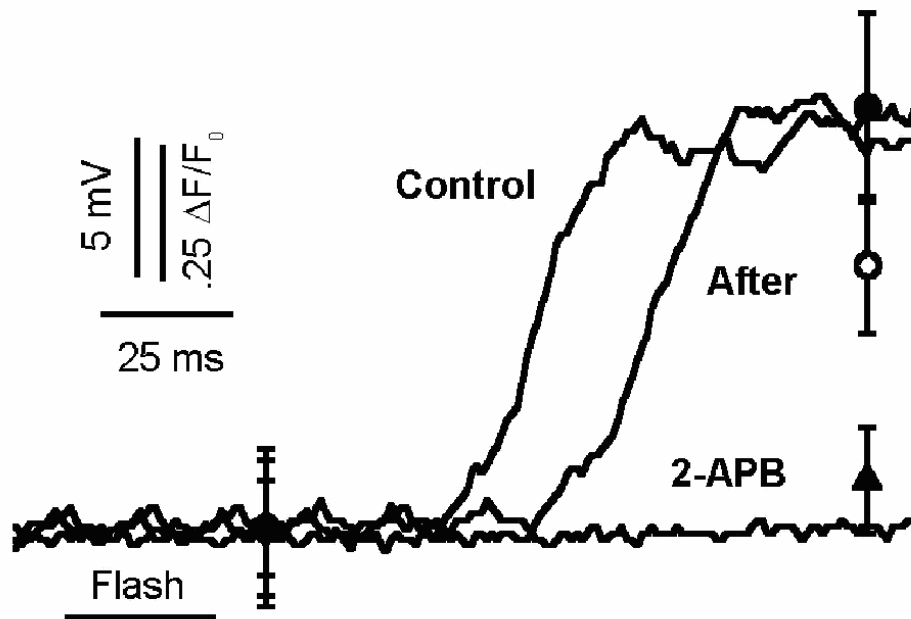


Figure 4: Inhibition of light-induced calcium release by 2-APB. Receptor potentials (lines) and relative fluorescence of Oregon Green-5N (symbols) recorded in response to a dim flash (duration 30ms, photoisomerizing approx. 300 rhodopsin molecules), recorded before (filled circles), during (triangles) and after (open circles) exposure to 100 μ M 2-APB. Relative fluorescence at the peak of the electrical response, but not during the latent period, is greatly reduced in the presence of 2-APB, accompanied by a comparable reduction in peak receptor potential amplitude.

2-APB reversibly inhibits the electrical response of ventral photoreceptors to pressure injections of IP_3 .

Since light-induced calcium release in ventral photoreceptors is known to be dependent upon light-induced IP_3 production (Frank and Fein, 1991; Faddis and Brown, 1992; review: Dorlochter and Stieve, 1997), we went on to determine the

effect of 2-APB on IP₃-induced electrical responses and on IP₃-induced calcium release. Pulsed pressure injections of 100 μM IP₃ were delivered in darkness into the R-lobe of the photoreceptor. Under current clamp, peak depolarizations in response to the injections were reversibly reduced to $30 \pm 9\%$ (n=5) of their control values following 10-15 min. treatment with 100 μM 2-APB (Fig. 5A). Under voltage clamp at the resting potential (-45 to -65 mV), peak inward currents produced in response to similar pulsed pressure injection of 100 μM IP₃ were reversibly reduced to $3 \pm 1\%$ of control (n=4; Fig. 5B). The much greater inhibition of the voltage-clamped response, compared to the current-clamped response, caused us to investigate the effect of 2-APB on voltage-gated currents, which may explain the discrepancy (see below).



Figure 5: Inhibition of electrical response to IP_3 by $100 \mu\text{M}$ 2-APB in one typical cell. A) Under current clamp, transient depolarizations elicited by injection of $100 \mu\text{M}$ IP_3 are reduced in the presence of 2-APB, complete recovering after washout of 2-APB. B) Under voltage clamp, 2-APB abolishes inward current elicited by IP_3 injection. The current response also completely recovers after washout of 2-APB.

2-APB reversibly inhibits IP_3 -induced calcium release.

The above result clearly shows that 2-APB can inhibit the ability of IP_3 to elicit an electrical response. The electrical response to IP_3 is thought to be mediated in two steps. IP_3 releases calcium ions, which activate a cationic plasma membrane conductance. In order to determine which of these steps was affected by 2-APB, we

first measured IP₃-induced calcium release, performing confocal fluorescence microscopy on cells filled with caged IP₃ (Fig. 6).

Cells were first desensitized to visible light by bleaching rhodopsin with hydroxylamine. Cells were then pressure-injected with a cocktail containing caged IP₃, GDP-βS (to further desensitize the physiological response to visible light) and the fluorescent calcium-indicator dye, Oregon Green-5N. Dye fluorescence was monitored during intense 488 nm laser excitation at a spot within 5 μm of the microvillar membrane. After injection, desensitized cells generated a small, delayed electrical response to 488 nm illuminations, and no calcium signal was detected at the position of the confocal spot (Fig. 6A). However, following a superimposed UV flash, so as to release caged IP₃, a rapid increase in the relative dye fluorescence signal ($\Delta F/F_0$) was observed within 20ms, indicating a calcium concentration increase at the confocal spot, accompanied by a rapid depolarization (Fig. 6B). This rapid response has previously been shown to arise from the photolysis of caged IP₃ and not from the UV flash per se (Ukhanov et al., 1997).

100 μM 2-APB reduced the peak $\Delta F/F_0$ following uncaging of IP₃ to 4 ± 4 % of its control value (n=5) and the accompanying depolarization to 6 ± 6 % (Fig. 6C). Partial recovery of both followed after washout of 2-APB (Fig. 6D). This result directly demonstrates that 2-APB is an inhibitor of IP₃-induced calcium release in ventral photoreceptors.

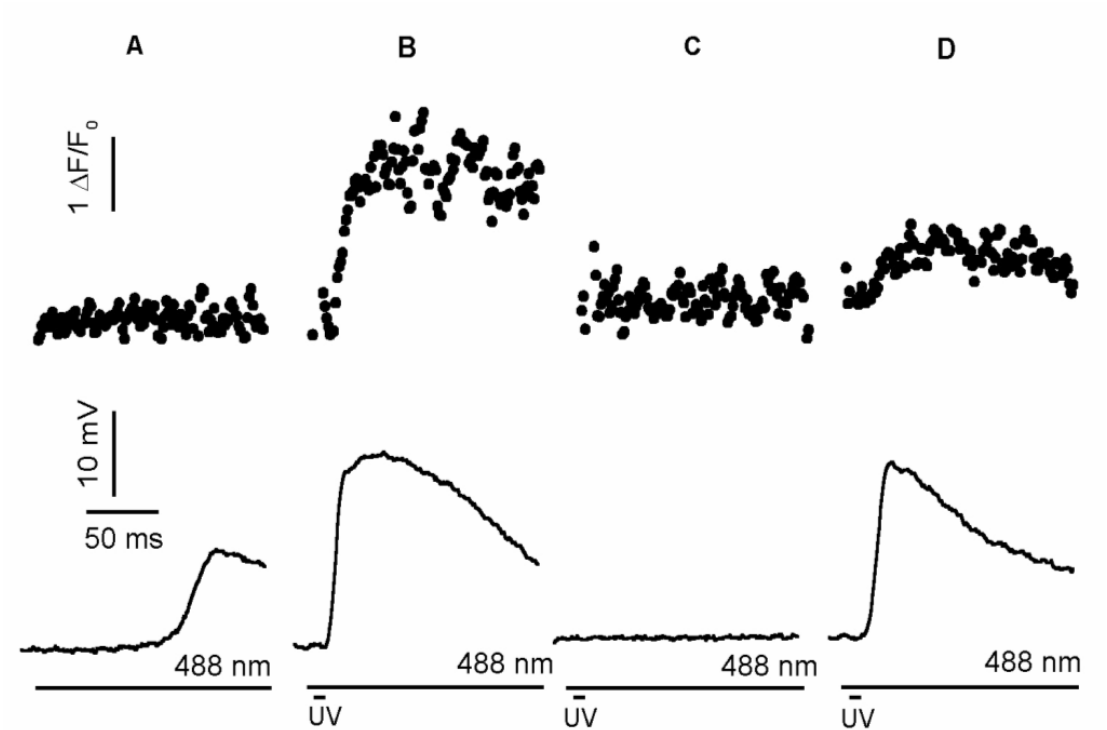


Figure 6: 2-APB inhibits IP₃-induced Ca²⁺ release in cells filled with caged IP₃, GDP-βS and the calcium indicator dye, Oregon Green-5N. Top traces show relative fluorescence of Oregon Green-5N, bottom traces show membrane potential. A) In the absence of UV light, an intense 488 nm step of light induces a small delayed depolarization and no detectable increase in calcium indicator fluorescence. B) Following a superimposed UV flash, to release caged IP₃, a rapid increase in fluorescence is observed indicating Ca²⁺ release. Rapid depolarization accompanies the Ca²⁺ release (bottom trace). C) Both Ca²⁺ release and depolarization are inhibited in the presence of 100 μM 2-APB. D) Partial recovery after washout of 2-APB.

2-APB's also acts downstream of Ca²⁺ release, reversibly inhibiting the amplitude of the current elicited by Ca²⁺ injections

For current clamp experiments, cells were impaled in their rhabdomeral lobe with a micropipette containing 2 mM Ca²⁺ for voltage recording and Ca²⁺ injections. For voltage clamp experiments, cells were impaled with a second micropipette filled with 3M KCl and were voltage-clamped to their resting potentials (-45 to -65 mV).

Under current clamp, the injection of Ca²⁺ into current clamped cells will induce depolarizations with amplitudes around 25 mV. The application of 100 μM 2-APB has no effect on the amplitudes of depolarizations induced by Ca²⁺ injections (n=4, paired T test) (Upper image, Fig. 7).

Whereas for cells under voltage clamp, pulsed pressure injection of Ca²⁺ elicited a rapid inward current of peak amplitude 2 - 8 nA (Payne et al., 1988). The Ca²⁺-induced current was reversibly reduced to 13 ± 5 % of its control values after 10 min treatment with 100 μM 2-APB (n=4; Fig.7, bottom image). This result shows that in addition to blocking calcium release, 2-APB also acts at a downstream site in the visual cascade, blocking the response to released calcium ions. Unlike our results, the experiments done by Chorna-Ornan et al. (2001) show that the Ca²⁺ activated Cl⁻ channels in *Xenopus* oocytes is not inhibited by 2-APB. Moreover, they found that after wash-out of 2-APB the injection of Ca²⁺ resulted in a highly facilitated response relative to control, while in our experiments, the difference is not significant.

Similar to the results of IP₃ injections, there is discrepancy between the results of the voltage-clamped response and those of the current-clamped response. The greatly reduced inhibition of the response to IP₃ and Ca²⁺ injections under current clamp indicates that 2-APB inhibits voltage gated channels.

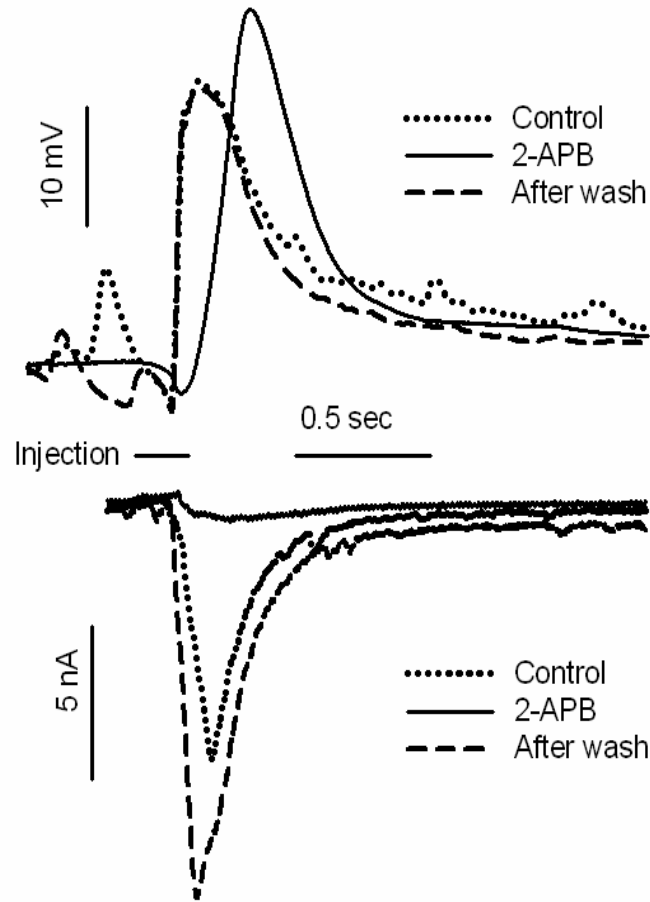
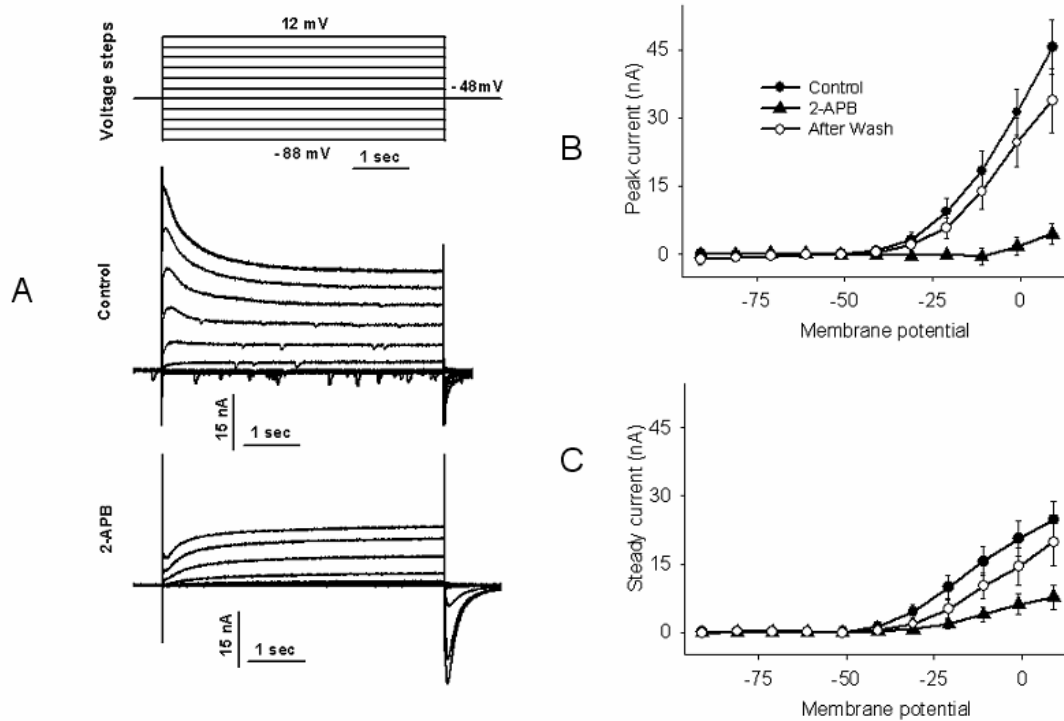


Figure 7: The effect of 100 μM 2-APB on Ca^{2+} injections-induced electrical responses in one typical cell. The dotted, dashed and line curve represents the corresponding electrical responses elicited by pulsed-pressure injections of 2mM calcium aspartate in photoreceptors before, after and during the application of 100 μM 2-APB. Upper image: 2-APB doesn't affect the amplitude of the rapid depolarizations elicited by Ca^{2+} injections into current-clamped photoreceptors. Bottom image: 2-APB greatly and reversibly reduces inward currents elicited by pulsed-pressure injections of 2mM calcium aspartate into voltage-clamped photoreceptors. For the cell shown, the amplitude of the current elicited by calcium injection following washout of 2-APB exceeded that of the control.

2-APB blocks voltage-sensitive K⁺ currents

Being a bulky organic amine, 2-APB is a potential blocker of voltage-gated potassium channels (review: Mathie et al., 1998). We therefore examined the effect of 2-APB on outward currents elicited by voltage steps. Voltage-activated outward currents of *Limulus* ventral photoreceptors comprise a delayed rectifier, giving rise to a maintained outward K⁺ current; and a rapidly-inactivating K⁺ conductance similar to the A current of molluscan neurons (Pepose and Lisman, 1978; Lisman et al., 1982). Both of these components of the outward current were blocked by 100 μM 2-APB (Fig. 8). Cells were first held at their resting potential. Voltage clamp currents were recorded during 5 s steps from the resting potential, ranging from -40 mV to +60mV. Average V-I curves for both peak transient and sustained currents, with the ohmic leakage current subtracted from the data, are shown in Fig. 8. For a step of +60 mV, treatment with 100 μM 2-APB for 10 min resulted in a reversible reduction in the peak transient outward current to $7\% \pm 6\%$ and the sustained current to $28 \pm 11\%$ of their control values respectively (n=8). The percent blockage was not significantly dependent on the magnitude of the voltage step, neither were ohmic leakage currents reduced by 2-APB. Therefore, 2-APB is a strong blocker of voltage-sensitive potassium conductances in ventral photoreceptors.



2-APB slowed down a depolarization-activated inward current

In the preceding experiments, when we investigated currents during hyperpolarizing steps, we held the membrane potential 20~40mV more negative than the resting potential (-40~-60mV) for 5 sec, then stepped it back to the resting potential. Under these conditions we observed a rapidly-inactivating inward current following the step (5 out of 8 cells, Fig. 9). This phenomenon has been reported previously: Pepose and Lisman (1978) found that depolarization of the photoreceptor from a holding potential of -70 or -80 mV would induce a fast inactivating current. Later, this current was found to be composed of sodium and calcium currents, each having a different voltage-dependence (Lisman et al., 1982).

In the presence of 100 μ M 2-APB, the time- to-peak of the transient inward current was increased from 17 ± 2 ms to 62 ± 11 ms and time constants of inactivation of this inward current were increased approximately 3 fold (45 ± 9 ms vs 169 ± 16 ms) (n=5)

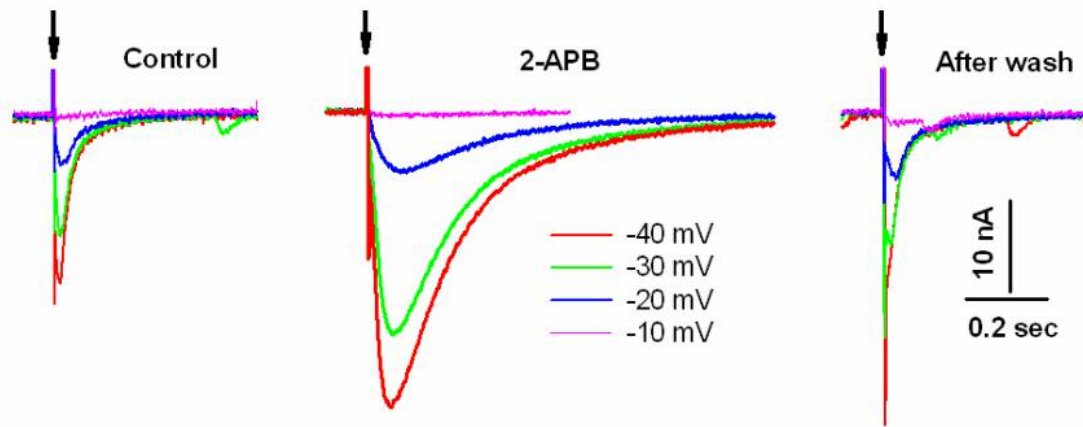


Figure 9. 2-APB slows down the activation and inactivation of depolarization activated inward currents. When the membrane potential is returned to the resting potential (-40~-60mV) following 5-sec -20~-40mV hyperpolarizing steps, a transient inward current is induced. The arrow indicates the end of the voltage step. In the presence of 100 μ M 2-APB, the times to peak and inactivation time constants of this inward current were increased approximately 3 fold.

Discussion

2-APB is clearly an effective, reversible inhibitor of the light response of *Limulus* ventral photoreceptors, acting in a concentration range (1-100 μM) that is similar to its actions in other cells, including *Drosophila* photoreceptors. At the highest concentration investigated, 100 μM , inhibition takes the form of an almost total loss of sensitivity to dim flashes, while the peak photocurrent produced by saturating flashes is reduced by only 16%. 2-APB does not, therefore appear to greatly block maximal ion permeation through the light-sensitive channels but rather reduces the efficiency with which the channels can be opened by dim flashes. The loss of the electrical response to dim, but not bright, flashes resembles the effect of other inhibitors of IP_3 -induced calcium elevation, including heparin, BAPTA and cyclopiazonic acid (Frank and Fein, 1991; Faddis and Brown, 1993; Ukhanov and Payne, 1995). This result also suggests that 2-APB either doesn't directly block the light sensitive channels on the membrane, or its direct inhibition effect is minor when compared with its other effects.

*2-APB is not a specific inhibitor of IP_3 -induced Ca^{2+} releases in *Limulus* ventral photoreceptors.*

2-APB inhibits multiple stages of the light response.

The high amplification achieved during the response of *Limulus* ventral photoreceptors to dim flashes is thought to depend on two cascaded processes,

calcium release due to light-induced production of IP₃ and the subsequent activation of the photocurrent by the released calcium (review: Dorlochter and Stieve, 1997).

As regards to the former process, we show that 100 μM 2-APB reversibly suppresses light- and IP₃-induced calcium release in ventral photoreceptors. 2-APB has been described as a non-competitive antagonist of IP₃-induced calcium release in a variety of cell types (Sugawara et al. 1997; Ma et al. 2000).

We also show that 100 μM 2-APB reversibly suppresses the activation of inward current by calcium ions. In blocking the response to calcium ions, 2-APB acts on a step in the visual cascade that is not blocked by heparin (Frank and Fein, 1991) and is therefore independent of IP₃-induced calcium release. The mechanism by which calcium ions activate cation channels in the plasma membrane is not understood and, to our knowledge, 2-APB is the first pharmacological agent shown to reversibly inhibit it. This second site of action may also reconcile the ability of 2-APB to inhibit phototransduction in *Drosophila* with the evidence that the IP₃ receptor is not required for phototransduction in that species. There are now several reports of 2-APB acting to inhibit plasma membrane conductances in mutant non-photoreceptor cell lines which lack all three IP₃ receptor isoforms, indicating an action of 2-APB at a site other than the IP₃ receptor (Prakriya and Lewis 2001; Ma et al. 2002).

The action of 2-APB at two consecutive independent stages of phototransduction may account for the steep Hill plot ($n=2.8$) of its overall inhibition of the cell's sensitivity to dim flashes.

2-APB also reversibly suppresses voltage-dependent potassium channels and slows depolarization activated sodium channels in Limulus ventral photoreceptors.

This may be expected from the structure of 2-APB. In general, bulky amines are inhibitors of voltage-sensitive potassium channels, including diphenylhydramine (Benadryl), a compound with a structure somewhat similar to that of 2-APB (Khalika et al., 1999). Since blockage of voltage-activated potassium channels by intracellular TEA or Cs^+ is routinely used in whole cell recordings of calcium currents, including those of *Drosophila* photoreceptors, it is possible that this effect of 2-APB has gone unreported in other cells. Clearly, if the potassium channels of *Limulus* photoreceptors are not unique in this respect, our finding constrains the interpretation of the effect of 2-APB on the electrophysiological behavior of intact cells

The effect of 2-APB on peak photocurrent-light intensity curve indicates the existence of two pathways that mediate the light-induced current in Limulus ventral photoreceptors.

Flashes with near saturating intensities ($-2.5 \sim -1.0 \log_{10}$ attenuation) induce currents that have two peaks in *Limulus* ventral photoreceptors (Stieve and Schlösser, 1989).

This and other observations have led to the hypothesis that the light response in *Limulus* photoreceptors may be mediated by up to three independent pathways. Our results partially support this concept. In the presence of 100 μM 2-APB, an initial peak in the time-course of the response to saturating light flashes reversibly disappears (Fig. 2B). This suggests that there may be at least two kinetically distinct pathways that mediate the light-induced current.

To obtain some hints about the pathways that lead to the opening of light activated channels, the peak photocurrent-light intensity curve (Fig. 1) was re-plotted as a curve of peak photocurrent vs number of effective photons (or activated rhodopsin molecules, Fig. 10). If we assume that the concentrations of intracellular messengers that bind and open light-activated channels are linearly proportional to the number of effective photons delivered per flash, then the intensity-response curve can be represented by the rectangular hyperbola equation (Baylor, Lamb and Yau, 1979).

$$I = \frac{I_{\max} \cdot n}{n_0 + n} \quad 1$$

Here “I” is the peak light-induced current produced by a light activated pathway in *Limulus* ventral photoreceptors, “ I_{\max} ” is the maximal peak light-induced current that can go through these channels, “n” is the number of effective photons delivered per flash (see Methods), “ n_0 ” is the number of effective photons eliciting half-maximal photocurrent.

Average peak photocurrent-light intensity curves in control groups have a complex shape that is similar to those in earlier reports (Fig. 1) (Brown and Coles, 1979; Stieve and Schlösser, 1989). Under control conditions, the average photocurrent can be fitted by the sum of two components, each obeying the rectangular hyperbola equation described above: one process is more sensitive to light (n_0 is 170 effective photons, corresponding to a light intensity around $-4.6 \log_{10}$ units with a saturating peak current, I_{\max} , of around 191~390 nA); The other component is less sensitive to light ($K_d = 132,000$ effective photons, corresponding to a light intensity around $-1.7 \log_{10}$ units with an I_{\max} around 370-517 nA). When the photoreceptors were bathed with 100 μM 2-APB, the average peak photocurrent-light intensity curve can be fitted by the less-sensitive process alone (with an I_{\max} of 593 nA). Similar results were obtained by fitting those curves of each individual cell and then averaging the resulting fits.

Although the above results imply the existence of a process with a peak current around 500 nA that is insensitive to 2-APB at concentrations up to 100 μM , this doesn't mean that this process is entirely 2-APB insensitive. The inhibition of the light-induced electrical response by 2-APB is concentration dependent and the effect of 2-APB shows no sign of saturation at 100 μM (Fig. 3). A recent paper by Fein (2003) demonstrates that application of 300 μM 2-APB further desensitizes the electrical response to light (Fein, 2003).

Nevertheless, the peak photocurrent-light intensity curves with and without 100 μM 2-APB suggest that there might be two pathways for the opening of the light activated channels. For dim light stimulus, the light-induced current is generated via a 2-APB sensitive pathway. When the light stimulus is stronger, a second pathway with less sensitivity to 2-APB is also engaged.

Interestingly, two possible mechanisms for the pathway downstream from Ca^{2+} or DAG have been proposed (See introduction for details, Fig. 1 of Chapter 1). Briefly, one candidate branch is to be through Ca^{2+} mediated activation of guanylyl cyclase, which will produce cGMP to open cGMP gated channels on the plasma membrane; while the other possible pathway is DAG and Ca^{2+} mediated TRPC channels.

To assign 2-APB sensitivities to these two possible pathways downstream from PLC, further experimental evidences are needed. 2-APB can be used as a useful pharmacological tool to separate these two possible pathways and then study the downstream mechanisms.

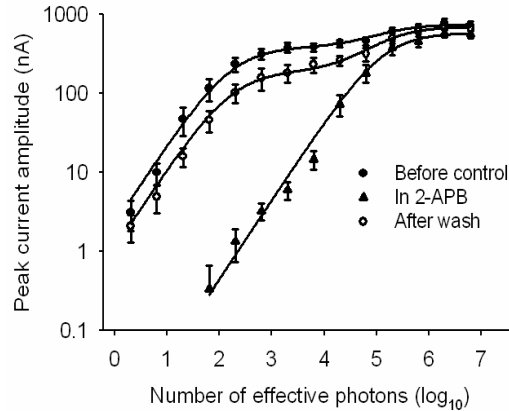


Figure 10. The curve of peak photocurrent-effective photons can be fitted by the sum of two components, each obeying the rectangular hyperbola equation (a replot of Fig. 1). These curves were generated following light flashes of different intensities in voltage clamped *Limulus* ventral photoreceptors. The light stimulus (20 ms flashes) was delivered every minute. Traces of filled circles, triangles, and open circles represent the corresponding peak light-induced-currents obtained before, during the application of 100 μ M 2-APB and after the washout of 2-APB. The corresponding lines that go through the above three traces are fits obtained by the sum of two components, each obeying the rectangular hyperbola equations (The goodness of all three fits are larger than 99.2%). The first component is relatively sensitive to light (“ n_{01} ” = 170 effective photons); whereas the second component is less sensitive to light (“ n_{02} ” = 170 effective photons). In the presence of 100 μ M 2-APB, the maximum peak light-induced current of the first component, $I_{\max 1}$, was abolished (191~390 nA as compared to 0 nA), whereas the change of $I_{\max 2}$ is not that significant (370~517 nA as compared to 593 nA). This indicates that the light response of *Limulus* ventral photoreceptors has at least two pathways: one is light and 2-APB sensitive, while the other is not.

Estimating the Diffusion Coefficients of Substances with Known Molecular Weights

Abstract

In order to get a better understanding of the dynamics of the Ca^{2+} signal, we estimated the diffusion coefficient, D , of Ca^{2+} ions, a Ca^{2+} buffer (Dextran fluo4) and inositol trisphosphate (IP_3), as well as the uniformity of the cytoplasm. We first developed a method for measuring the D value of injected fluorescent dyes by fitting confocal line scan images with diffusion equations. The D values of various dyes were paired with their corresponding molecular weights, and the D values of IP_3 and Ca^{2+} inside the cytoplasm of the cell were then estimated using Graham's Law. The estimated D for Ca^{2+} , $217 \mu\text{m}^2/\text{s}$, is similar to previous reports, and those of IP_3 ($74 \mu\text{m}^2/\text{s}$) and Dextran fluo4 ($23 \mu\text{m}^2/\text{s}$) fall within the range of D values of substances with similar molecular weight in other cellular systems. However, the D value of IP_3 is significantly lower than that in a cellular extract of *Xenopus* oocytes. This might be caused by differences among species and the possible loss of cellular content during preparation of the cellular extract. There was no difference between D values of Dextran alexa fluo488 measured along different directions and in different locations

of the cell. The cytoplasm of the cell is therefore uniform and has no role in generating non-uniform light-induced Ca^{2+} signals.

Introduction

As an important intracellular messenger, the multifunctional role of Ca^{2+} is accomplished by modulating its amplitude, temporal and spatial features through combinations of different Ca^{2+} release, termination and effector machineries (Berridge, et al., 2001). Among all those termination modulators, Ca^{2+} buffers are an important factor that can affect the range and amplitude of Ca^{2+} signals. Most importantly, the mobility of Ca^{2+} ions is mainly determined by Ca^{2+} buffers: “fixed Ca^{2+} buffers tend to retard the signal”, “whereas mobile buffers contribute to Ca^{2+} redistribution” (Gabso, Neher and Spira, 1997). Similarly, in cells where Ca^{2+} ions are released via a diffusible agonist such as IP_3 , the diffusion of such agonist is also important in determining the spreading of Ca^{2+} signals (Jafri and Keizer, 1994). Therefore, estimations of the diffusion coefficients of substances like Ca^{2+} buffers and agonist are needed to understand the dynamics of the Ca^{2+} signal.

Many methods have been used to measure the diffusion coefficients (D) of substances inside cells. The D value can be obtained directly by fitting the spread of radioactivity-labeled ions with diffusion equations or by calculations using Nernst-Einstein equation and the movement of the radio-active ions in electrical fields (Hodgkin and Keynes, 1953, 1957; Kushmerick and Podolsky, 1969). The usage of this method is restricted by the requirement of a large specimen and radioactive materials. Similarly, the D value of fluorescent indicators can also be obtained by fitting the spreading of injected dyes with diffusion equations (Gabso, Neher and Spira, 1997). Or the D value of fluorescent molecules can be obtained through other

methods. For example, fluorescence photobleach recovery (FPR) is routinely used to determine diffusion coefficients (Axelrod et al., 1976; Blatter and Wier, 1990; Tansey et al., 1994); The value of D for fluorescent macromolecules in a finite volume can also be obtained by fluorescence (fluctuation) correlation spectroscopy (FCS) (Elson, 1974; Chen et al., 1999; Digman et al., 2005).

Here we measured the D value of fluorescent indicators using a similar method to that of Gabso, Neher and Spira, 1997, and from these measurements the D values of IP₃ and mobile Ca²⁺ buffers were estimated (Bruins et al., 1931).

Material and methods:

Preparation of the nerves, dyes and electrodes:

The ventral nerves of the *Limulus* were treated as described before (Millecchia and mauro, 1969; Fein and DeVoe, 1973). Then, they were placed for stimulation and recording in a chamber filled artificial sea water (ASW), which contained (in mM) 435 NaCl, 10 KCl, 10 CaCl₂, 20 MgCl₂, and 25 MgSO₄ (pH 7.0~7.4).

All four dyes, dextran-alexa fluor 555 (MW:10,000), dextran-alexa fluo 488 (MW:3,000), alexa-fluor 555 and ANTS, were bought from Molecular Probes. They were dissolved in a carrier solution (100mM KAsp, 10mM HEPES, PH 7.0) before being loaded into injection electrodes.

A sharp electrode loaded with fluorescent molecules was placed into ASW or used to impale cells. The dyes were then injected into solutions or cells via pulse air pressure. A single such injection will eject a 1-10 pl volume of solution into ventral photoreceptors (Corson & Fein, 1983).

Fluorescence measurements:

All measurements were performed using Zeiss confocal microscopes. For ANTS measurements, a Zeiss LSM410 was used. In order to excite ANTS the 364 nm laser beam from an Ar laser (Innova Technologies), was focused onto the cell by a 40X

objective (Zeiss, 40X, Neofluar, NA 0.75). Fluorescence was collected through a dichroic mirror (FT395). Before collection, the resulting fluorescence was filtered by a 515 nm long pass filter (Ukhanov and Payne, 1995a). For the other three dyes, a Zeiss LSM510 and a 40X oil lens (Zeiss, NA: 1.3) were used for measurements. Dextran alexa fluor555 and alexa fluor555 were excited by a 543 nm laser beam from a HeNe laser, and dextran alexa fluor 488 was excited by a 488 nm laser line from an Argon laser. Before reaching the specimen, the exciting laser beam excitation first went through an appropriate beam splitter (HFT488/543). Before collection by the photomultiplier tube, the emitted fluorescence was filtered by appropriate long pass filters (a 560 nm long pass filter for emissions from the first two dyes and a 505 nm long pass filter for emissions from dextran alexa fluor 488)

The line scan (X-t scan) mode of the microscope was used: The laser beam sweeps back and forth along a pre-selected line. The resulting fluorescence of each pixel along this line is collected so that the fluorescence change with time across this line can be obtained. Therefore, both spatial and temporal information about the fluorescence change can be obtained by this method. Since one sweep scan takes around one or two milliseconds, this method is used for collecting both spatial and temporal information.

Data collection: A two-second duration confocal line scan across the electrode tip was taken to collect the fluorescence beneath the electrode tip. The line was perpendicular to the axis of electrode. 50 ms after the onset of the line scan,

fluorescent molecules were introduced into ASW or cells by a 0.1 sec pressure injection. The resulting fluorescence changes were collected and stored onto a computer. The above procedures were repeated with two-minute intervals to get 9 or 12 images.

To reduce noise level, one average image was obtained from the raw images. The resulting image was then filtered with a 2D Gaussian window (2.25 $\mu\text{m} \times 7.68 \text{ ms}$). Background fluorescence before injection was subtracted from this filtered image to obtain the two dimensional image of the injection and subsequent diffusion of fluorescent molecules. Diffusion equations were fit to the spread of fluorescence after the end of the injection period.

Equations used for fitting diffusional spread: Equation (1) is the solution to diffusion from a point source into an infinite volume (Crank, 1956).

$$C = \frac{M}{8(\pi \cdot D \cdot t)^{1.5}} \cdot \exp\left(\frac{-r^2}{4D \cdot t}\right) \quad (1)$$

Where 'C' is the concentration of the diffusion molecule, 'M' is the total mass injected, 'D' is the diffusion coefficient, 't' is time, and 'r' is the distance from the point source.

We modify equation (1) by adding an extra factor ‘ σ ’ to describe an initial Gaussian concentration profile of fluorescent molecule following injection.

$$C = \frac{M}{8(\pi \cdot D \cdot (t + \sigma))^{1.5}} \cdot \exp\left(\frac{-r^2}{4D \cdot (t + \sigma)}\right) \quad (2)$$

The spatial-temporal distribution pattern of pressure injected fluorescent molecules was fitted with this equation. The extent of similarity between simulated and experimental results was estimated by the least square method. Then ‘ σ ’ and ‘ D ’ in equation (2) were varied and the above procedures were repeated until a best fit was found. If the maximal correlation coefficient was better than 95%, then the corresponding D was accepted as the diffusion coefficient of this molecule.

Results and Discussion

The diffusion coefficients of several dyes in the cell and in ASW: We estimated the diffusion coefficients of dextran alexa fluor546, ANTS, Alexa fluor 555 and Dextran alexa fluo 488.

An example of using the fitting method to estimate D values

Using the least square method, the spatial-temporal distribution pattern of pressure injected fluorescent molecules from a sharp electrode was compared with that from calculations of diffusion from an initially Gaussian concentration profile. When the simulated pattern generated from a certain diffusion coefficient fitted the experimental data with a correlation coefficient of >95%, then the corresponding D was accepted as the diffusion coefficient of this molecule (Fig 1).

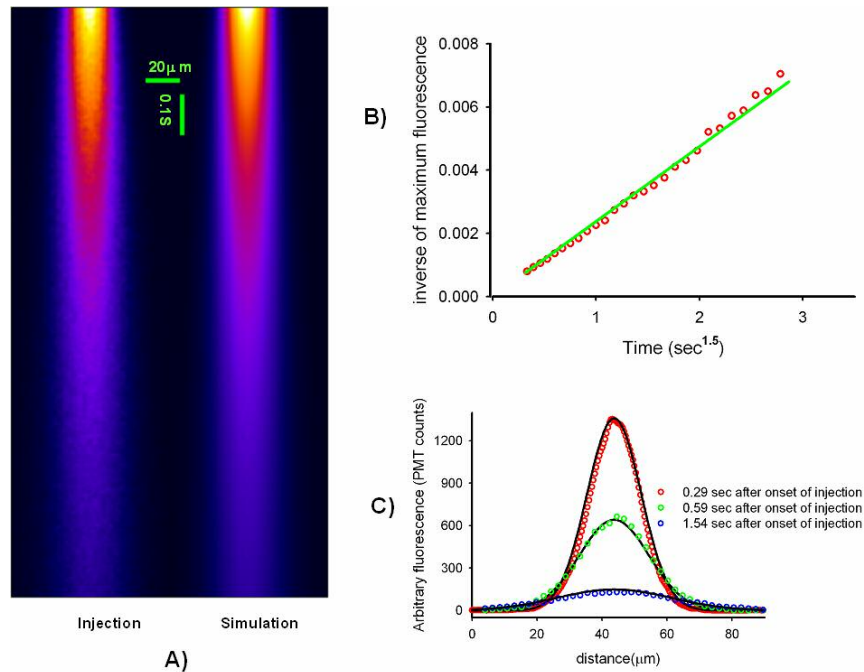


Figure 1. The diffusion coefficient of dextran alexa fluor. A) Figure on the left: Line scan image of the spread of dextran alexa fluor beginning 0.29 sec after the onset of injection. The laser beam sweeps back and forth along a pre-selected line. Successive lines of fluorescence are then stacked so that the fluorescence change with time across lines can be obtained, while spatial information is indicated by the intensity of the fluorescence along the lines. Figure on the right, the best fit of equation (2) to the experimental data. Parameters used: $D = 76 \mu\text{m}^2/\text{s}$, $\sigma = 0.17 \text{ sec}$, $M = 1.25\text{e}7$. The correlation coefficient is 99.8%. The pseudo-colors in both figures have the same scale. The higher the fluorescence, the brighter the color. B) Linear plot of $(t+\sigma)^{1.5}$ vs the inversion of peak fluorescence obtained from figure A. Red curve: experimental data. Green line: equation (2). C) The spatial distribution of fluorescence of dextran alexa fluor and the corresponding fits to equation (2) at three different times. Colored curve of circles are experimental data, black curves are the corresponding fits to equation (2).

From equation (2), two conclusions about three dimensional diffusion from a Gaussian profile can be made: (1) The spatial concentration profile of the diffusion substance at any time point is a Gaussian distribution (Fig 1 C). (2) The decay of peak concentration (C_{peak}) with time follows equation (3) (Fig 1 B)

$$\frac{1}{C_{\text{peak}}} = \frac{8(\pi \cdot D \cdot (t+\sigma))^{1.5}}{M} \quad (3)$$

A simplified version of equation (3) is equation (4), where K is a constant. From equation (4) it is clear that there is a linear relationship between $1/C_{\text{peak}}$ and $(t+\sigma)^{1.5}$. (Fig 1. C and Fig 2.C)

$$\frac{1}{C_{\text{peak}}} = K \cdot (t+\sigma)^{1.5} \quad (4)$$

From Figure 1 and 2, it is clear that the diffusion of dextran alexa fluor after injection strictly follows the two above characteristics of diffusion from an initial Gaussian profile. Therefore, it is reasonable to estimate the diffusion coefficients of fluorescent molecules with this method.

Through this method, the diffusion coefficients of dextran alexa fluor 546 in ASW and in cells were determined to be $74 \pm 9 \mu\text{m}^2/\text{s}$ (n=6) and $12.4 \pm 0.8 \mu\text{m}^2/\text{s}$ (n=4) respectively (Fig. 1 and 2).

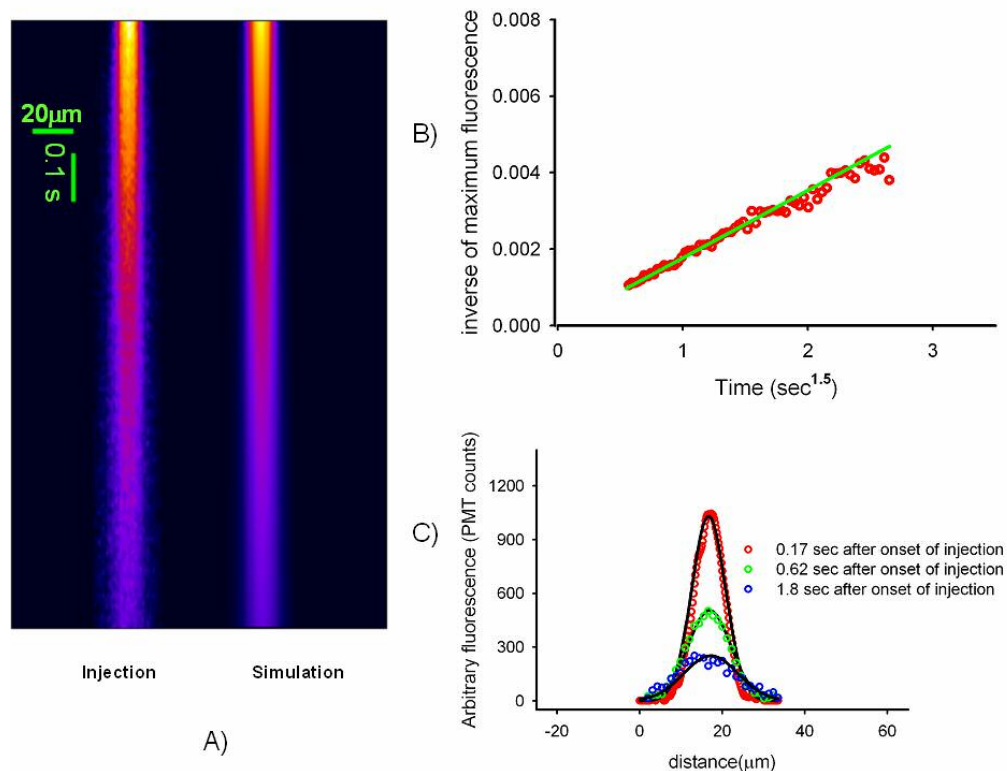


Figure 2. The diffusion coefficient of dextran alexa fluor inside cells. A) Figure on the left: Line scan image of the spread of dextran alexa fluor beginning 0.17 sec after the onset of injection. Figure on the right, the best fit of equation (2) to the experimental data. Parameters used: $D = 12.6 \mu\text{m}^2/\text{s}$, $\sigma = 0.52 \text{ sec}$, $M = 1.13\text{e}6$. The correlation coefficient is 99.6%. B) Plot of $(t+\sigma)^{1.5}$ vs the inverse of peak fluorescence of figure A. Red curve: experimental data. Green line: fitting of experimental data. C) The spatial distribution of fluorescence of dextran alexa fluor and their corresponding Gaussian fits at three different time points in figure A). Colored curve of circles are experimental data, black curves are their corresponding fittings.

The cytoplasm of the photoreceptor is uniform

As described in the next chapter, the spread of the light-induced Ca^{2+} signals has two phases. The initial fast phase is mainly confined within the R lobe, while the later slow phase often occurs at the junction between the two lobes (See chapter 3 for details). To test whether this difference in spread speed is caused by non-uniformity of the cytoplasm, the D values of Dextran alexa fluo 488 in different lobes and along different directions relative to the long axis of the cell were measured.

The D value of Dextran alexa fluo 488 in the A and that in the R lobe was determined to be 46 ± 5 and $43 \pm 6 \mu\text{m}^2/\text{s}$. There was no significant difference between these two values ($p=0.28$, paired T test, $n=4$). Similarly, D values measured along the longitudinal axis of the cell, $42 \pm 4 \mu\text{m}^2/\text{s}$, showed no difference to those measured perpendicular to the longitudinal axis of the cell ($46 \pm 5 \mu\text{m}^2/\text{s}$) ($p=0.26$, paired T test, $n=7$). These results indicate that the cytoplasm of the cell is uniform.

This uniformity of the cytoplasm is consistent with previous reports. Although the A and the R lobe of the *Limulus* ventral photoreceptors are structurally and functionally different, there are no physical barriers between them and the ER network is uniform and continuous throughout the entire cytoplasm (Stern et al., 1982; Calman & Chamberlain, 1982; Feng et al., 1994). Cytoplasmic viscosity, the major factor that affects apparent D values, is usually uniform for substances that do not bind significantly to immobile intracellular components (Luby-Phelps, 2000). The D

values of the other indicator dyes within the R and the A lobe were therefore considered to be the same and were not measured separately.

The diffusion coefficients of indicator dyes in the cell and in ASW through the fitting method (table 1).

Table 1. The diffusion coefficients of dyes inside Cells and in ASW

Dye	MW	Diffusion coefficient ($\mu\text{m}^2/\text{s}$)			
		N		In ASW	In Cells
		In ASW	In Cells	In ASW	In Cells
ANTS	381	7	4	290 \pm 29	72 \pm 10
Alexa fluo 555	1029	6	4	225 \pm 10	57 \pm 14
Dextran alexa fluo 488	3000	11	4	129 \pm 6	43 \pm 4
Dextran alexa fluo 555	10,000	6	4	74 \pm 9	12 \pm 1

From figure3, it is clear that the D values we obtained fall within the range of reported values of molecules with similar sizes in other cellular systems. Also, the D values of these dyes inside cells are reduced by a factor of approximately 4.6 relative to their D values in ASW. Similar reductions have been reported in many other cellular systems (Swiss 3T3 cells, Luby-Phelps et al., 1986; Nerve processes, Popov and Poo, 1992; Muscle cells, Arrio-Dupont, 1996; Hela cells, Lukacs et al., 2000).

There are many reasons for this reduced mobility of substances inside cells. Firstly, according to Stokes-Einstein equation, the D of molecules is inversely proportional to viscosity. The cytoplasm of the cells has a greater viscosity relative to that of the extracellular solution, which usually results a 2-5 fold reduction in D values (Kushmerick and Podolsky, 1969; Strautman et al., 1990, Popov and Poo, 1992; for review: Luby-Phelps, 2000). Secondly, the cytoskeletal network may restrict the apparent diffusion of macromolecules that have a hydrodynamic diameter larger than 10 nm or a MW bigger than 580 kDa (Luby-Phelps, 2000; Lukacs et al., 2000). Considering the sizes of the dyes we used, it is unlikely that the cytoskeleton will hinder their diffusion. Thirdly, the binding of diffusible substances with immobile cellular components will greatly reduce apparent D values (Crank J, 1957; Blatter and Wier, 1990; Luby-Phelps et al., 1995). However, it has been shown that the inert tracer Dextran does not bind with immobile cellular structures (Luby-Phelps et al., 1985). Since the two other dyes we tested show a similar reduction in D value to those of Dextran dyes and the reduction in apparent D value is similar to those reported in the literature (Swiss 3T3 cells, Luby-Phelps et al., 1986; Nerve processes, Popov and Poo, 1992; Muscle cells, Arrio-Dupont, 1996; Hela cells, Lukacs et al., 2000), it is probable that none of the dyes we used bind significantly to cellular structures.

Estimations of the diffusion coefficients of Dextran fluo4 and IP₃ inside cells.

Although there are many factors that affect the diffusion coefficient of a molecule, the molecular weight (M) and the diffusion coefficient (D) of a molecule are strongly related (Blatter and Wier, 1990). This relationship can be described by the Graham's Law (equation (5), Bruins et al., 1931).

$$D = \frac{c}{M^{0.5}} \quad (5)$$

In which c is a constant dependent on the nature of the solvent and the temperature.

The diffusion coefficients and molecular weight of dextran alexa fluor, alexa fluor 555 and ANTS can therefore be used to calculate the value of "c" inside cells and in ASW (Fig 3). Then, the diffusion coefficients of Dextran fluo4 (MW: 10,000) and IP₃ (MW: 414.6) inside cells and in ASW can be estimated through equation (5).

For Dextran fluo4 the diffusion coefficients inside cells and in ASW are 23 μm²/s and 86 μm²/s respectively. For IP₃, they are 74 μm²/s inside cells and 293 μm²/s in ASW.

The predicted diffusion coefficients of free Ca²⁺ ions in ASW and inside cells (866 and 217 μm²/s respectively) are close to those reported in the literature (700-780 μm²/s in aqueous solution, (Wang, 1953); 223 μm²/s in cellular extract (Allbritton et al., 1992). Moreover, the predicted diffusion coefficient of Fura-2 (MW 636.5) is 62 μm²/s in *Limulus* ventral photoreceptors. This is also close to the values reported in

cells with similarly dense ER networks, like cardiac and muscle cells (32-43 $\mu\text{m}^2/\text{s}$, Miura et al., 1998; Blatter and Wier, 1990; Timmerman and Ashley, 1986; Baylor and Hollingworth, 1988).

Our estimation of D for IP_3 is lower than the measurements in cellular extract (283 $\mu\text{m}^2/\text{s}$, Allbritton et al., 1992). Besides variation of cytoplasm viscosity in different species, the other possible explanation for this is that during the procedure of extract preparation some content of the cytoplasm was lost, thus reducing its viscosity. Moreover, the ER network in the cellular extract might be ruptured, reducing any physical obstacles for IP_3 diffusion.

The size of all known Ca^{2+} binding proteins in neurons (Baimbridge et al., 1992; Burgoyne and Weiss, 2001; Haeseleer et al., 2002) is larger than 10 kDa. The reported D values of similar sized macromolecules in different cytoplasm all fall within the range of 0.1~23 $\mu\text{m}^2/\text{s}$ (Figure 3). Therefore, the mobility of Ca^{2+} binding proteins in the cytoplasm of the photoreceptors should be low. If they have a similar binding ratio to fixed intracellular components to the dyes we used here, then according to our estimation, their diffusion coefficient inside *Limulus* ventral photoreceptors is estimated to be smaller than 14 $\mu\text{m}^2/\text{s}$. This indicates that when the intracellular Ca^{2+} signal is small relative to the buffering capacity of immobile and mobile Ca^{2+} binding proteins, the spread of the Ca^{2+} signal is expected to be slow.

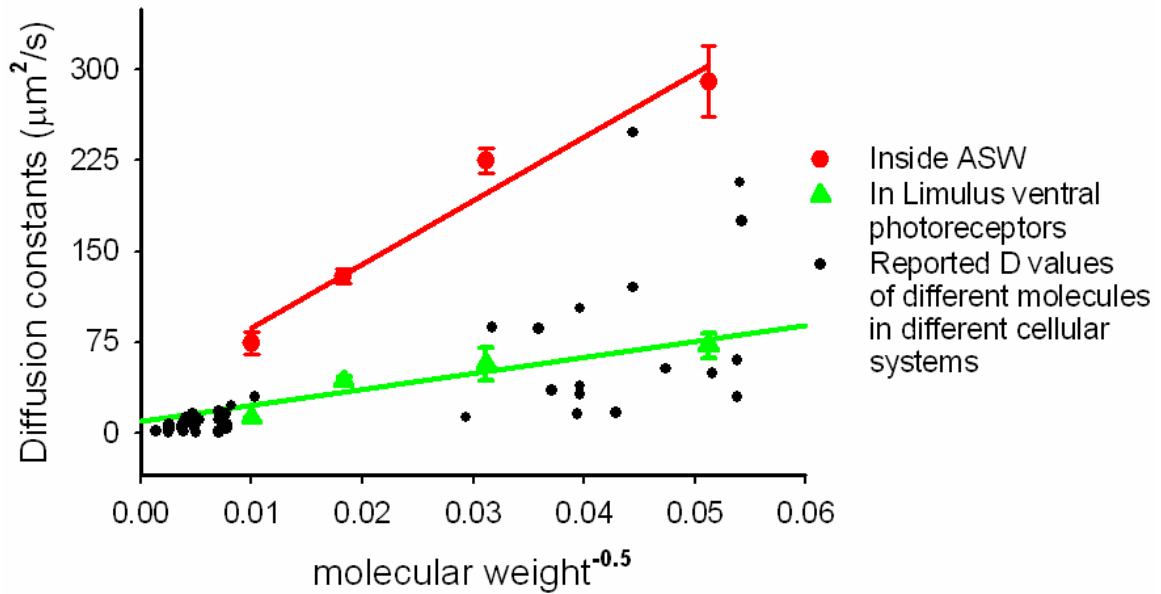


Figure 3. The diffusion coefficient inside cells and in ASW as a function of molecular weight. Red dots and line: diffusion coefficients of dyes in ASW and their linear regression curve; Green dots and line: diffusion coefficients of dyes inside *Limulus* ventral photoreceptors and their linear regression curve. The values of c in ASW and cells are 5253 and $1466 \mu\text{m}^2/\text{s}$ respectively. Black dots are the D values of different molecules in different cellular systems as reported in the literature. Fluorescent labeled macromolecules used include: various sized dextran (Tansey et al., 1994; Braga et al., 2004; Arrio-Dupont et al., 1996; Luby-Phelps et al., 1985; Horne and Meyer, 1999), Calmodulin (Tansey et al., 1994; Luby-Phelps et al., 1985); bovine serum albumin and IgG (Wojcieszyn et al., 1981; Luby-Phelps et al., 1985; Popov and Poo, 1992); lactalbumin and ovalbumin (Luby-Phelps et al., 1985; Popov and Poo, 1992); actin (Luby-Phelps et al., 1985); Na^+/H^+ exchanger-regulatory factor 1 (Haggie et al., 2004); and myoglobin (Baylor and Pape, 1988); small molecules include indicators and dyes like: indo-1 (Blatter and Wier, 1990), Fura-2 (Blatter and

Wier, 1990; Gabso et al., 1997; Strautmann et al., 1990; Timmerman and Ashley, 1986); Tetramethylmurexide, Arsenazo III, and antipyrylazo III (Maylie et al., 1987a~c); Calcium green (Brown et al., 1999), Alexa fluor 488 and Lucifer yellow (Holcman and Korenbrot, 2004), carboxyfluorescein and dichlorofluorescein (Brink and Ramanan,1985), and other small molecules like glycine (Timmerman and Ashley, 1986), sucrose, ATP (Kushmerick and Podolsky, 1969; Hubley et al., 1995), and cGMP (Koutalos et al., 1995).

Investigation of the Mechanisms that Define the Spatial-temporal Profile of the Ca^{2+} Signal and Estimation of the Peak Ca^{2+} Signal Inside *Limulus* Ventral Photoreceptors

Abstract

As an important intracellular messenger, Ca^{2+} signals mediate both light-induced excitation and adaptation in *Limulus* ventral photoreceptors. To get a better understanding of its multiple functional roles, the dynamics of the Ca^{2+} signal were studied. The light-induced Ca^{2+} release was shown to originate at the rhabdomeral membrane of the R lobe. Consistent with its role in mediating the light response, the Ca^{2+} signal under the microvillar membrane rises to its peak with a similar time course to that of the photoreceptor's electrical signal. The Ca^{2+} signal then spreads into the interior of the cell with two phases. The initial fast phase is a diffusion driven process that needs both the diffusion of IP_3 and of Ca^{2+} released by IP_3 . Experimental manipulation of either the apparent diffusion coefficient (D) of Ca^{2+} ions or the life span of IP_3 molecules change the spread of the fast phase. The peak $[\text{Ca}]_i$ close to the rhabdomeral lobe is high enough (300 μM) to enable it to diffuse freely and contribute to the initial spread. Minimizing the D values of Ca^{2+} ions by buffering the

Ca^{2+} signal through injection of excess slow moving Ca^{2+} buffer, Dextran-fluo4, can slow down the speed of the initial spread. Thus the diffusion of Ca^{2+} ions contributes to the fast phase. In the presence of excess Dextran fluo4, the existence and the unaltered duration of the fast spread indicates the participation of IP_3 diffusion. Moreover, prolonging the life span of IP_3 through injection of the analog and IP_3 -ase inhibitor, L-chiro-I (1,4,6) PS_3 , increases the duration of the initial spread. Thus the diffusion of IP_3 also contributes to the initial fast spread, and it determines the duration of the fast phase. Model simulations indicate that the diffusion of both IP_3 molecules and Ca^{2+} ions released by IP_3 are both necessary and sufficient to explain the initial fast phase of spread. This model also indicates that the diffusion of IP_3 might account for the spread of excitation and the facilitation of light responses in responses to dim flashes, while the diffusion of both Ca^{2+} ions and IP_3 molecules are needed for the spread of excitation and the saturation of light responses in responses to intense flashes.

Introduction

Calcium (Ca) is a very important intracellular messenger that controls many cellular processes, such as visual transduction, exocytosis, gene transcription, and muscle contraction. This vital, multifunctional role of Ca^{2+} is accomplished by modulating its amplitude, temporal and spatial features through combinations of different Ca^{2+} release, termination and effector machineries (Berridge, et al., 2001). Therefore, accurate estimate of Ca^{2+} amplitude, timing, temporal and spatial properties is important to understand the role of Ca^{2+} in those cellular responses.

In *Limulus* ventral photoreceptors, a light stimulus will lead to the release of IP_3 from plasma membrane. IP_3 molecules then diffuse to the endoplasmic reticulum (ER) and release calcium (Ca) stored in the ER by opening IP_3 receptors. Ca^{2+} mediates both excitation and adaptation of the light responses (for review, see Nasi E, et al., 2000; Lisman et al., 2002). To get a better understanding of the molecular mechanism of the light response, more information about the light-induced Ca^{2+} signal is needed. It is known that the light-induced Ca^{2+} signal initiates within the light sensitive rhabdomeral lobe (R lobe) (Payne and Fein, 1987). However, the spatial relationship between the light-induced Ca^{2+} signal and the microvillar membrane of the R lobe has not been demonstrated directly. In response to weak or moderate intensity stimuli it has been shown previously that the time to peak of the Ca^{2+} signal is highly correlated with that of the light-induced receptor potential (Payne & Demas, 2000). But we do not know whether this relationship holds true for responses to intense stimulus.

Moreover, because high affinity calcium indicators were used in previous studies, the peak Ca^{2+} signal in response to intense flashes may have been greatly underestimated (Brown and Blinks, 1974; Brown et al., 1977; Levy and Fein, 1985; O'Day and Gray-Keller, 1989; Ukhanov & Payne, 1995a,b).

Under very dim illumination, light-induced excitation is confined to the locality of a photoisomerized rhodopsin molecule. Within 100ms excitation appears to spread a distance of 1.5~4 μm . Saturation of the light response (competition between excitatory products released by individual photoisomerisations therefore begins when only 200 photons are effectively absorbed across the entire photoreceptive membrane (Brown JE and Coles JA, 1979; Payne R and Fein A, 1986). It is not known whether the diffusion of Ca^{2+} and IP_3 can account for this spread.

In response to a stronger stimulus “global” Ca^{2+} signals are generated in many cell types. They are usually triggered from local Ca^{2+} “hot spots” and then propagate as waves across the cell. (Berridge MJ, 1997; Bootman et al., 2001). In *Limulus* ventral photoreceptors, it is known that the light-induced Ca^{2+} signal first spreads rapidly across the R lobe and then slows down and hardly penetrates the light insensitive arahbdomeral lobe (A lobe) (Ukhanov & Payne, 1995a). But whether this spread results from diffusion or a regenerative “ Ca^{2+} wave” has not been demonstrated. Detailed description of two-phase spreading and the possible molecular mechanism behind it is unknown.

In this chapter, the above questions will be investigated with the help of various dyes, buffers and model simulations.

Material and methods

Preparation of the nerve

The ventral nerves of *Limulus* were taken out of the animal, desheathed, and softened with 1 % Pronase in (Millecchia and Mauro, 1969; Fein and DeVoe, 1973). Then they were placed in a chamber filled artificial sea water (ASW), which contained 435 mM NaCl, 10 mM KCl, 10 mM CaCl₂, 20 mM MgCl₂, and 25 mM MgSO₄ (pH 7.0~7.4) for stimulation and recordings. For some experiments, a component of ASW was modified: 0 Ca²⁺ ASW, contained no CaCl₂ but 1mM EGTA

Chemicals and solutions:

D-myo-IP₃ (100μM) and L-chiro-IPS₃ (L-chiro-Inositol 1,4,6-tris-phosphorothioate triethylammonium salt, 500mM) were obtained from Sigma Chemical Corp. All dyes, ANTS (8-aminonaphthalene- 1,3,6-trisulfonic acid), Dextran-fluo4 (5 mM), FM4-64 (N-(3-triethylammoniumpropyl)-4-(6-(4-(diethylamino) phenyl) hexatrienyl) pyridinium dibromide, 100μM); Fluo-4 (1 mM), Fluo-5N (1 mM), and Calcium Green 5N (1 mM), were obtained from Molecular Probes Inc.

Chemicals were dissolved in ASW or modified ASW and introduced to the cells in the solution bathing cells or dissolved in a carrier solution (100mM KAsp, 10mM HEPES, PH 7.0) and injected into the photoreceptors via air pressure pulses.

Photoreceptors were impaled with blunt glass micropipettes containing injection solutions. In some experiments, another blunt electrode was introduced into the cells for injections of a second substance. The injection method was pulse-pressure injection. A single such injection will introduce a 1-10 pl solution into the cells (Corson & Fein, 1983). For voltage clamp studies, the cells were impaled with a second sharp electrode containing 3M KCl and were clamped at the resting potential. Data was collected by a CODAS data acquisition board in a personal computer with a sampling rate of 1K HZ and high pass filtered to reduce the noise level (455 HZ for voltage trace, 177 HZ for current trace)

Fluorescence measurements and calibration

Most measurements were performed using Zeiss confocal microscopes. For ANTS measurements a Zeiss LSM410 with UV excitation was used. ANTS is excited by After reflected by a dichroic mirror (FT395), the 364 nm laser beam from an Ar laser (Innova Technologies), is focused onto the cell by a 40X objective (Zeiss, 40X, Neofluar, NA 0.75) to excite the cells and ANTS. Before collection, the resulting fluorescence was filtered by a 505 nm long pass filter (Ukhanov and Payne, 1995a). For those Ca²⁺ indicators, a Zeiss LSM510 and a 40X oil lens (Zeiss, NA: 1.3) were used for measurements. They were excited by a 488 nm laser line from an Argon laser. Before reaching the specimen, the laser beams for excitation first went through

a primary beam splitter (HFT488/543). Also, the emitted fluorescence was filtered by a 505nm long pass filters before being collected by a photomultiplier tube.

In experiments where both FM4-64 and Dextran-fluo4 is used, the 488 nm laser served as an excitation source for both dyes. The fluorescence emitted from the samples was then encountered by a secondary beam splitter (HFT635). After passing a 505~530 nm band pass filter, the fluorescence reflected from HFT635 is collected as the signal from the binding of Dextran fluo4 to Ca^{2+} ions (Ca^{2+} channel); while the fluorescence that went through HFT635 splitter was further filtered by a 650 nm long pass filter before it was collected as FM4-64 signal (Membrane channel).

Besides the line-scan mode (see methods of Chapter 3), two other modes were used. Spot scan: The laser beam is kept stationary on a pre-selected focal spot (an ellipsoid with a diameter of $5 \times 1 \mu\text{m}$) (Ukhanov and Payne, 1995). The resulting fluorescence is collected by the photomultiplier of the confocal microscope. The highest sampling rate of this method is less than two microseconds, so this method is used for tasks that need high temporal resolution. Frame scans (X-Y scans): The laser beam performs X-Y scans across a selected area to collect fluorescence from the entire region. In this mode, each X scan at one Y position is a single line scan. To finish one frame scan, the laser beam needs to go through all the lines at each Y position. It usually takes one or two hundred milliseconds to collect one single image of *Limulus* ventral photoreceptors. Therefore this method is used to obtain most detailed spatial information about the Ca^{2+} signals with a price of losing most temporal information.

Dye calibration:

External calibration — (affinity) k_d of Fluo-5N: Fluorescence was measured by a conventional epiillumination system for ratio-fluorescence microscopy (Deltascan; PTI Inc., South Brunswick, NJ). Solutions (PH 7.0) containing 1 μ M dye, 400 mM KCl, 10 mM HEPES and various $[Ca]_i$ were used to check their fluorescence. The k_d is then decided from the $[Ca]_i$ -fluorescence curve (Ukhanov et al., 1995). The K_d of Fluo-5N got from this method is 500 μ M.

In vivo calibration — determining $[Ca]_i$: Fluorescence was measured by a Zeiss LSM 410 laser scanning confocal microscope. In such measurements, depth resolution was 5 μ m at 488 nm and 7 μ m using the 364 nm laser beam). The stationary spot and line scan mode were chosen because they have higher time resolution. In spot scan mode, the sampling rate is 125 KHZ. In the line scan mode, fluorescence was sampled along a pre-selected line, composed by 512 points, at the rate of 4 ms per line. The fluorescence trace was then integrated at suitable intervals for the convenience of display

Carrier solution that contains 10 mM of the Ca-insensitive dye ANTS and 1 mM Fluo-5N was pressure injected into cells. The ratio (R) of 488 nm fluorescence from Fluo-5N to 360 nm fluorescence from ANTS was determined after subtraction of the appropriate backgrounds. Using equation $[Ca]_i = K_d \cdot (R - R_{min}) / (R_{max} - R)$, $[Ca]_i$ was then estimated by comparing this ratio to that of the minimum (R_{min}) and maximum ratios

(R_{\max}) determined in droplets containing 1 μM Calcium Green-5N, 100 μM ANTS and either 10 mM EGTA or 10 mM CaCl_2 , placed on a microscope cover slip glass. (Ukhanov & Payne, 1995).

Simultaneous recording of electrical signal and fluorescence signal were done as described previously (Ukhanov & Payne, 1995).

Data collection: The laser beam sweeps back and forth along a pre-selected line. The resulting fluorescence of each spot along this line is collected so that the fluorescence change with time across this line can be obtained.

Analysis and Simulations

All analysis and simulations described below were accomplished through a combinational use of Matlab, SigmaPlot, and Image J

Measurement of the speed of the initial and the later spread of Ca^{2+} signal

Depending on the affinity of the dye used in experiments, two methods were used to measure the speed of spread of the Ca^{2+} signal.

High affinity dyes were used in most of our experiments. To avoid distortions caused by dye saturation, we use the spread of the first reliably detectible fluorescence

increase to define the speed of the spread. For a line scan image obtained either through experiment or through simulations, as described below, the time taken for the ratio between increased and resting fluorescence (F and F_0) at a given point to exceed a criterion value of 2 was used to calculate the speed. A curve relating distance from the microvillar membrane to this time was then constructed.

In some experiments, a low affinity dye was used to get a better understanding of the Ca^{2+} signal. In these experiments, F_0 was so small that it was too noisy to obtain a good fit using the above method. Instead of using $F/F_0=2$, we therefore used the half maximum width of the fluorescence signal to define the speed of spread of Ca^{2+} signal. Here F_{max} is the maximal fluorescence of each corresponding line image obtained at certain time.

Model of IP_3 diffusion within the R-lobe

To explain the initial spread of the light induced Ca^{2+} signal in the presence of large amount of slow moving Ca^{2+} buffer, a model of IP_3 diffusion within the R-lobe was made. The model of the R lobe is sphere with a radius of 30 μm , divided into 1 μm hypothetic shells (Fig 1). All properties of the rhabdomeral membrane or the cytoplasm of the R lobe are considered to be uniform (table 1)

Table1: Contents of the R lobe assumed for modeling

Parts	Contents	Source
	6e5 microvilli ①	Brown and Coles, 1979
The rhabdomeral membrane	Diameter: 0.1 μm , length: 1.5 μm 3% of the lipids of inner layer of the membrane of the microvillus are PIP_2 molecules	Clark et al., 1969 Zinkler et al., 1985; Hardie et al., 2001
	Phospholipase C	assumed
	IP_3 diffuses ($D=74 \mu\text{m}^2/\text{s}$) through a uniform cytoplasm	assumed
The cytoplasm	Enough IP_3 5-phosphatase uniformly distributed in the cytoplasm to hydrolyze IP_3	assumed
	IP_3 molecules are hydrolyzed with a time constant of 50ms	assumed

① In simulations, the shape and the volume of the microvilli were not considered.

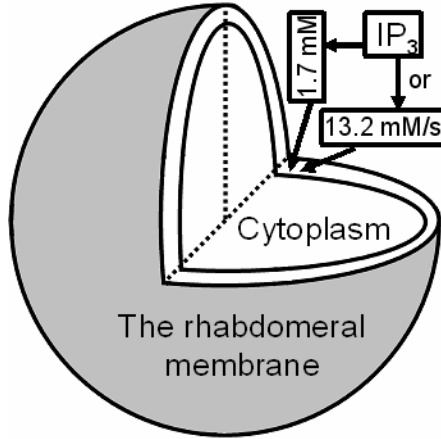


Figure 1: The model of the R lobe and the generation of the IP₃ molecules. The R lobe is a sphere that has a radius of 30 μm. The sphere is cut open to show its structure and contents. The gray surface of the R lobe is the rhabdomeral membrane, and the white content of the R lobe is its cytoplasm. The cytoplasm is divided into 1 μm hypothetical shells. During simulations, all IP₃ molecules will be produced in the outmost shell of the R lobe in the following two ways: either the simulation starts with [IP₃] = 1.7mM and there is no more IP₃ production, or the simulation starts with [IP₃] = 0 mM, and IP₃ is produced with a rate of 13.2 mM/s for 100ms.

Equations: According to Fick's first law, for a given shell inside the cytoplasm:

$$\text{Its influx (j}_i\text{) or efflux (j}_e\text{) is } \mathbf{j = D \cdot A \cdot \frac{\partial C}{\partial x}} \quad (1)$$

Where A is the surface area between two shells, 'C' is [IP₃], x is position.

$$\text{The hydrolysis rate of [IP}_3\text{] (K}_h\text{) is } \mathbf{K_h = - \frac{C}{\tau}} \quad (2)$$

Where C is $[IP_3]$, τ is the time constant of the hydrolysis of IP_3 molecules.

The rate of net concentration change (K_c) in this given shell caused by net flux and hydrolysis of IP_3 can then be calculated

$$K_c = \frac{j_i - j_e}{Vol} - K_h \quad (3)$$

Where Vol is the volume of the shell.

The Euler method was used to integrate these equations so as to calculate the $[IP_3]$ in any given shell at any given time.

Relating the diffusion of IP_3 to the Ca^{2+} release and the spread of Ca^{2+} signal shown by fluorescent dyes. With all the following assumptions and facts, the speed of the initial spread of the Ca^{2+} signal can be determined in terms of the velocity with which a threshold $[IP_3]$ spreads into the interior of the R lobe. The ER network (Feng et al., 1994) of the R lobe, including the distribution of IP_3 receptors (Ukhanov et al., 1998) and Ca^{2+} stores, is assumed to be uniform. IP_3 molecules diffuse ($D = 74 \mu m^2/s$) from the outermost shell into the interior of the R lobe. As diffusion proceeds, Ca^{2+} ions will be released if an $[IP_3]$ threshold is exceeded. In the presence of excess injected Dextran fluo4, the released Ca^{2+} ions are assumed to be detectable immediately after their release and are then assumed to be immobilized. The diffusion coefficient (D) of Dextran fluo4 in the cytoplasm is assumed to be negligible.

Model of IP_3 induced Ca^{2+} release and diffusion within the R-lobe

To explain the initial spread of the light induced Ca^{2+} signal under normal conditions, a model of IP_3 diffusion was modified into a model of a diffusion -reaction-diffusion type. Firstly, after $[\text{IP}_3]$ reached threshold in a given shell, Ca^{2+} ions would release after a delay of 17 ms (Ukhanov et al., 1995). Secondly, the observed release rate of light induced Ca^{2+} signal in the outermost shell was used as the maximal rate of Ca^{2+} release, K , in other shells. Thirdly, after opening, IP_3Rs remain open during the entire period of simulation. They do not inactivate, nor are they affected by Ca^{2+} ions. The rate of increase of Ca^{2+} (K_r) in one given shell is given by equation (4)

$$K_r = \frac{K \cdot C \cdot dt}{(C + 7.5 \cdot \text{thr})} \quad (4)$$

Where ‘thr’ is the threshold $[\text{IP}_3]$ to release Ca^{2+} ions, ‘C’ is the concentration of IP_3 in one given shell, and the value of ‘7.5·thr’ is an estimate of the affinity of IP_3 molecules to IP_3Rs , obtained by multiplying the threshold $[\text{IP}_3]$ by 7.5. Thirdly, once released, Ca^{2+} ions were assumed to diffuse freely through the cytoplasm ($D=217 \mu\text{m}^2/\text{s}$, see Chapter 3 for details). There was no buffering, uptake or extrusion of Ca^{2+} ions during simulation. Except the above modifications, all the other assumptions, parameters of this model are the same as those in the model of IP_3 diffusion. Therefore, by combining equation (2) with equation (4), and using the same approach as those used in the model of IP_3 diffusion, the $[\text{Ca}]_i$ in any given shell can be calculated at any given time.

Results

The light-induced calcium signal originates at the plasma membrane.

The plasma membrane of ventral photoreceptors was visualized by bathing the cells in ASW containing 100 μM FM4-64, as described in Methods. Fluorescent Ca^{2+} signals were recorded from cells injected with an excess amount of 5 mM Dextran fluo4, so as to maximize the fluorescent Ca^{2+} signal and minimize Ca^{2+} diffusion from release sites. Confocal line scans across the R lobe of dark-adapted photoreceptors were initiated, and the resulting Dextran fluo4 and FM4-64 fluorescence were recorded simultaneously.

Regions of the cell periphery that displayed a high intensity of FM4-64 staining were presumed to be microvillar in nature, since the surface area of the microvillar membrane is 10-fold greater than that of non-microvillar plasma membrane (Fig. 2) (Brown and Coles, 1979). The half-maximum width of the fluorescence from these regions was $1.7 \pm 0.1 \mu\text{m}$ ($n=7$), consistent with the length of microvilli in electron micrograph images ($1.5 \mu\text{m}$, Clark et al., 1969)

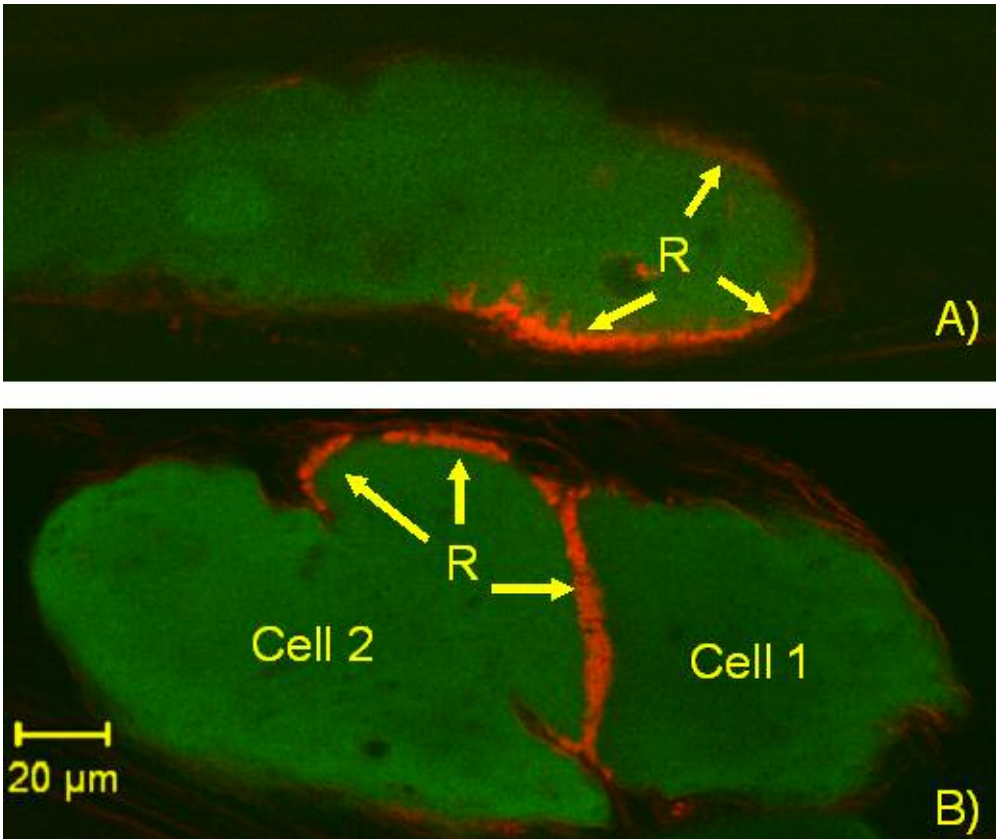


Figure 2. The staining of rhabdomeral membrane by FM4-64 in several typical cells. The fluorescence signal from the plasma membrane is shown by FM4-64 (red), and the positions of assumed rhabdomeral membrane (R) are indicated by arrows, whereas the cytoplasmic volume is shown by fluorescence of injected Dextran fluo4 (Green). A) Typical cell with a distinct R lobe. B) Parts of the R lobe from two different cells are piled together

Following the onset of the line-scan stimulus, Ca^{2+} signals originated from areas adjacent to rhabdomeral membranes with a latency of 15 ± 6 ms ($n=5$). The spatial profiles of Ca^{2+} signals, averaged during the first 10ms of the response overlapped the spatial profiles of FM4-64 staining, with the two peaks of fluorescence located $1.4 \pm$

0.3 μm apart (n=6) (Fig 2). Considering the 1.5 μm length of microvilli (Clark et al., 1969) and the 0.45 μm optical resolution of the microscope, this result is consistent with the Ca^{2+} signal originating at the base of the microvilli.

Smaller Ca^{2+} signals with longer latency (70 ± 16 ms, n= 5) were also observed to originate at regions of the cell periphery that that were stained by FM4-64 with very low intensity. We do not know whether these regions represent secondary rhabdomeral-lobes or some previously unreported light-sensitivity of the non-microvillar membrane.

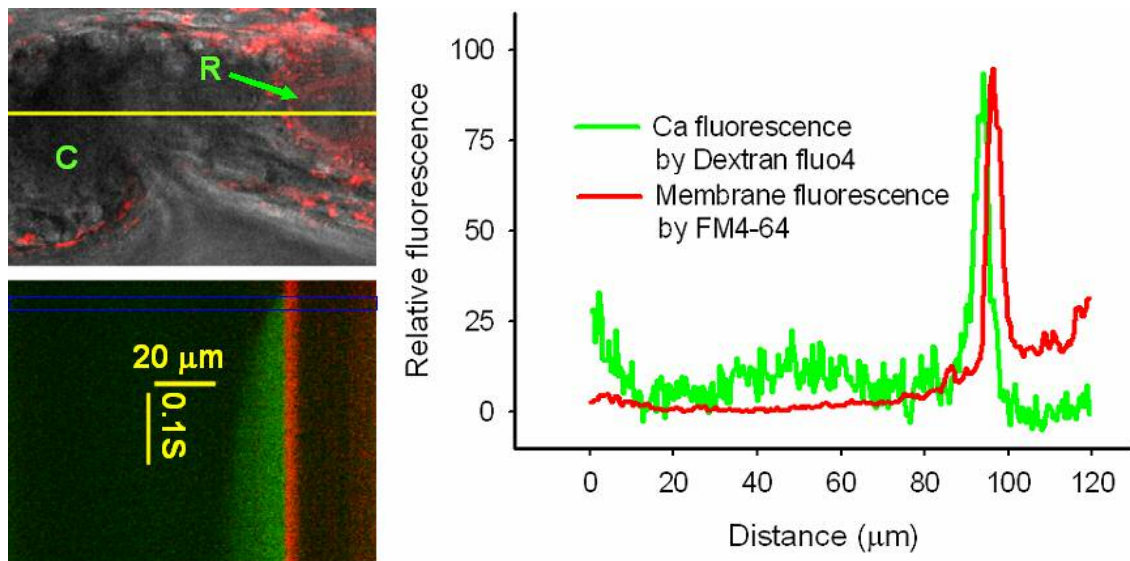


Figure 3. The distance between onset spots of Ca^{2+} release and the rhabdomere membrane. A) The upper image: part of one cell that shows the position of the rhabdomeral membrane (the curved line of red fluorescence indicated by the arrow) and that of the line scan (yellow line). “C” represents the cytoplasm of the cell. The bottom image: The corresponding line scan image of the above cell during excitation. Red: FM4-64 fluorescence shows the position of the rhabdomere membrane where it intersects with the line scan; Green: Dextran fluo4 fluorescence shows the temporal-spatial pattern of light-induced Ca^{2+} release. The higher the fluorescence, the brighter the color is. B) The distance between the initial Ca^{2+} release and the rhabdomere membrane. Plots were obtained from the temporal average of the corresponding fluorescence signals within the blue box (10 ms) shown in Figure A. Red curve: FM4-64 signal; Green curve: Dextran fluo4 signal. The distance between the two peaks is considered to be the distance between the rhabdomere membrane and the initial site of Ca^{2+} release spot. It was 2.3 μm in this cell.

The Ca²⁺ signal beneath the microvillar membrane rises to its peak with a similar time course to that of the light-induced electrical signal

Using a similar method as described by Ukhanov and Payne (1995), Ca²⁺ signals were measured at their points of origin using spot scans and the low affinity dye Fluo-5N ($K_d = 500 \mu\text{M}$) (See methods for details).

The latency and time to peak of the Ca²⁺ signal is similar to that of the electrical signal: The latency of the Fluo-5N signal was 16 ± 3 ms (n=5), reaching its peak after 82 ± 8 ms. The latency and time-to-peak and delay times for the accompanying receptor potentials were 30 ± 6 ms and 70 ± 10 ms and respectively (n=5) (Fig. 4A). We found no significant difference between the latencies or times-to-peak of the Ca²⁺ signals and the electrical response. (p>0.16; Paired T test, n=5).

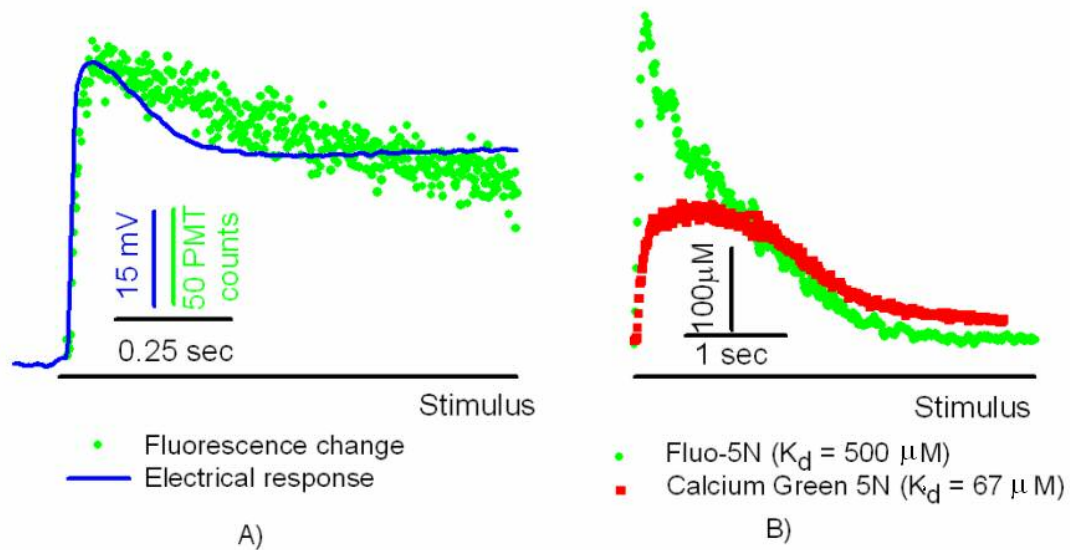


Figure 4: The timing and amplitude of light-induced Ca^{2+} signal in typical cells in response to a spot scan. The black bar beneath represents the light stimulus. The laser light intensity is around $\sim 10^8$ effective photons per sec. A) The latency and time to peak of the light-induced Fluo-5N signal (the green dotted trace) is similar to that of the electrical signal (the blue line). The fluorescence signal from Fluo-5N is shown as arbitrary photon-multiplier tube counts. In this cell, both the onset and time-to-peak of Fluo-5N precede those of receptor potential by one millisecond. B) The amplitude of the light-induced Ca^{2+} signal shown by dyes with different affinity in two typical cells. When measured with Fluo-5N in one cell, there is no plateau and the $[\text{Ca}]_i$ reaches its peak ($400 \mu\text{M}$) within 200ms and then decays with a time constant of 1 sec. Whereas the $[\text{Ca}]_i$ shown by Calcium Green 5N (Ukhanov & Payne, 1995) bears a plateau and its peak amplitude is smaller ($150 \mu\text{M}$)

The peak amplitude of Light-induced Ca²⁺ signal is as high as 300 μM: Our previous estimate of Ca²⁺ peak using the middle affinity dye Calcium Green 5N (k_d=67 μM) was approximately 150 μM, with a very broad peak, more like a plateau ((Fig 3B; Ukhanov & Payne, 1995)). There is no plateau in the calcium signal measured with Fluo-5N: right after the Ca²⁺ signal reaches its peak, it begins to decrease immediately (Figure 3B). Moreover, the Ca²⁺ peak shown by Fluo-5N is 300 ± 55 μM (n = 7; Fig. 3A), almost doubles the size of our previous measurements. This discrepancy in the time course and calculated amplitude of Ca²⁺ signals determined by Fluo-5N and Calcium Green 5N, is expected if Ca²⁺ release is localized to confined spaces within the confocal spot where Calcium Green 5N saturates (Tillotson and Nasi, 1998).

Similarly large Ca²⁺ transients have been observed in other cell types, but they are shorter lasting and more spatially confined. In the micro-domain of squid giant synapses (diameter: 0.5 μm), the peak Ca²⁺ transient caused by Ca²⁺ influx is also around 300 μM but lasts less than 20 ms (Silver et al., 1994). In the rhabdomeres (packed microvilli) of *Drosophila* photoreceptors, the peak amplitude of the C signal is estimated as 600 μM, lasting for less than 500 ms (Oberwinkler & Stavenga, 2000). The prolonged Ca²⁺ signal that spreads over a large region of the R-lobe of *Limulus* ventral photoreceptors therefore appears to be unique. We therefore decided to investigate the mechanism of its propagation.

The Ca²⁺ signal spreads into the interior of the cell in two phases.

To examine the spread of light-induced Ca^{2+} signals, dyes with different affinities and different methods for calculating the speed of the spread were used. Similar to previous reports (Ukhanov and Payne, 1995), all results show a two-phase spreading. The light-induced Ca^{2+} signal initiates from the edge of the cell (Fig. 3), spreads within 200 ms up to 40-50 μm into the cell interior following which there is little further spread while $[\text{Ca}]_i$ remains elevated for several seconds (Fig. 5 and table 2).

The existence of the two-phase spread of the Ca^{2+} signal is not dependent on the criterion $[\text{Ca}]_i$ or the dye used to measure the spread.

The high affinity of Fluo-4 ($K_d = 2 \mu\text{M}$) makes it suitable to catch small Ca^{2+} signals. Therefore, Fluo-4 was used to follow the leading edge of the Ca^{2+} signal as it spreads. The leading edge was defined as the point at which F/F_0 exceeds a criterion of 2. The results show that for the first $154 \pm 17 \text{ms}$ of Ca^{2+} release ($n=7$) the Ca^{2+} signal spreads $20 \pm 4 \mu\text{m}$ into interior of the cell with a square-root speed, V , of $81 \pm 7 \mu\text{m/s}^{0.5}$. After this, the value of V slows down to $26 \pm 3 \mu\text{m/s}^{0.5}$. This slower phase of spread continues for several seconds.

The low affinity dye, fluo-5N, was used to estimate the spread of the $\frac{1}{2}$ maximal fluorescence signal. During the first $114 \pm 38 \text{ms}$ ($n=6$) of Ca^{2+} release, the Ca^{2+} signal spreads about $11 \mu\text{m}$ into interior of the cell with a speed of $39 \pm 5 \mu\text{m/s}^{0.5}$. After this, the spread slows down to a speed of $15.5 \pm 2.4 \mu\text{m/s}^{0.5}$. This slower phase also lasts for seconds.

To test whether the light-induced Ca^{2+} entry has any role in this two phase spreading, the spread of Ca^{2+} signals in cells loaded with fluo-4 and bathed in 0 Ca^{2+} ASW with 2mM EGTA was measured. In 0 Ca^{2+} ASW, the speed ($85 \pm 12 \mu\text{m}/\text{s}^{0.5}$), duration ($159 \pm 53 \text{ms}$) and distance ($22 \pm 2 \mu\text{m}$) of the initial spread is no different to cells bathed in normal ASW ($p > 0.5$, T-test, $n=5$). Similarly, the speed of the later spread ($24 \pm 5 \mu\text{m}/\text{s}^{0.5}$) is also unaltered. This indicates that the spread of the light-induced Ca^{2+} signal is independent of light-induced Ca^{2+} entry, consistent with the previous finding that the light-induced Ca^{2+} release is from ER Ca^{2+} stores (Ukhanov and Payne, 1995).

In order to control for the possibility that the rapid initial spread of the Ca^{2+} signal was related to rapid diffusion of Ca-loaded dye, cells were loaded with a small quantity of Dextran fluo4 by 2-5 pressure injections. Dextran fluo4 diffuses slowly inside *Limulus* ventral photoreceptors ($23 \mu\text{m}^2/\text{s}$, see Chapter 3 for details). We also co-labeled these cells with FM4-64 so as to make sure that the scan line ran perpendicular to the rhabdomeral membrane and that no infoldings of the rhabdomeral membrane existed along the scan line that could initiate Ca^{2+} signals deep within the R-lobe. Under these conditions, the speed of the initial spread of the Ca^{2+} signal was measured as $67 \pm 8 \mu\text{m}/\text{s}^{0.5}$ ($n=9$) (Fig. 8). This result is not significantly different from the value obtained using fluo4. Therefore the rapid spread of the Ca^{2+} signal in the presence of fluo-4 cannot be ascribed to diffusion of the

measuring dye or due to Ca^{2+} signals initiated from infoldings of the plasma membrane.

Table 2. The initial and later spread of light-induced Ca^{2+} signal shown by different Ca^{2+} indicator dyes.

Methods	Dyes used	N	Initial spread			Later
			V ($\mu\text{m}/\text{s}^{0.5}$)	Duration (ms)	Distance (μm)	spread V ($\mu\text{m}/\text{s}^{0.5}$)
Half maximum width	Fluo-5N	6	39±5	114±38	9±1	15.5±2.4
	Calcium Green 5N	4	62±18	157±48	14±2	10.8±5.2
	Calcium Green 5N	4	88±9	151±28	17.3±0.	3.3±5
F / F ₀ =2				4		
	Fluo4	7	81±7	154±17	19±6	26±3
	Dextran fluo4	9	67±8	163±18	17±2	20±3

The initial spread of the light-induced Ca^{2+} signal might be determined by the diffusion of both Ca^{2+} ions and IP_3 molecules.

The rapid phase of spread is not a regenerative calcium wave.

Pulsed pressure injection of Ca^{2+} (2 mM) or IP_3 (1mM) into dye-loaded cells did not initiate propagating Ca^{2+} waves that traveled through the R-lobe cytosol. Calcium

signals elicited by these injections were decremental and confined to the immediate surround of the injection site (Data not shown). In addition, the light-induced Ca^{2+} signal does not have the characteristics of a typical Ca^{2+} wave. As the light-induced Ca^{2+} signal measured with fluo-5N spread into the interior of the cell, both its amplitude and speed decreased (Fig. 5). Moreover, the spread of the leading edge of the light-induced Ca^{2+} signal has a characteristic typical of diffusion: The distance over which the fluorescence exceeds a criterion value is better fit by a square root rather than a linear function of the time elapsed after the initiation of the signal (Fig. 5D). We therefore used distance divided by the square root of time as the “speed” (V) to describe the spread.

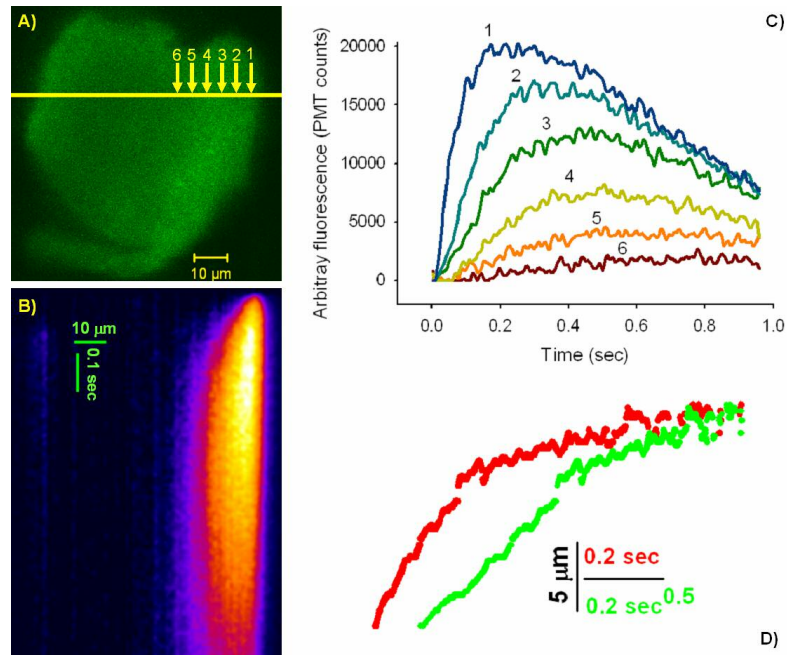


Figure 5. The rapid phase of the two-phase spread of light-induced Ca^{2+} signal is a diffusion driven process A) Image of the cell showing the position of the line scan (yellow line). The first arrow (1) indicates the position where the Ca^{2+} release originates. B) A typical line scan image that shows the two-phase spread of the light-induced Ca^{2+} signal in A). C) The increase of fluorescence with time in different locations of the photoreceptor (arrows in Figure A). The more interior the position of the spot is, the slower the rate of rise of the fluorescence and the smaller the maximum fluorescence. The distance between two adjacent measurement positions is $4.5 \mu\text{m}$. C) The spread of a criteria fluorescence intensity into the interior of the R lobe with time (t) plotted on two scales. Red trace is a plot of x vs. t ; while the Green trace is the plot of x vs. $t^{0.5}$. For the initial spread, it is clear that $x/t^{0.5}$ is constant. This is a typical characteristic of a diffusion driven process. The slope, $x/t^{0.5}$, defines the “speed” of the diffusion front, V .

This diffusion driven process cannot be explained by simple diffusion of one single substance like free Ca^{2+} ions or IP_3 molecules. Similar to previous reports (Allbritton et al., 1992), the D of free Ca^{2+} ions in the R-lobe was estimated to be $217 \mu m^2/s$ (see Chapter 3). We constructed a simple, spherical model of the R-lobe ((see methods) which ignored calcium buffering or uptake in the cytoplasm. Ca^{2+} ions are released only at the outmost $1 \mu m$ shell of our model cell at a rate that replicates the rate of rise of $[Ca]_i$ under the microvillar membrane in our spot scan measurements (Fig. 4). With these conditions, the fastest speed of spread of the Ca^{2+} signal, determined by half maximum width, $10 \mu m/s^{0.5}$, is still much lower than that of the experimental values ($39 \pm 5 \mu m/s^{0.5}$). The speed of spread would diminish further due to the reduced mobility of Ca^{2+} ions in a more realistic model that included buffering or uptake of Ca^{2+} ions in the cytoplasm. These calculations indicate that Ca^{2+} release is unlikely to be confined to within the immediate vicinity of the microvillar membrane.

An obvious development of our model is to include the diffusion and calcium-releasing action of IP_3 . We distributed Ca^{2+} stores uniformly throughout the R-lobe and allow diffusion of IP_3 from the rhabdomeral membrane to propagate the Ca^{2+} signal deep into the cell. There is solid experimental evidence both for a continuous network of ER within the R-lobe that can release Ca^{2+} in response to IP_3 (Feng et al. 1994, Ukhanov & Payne, 1997). We first considered whether diffusion of IP_3 alone could account for the rapid spread of the Ca^{2+} signal. We constructed a simple model (see Methods) in which the flash instantaneously hydrolyzed all of the PIP_2 in the

microvillar membrane so as to produce a calculated initial IP₃ concentration in the outmost shell of 1.71 mM of a spherical R-lobe. No hydrolysis of IP₃ occurs and IP₃-release is assumed to initiate detectable Ca²⁺ release at a threshold concentration of 0.01 μM. Under these conditions the speed of spread, V, of the resulting Ca²⁺ signal would only be predicted to reach (45 μm/s^{0.5}). Thus the diffusion of IP₃ molecules alone is also insufficient to explain the fast spread of the Ca²⁺ signal. The diffusion of both IP₃ and mobile Ca²⁺ ions released at high concentrations at sites throughout the R-lobe may therefore be required.

An excess amount of a slowly-moving Ca²⁺ buffer slows down but does not eliminate the rapid phase of spread.

In order to experimentally investigate the role of IP₃ and Ca²⁺ diffusion in the spread of the Ca²⁺ signal we injected cells with an excess of the fluorescent calcium indicator Dextran fluo4. As well as being a calcium indicator, Dextran fluo4 is a slow moving, high affinity Ca²⁺ buffer ($k_d=0.77$ μM, $D=23$ μm²/s). If it is able to effectively buffer Ca, a high cytoplasmic concentration of Dextran fluo4 should minimize the elevation of the light-induced Ca²⁺ and the diffusion of Ca²⁺ ions. Under these conditions, we would expect diffusion of IP₃ alone would dominate the spread of the Ca²⁺ signal and we could then test the predictions of our simple model of IP₃ diffusion.

We first demonstrated the effectiveness of dextran-fluo4 as a Ca²⁺ buffer. Like other Ca²⁺ buffers, when injected into *Limulus* photoreceptors, Dextran fluo4 is able to

greatly desensitize the electrical response to dim light and eliminate the peak-plateau response transition to bright light (n=4, Fig. 6) (Lisman and Brown, 1975). Given this physiological evidence that Dextran fluo4 effectively buffered calcium during the light response, we investigated the spread of the Ca^{2+} signal after injection of an excess of Dextran fluo4.

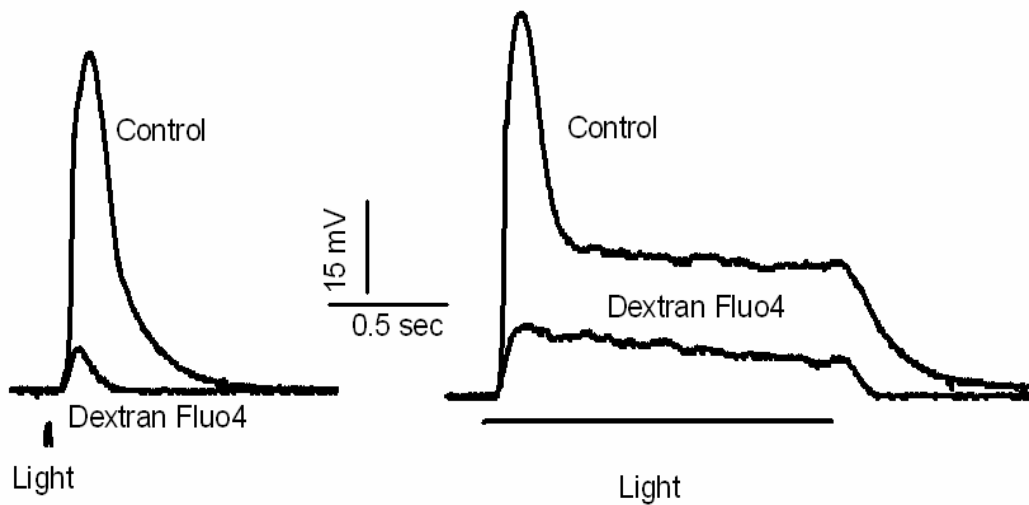


Figure 6. Injection of Dextran fluo4 desensitizes the electrical response to dim light and eliminates the peak-plateau response transition to bright light in one typical cell. The cell was loaded by 9 injections of 1mM Dextran fluo4. A) The electrical response to dim flashes ($-3.5 \log_{10}$ unit) was greatly inhibited by Dextran fluo4 injections. B) The peak-plateau response transition in response to strong flashes ($-2.0 \log_{10}$ unit) was abolished by Dextran fluo4 injections.

As noted above, 2-5 injections of Dextran fluo4 had little effect on the initial speed of spread of the Ca^{2+} signal. However, injection of more dye slowed the speed of the

initial spread from $67 \pm 8 \mu\text{m}/\text{s}^{0.5}$ to $32 \pm 3 \mu\text{m}/\text{s}^{0.5}$, ($p=0.0002$, T test, $n=19$) (27-36 injections were injected, creating an estimated final dye concentration of 300-2000 μM). The duration of the initial rapid spread $171 \pm 15\text{ms}$, however, was not significantly different from that of controls. As a result, the distance of the initial spread decreased from $17 \pm 2 \mu\text{m}$ ($n=8$) to $8 \pm 1 \mu\text{m}$ ($n=9$) (Fig. 7).

This result demonstrates that the abrupt slowing down of the spread of the Ca^{2+} signal as it enters its second phase is not due to a physical barrier placed at a fixed distance from the rhabdomeral membrane or due to a reduction in the density of Ca^{2+} stores and IP_3 receptor proteins.

Excess Dextran fluo4 also decreased the speed of the slow phase from $20 \pm 3 \mu\text{m}/\text{s}^{0.5}$ to $7 \pm 1 \mu\text{m}/\text{s}^{0.5}$ ($n=10$, T-test, $p=0.001$) (Fig6. B). This would be consistent with the later phase of spread being dominated by the diffusion of buffered Ca^{2+} ions alone.

The decrease in the speed of both phases of spread in the presence of an excess of Dextran fluo4 is consistent with a role for Ca^{2+} ions in both phases of the Ca^{2+} signal.

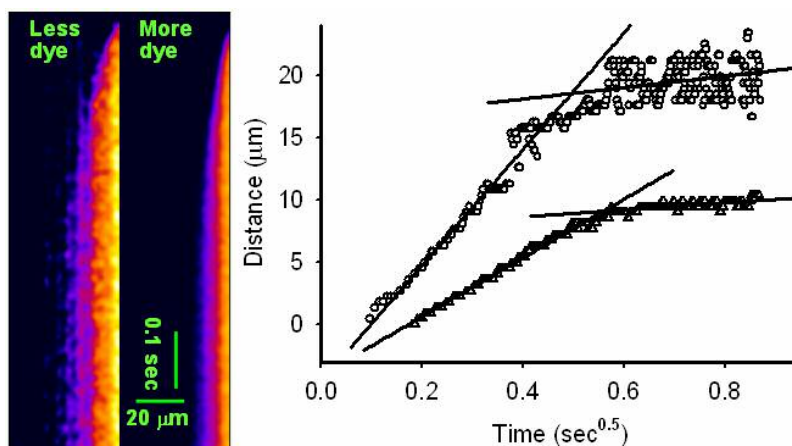


Figure 7. Injection of excess amount of Dextran fluo4, a high affinity Ca^{2+} buffer, decreases the speeds of both the fast and slow spread. A) Figure on the left: Line scan image of the R lobe of one ventral photoreceptor loaded with less dye. Figure on the right, same line scan at the same position of the cell after more dye is loaded. To make a direct comparison between these two line scan images possible, their background fluorescence were scaled to the same value. The pseudo-colors in both figures have the same scale. The higher the concentration of Ca^{2+} is, the brighter the fluorescence. B) The movement of the light-induced fluorescence that is two folds of the background fluorescence ($F/F_0=2$). It is obtained from the contour of $F/F_0=2$ from images in A). Open circles, the spreading of light-induced fluorescence increase when the cell is loaded with low concentration of dye. Open triangles, light-induced signals in the same cell filled with high concentration of dye. Black lines are the linear fitting of the initial/late spreads part of corresponding curves. The intercepts of the fittings are the speeds of the spreads. When the above cell is loaded with less dye, the speed of the initial spread is $47 \mu\text{m}/\text{s}^{0.5}$. After more dye is injected into the cell, the speed decreases to $23 \mu\text{m}/\text{s}^{0.5}$. Similarly, more Dextran fluo4 injection reduces the speed of the later spread from $6 \mu\text{m}/\text{s}^{0.5}$ to $3 \mu\text{m}/\text{s}^{0.5}$.

The diffusion of IP₃ molecules also contributes to the fast initial spread

The initial spread of the light-induced Ca²⁺ signal in the presence of excess Dextran fluo4 is also a diffusion driven process.

In the presence of excess dextran-fluo4, the Ca²⁺ signal still spreads quite rapidly. We wished to determine whether spread under these conditions might be entirely explained by diffusion of IP₃ from the plasma membrane.

We first verified that the spread of the light-induced Ca²⁺ signal in the presence of Dextran fluo4 had the characteristics of a diffusion driven process. We found this to be the case: As the Ca²⁺ signal spreads into the interior of the cell, both its amplitude and the rate of [Ca]_i increase decrease. And there is a linear relationship between the square root of the time elapsed and the distance over which the fluorescence exceeds a criterion value

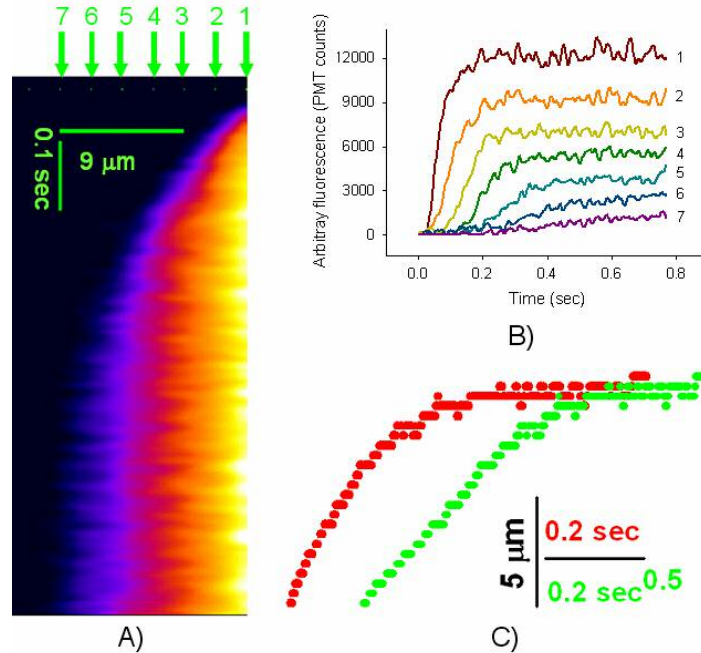


Figure 8. The spread of the light-induced Ca^{2+} signal has the characteristics of a diffusion driven process. A) A typical line scan image that shows the two-phase spread of the light-induced Ca^{2+} signal. The first Arrow indicates the position where the Ca^{2+} release starts. B) The increase of fluorescence with time in different locations of the photoreceptor. The more interior of the position of the spot is, the slower the rise rate of fluorescence and the smaller the maximum fluorescence is. The locations are indicated by numbers and their positions are shown by arrows in figure A), the distance between two adjacent positions is $2.25 \mu\text{m}$. C) The spread (x) of arbitrary fluorescence intensity into the interior of the R lobe with time (t) plotted on two scales. Red trace is the direct plot of $x-t$; while the Green trace is the plot of $x-t^{0.5}$. For the initial spread, it is clear that $x/t^{0.5}$ is equal to a constant. This is a typical characteristic of a diffusion driven process. The slope, $x/t^{0.5}$, defines the “speed” of the diffusion front, V . When cells are loaded with large amount of Dextran fluo4, $V = 35 \pm 5 \mu\text{m}/\text{s}^{0.5}$ ($n=10$).

The speed with which the Ca^{2+} signal spreads in the presence of excess Dextran fluo4 may be explained by simple diffusion of IP_3 from the rhabdomeral membrane to activate high-affinity receptors in the R-lobe cytoplasm. Given the evidence that the rapid spread of the calcium wave is diffusive and is quite resistant to an excess of Dextran fluo4, we constructed a simple model of IP_3 release and diffusion within the R-lobe in the presence of excess Dextran fluo4. The main assumptions of this model are that an extremely high concentration of IP_3 , in the mM range, is generated beneath the microvillar membrane and that the threshold of IP_3 receptors (IP_3Rs) uniformly distributed in the cytoplasm is comparatively very low, in the μM range. Also, the IP_3 molecules are hydrolyzed fast ($\tau = 50ms$). If IP_3 molecules are produced with a constant speed and its threshold to release Ca^{2+} ions is in the range of $0.1\sim 1 \mu M$, the experimental values of the speed and the duration of the initial spread can be approximately accounted for (Fig. 9). It is therefore possible that simple diffusion of IP_3 is responsible for the spread of light-induced Ca^{2+} signal in the presence of excess Dextran fluo4.

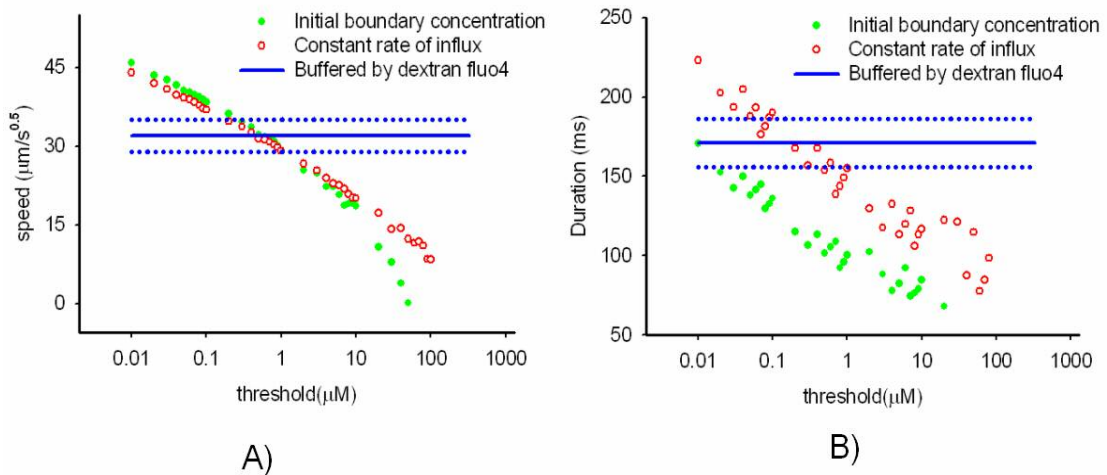


Figure 9. The simulated dependence of the speed, V , and duration of the initial spread of the Ca^{2+} signal on the dynamics of the release of IP_3 and the threshold of IP_3 receptors. Red and green curves are simulation results, while blue lines are the mean and SE of experimentally determined values measured in cells loaded with excess of Dextran fluo4. For details of the simulations, see the Methods section. A) The dependence of V on the dynamics of the release of IP_3 and the threshold of IP_3R . B) The dependence of the duration of the initial spread on the dynamics of the release of IP_3 and the threshold of IP_3R . The results show that no matter how the IP_3 molecules are released, the smaller the threshold criterion for Ca^{2+} release, the larger the V and the longer the duration are. If IP_3 molecules are produced at a constant rate, and the threshold $[\text{IP}_3]$ to IP_3R is around $0.1\sim 1\ \mu\text{M}$, the experimental values can be explained by the diffusion of IP_3 only.

Injection of L-chiro- IP_3 increases the speed and duration of the rapid phase of spread.

We sought experimental evidence that diffusion of IP₃, limited by hydrolysis, is responsible for the spread of the Ca²⁺ signal in the presence of excess Dextran fluo4. L-chiro-I(1,4,6)PS₃ is a non-hydrolysable IP₃ stereoisomer that can act as an inhibitor of the enzyme, myo-Inositol 1, 4, 5-trisphosphate 5-phosphatase, that metabolizes I(1,4,5)P₃ to inactive I(1,4)P₂. The influence of L-chiro-Ins(1,4,6)PS₃ on the initial spread of Ca²⁺ signal was tested by introducing 30-40 injections of Dextran fluo4 (5mM) into cells with or without the addition of L-chiro-Ins(1,4,6)PS₃ (500 μM).

When compared with control cells that were only loaded with Dextran fluo4 (0.3~2mM), the speed and duration of the initial spread in the presence of L-Chiro-IPS₃ was significantly greater: 59 ±6 μm/sec^{0.5} vs 35±5 μm/sec^{0.5}; 245±19 ms vs 148±19 ms. As a result, the distance of the initial spread is prolonged by L-chiro-IPS₃ from 5±1 μm to 24±2 μm. However, the speed of the later slow phase of spread of the Ca²⁺ signal was not altered by L-Chiro-IPS₃: 16 ±3 μm/sec^{0.5} vs 12±1 μm/sec^{0.5} (P=0.17, T test) (Fig. 10).

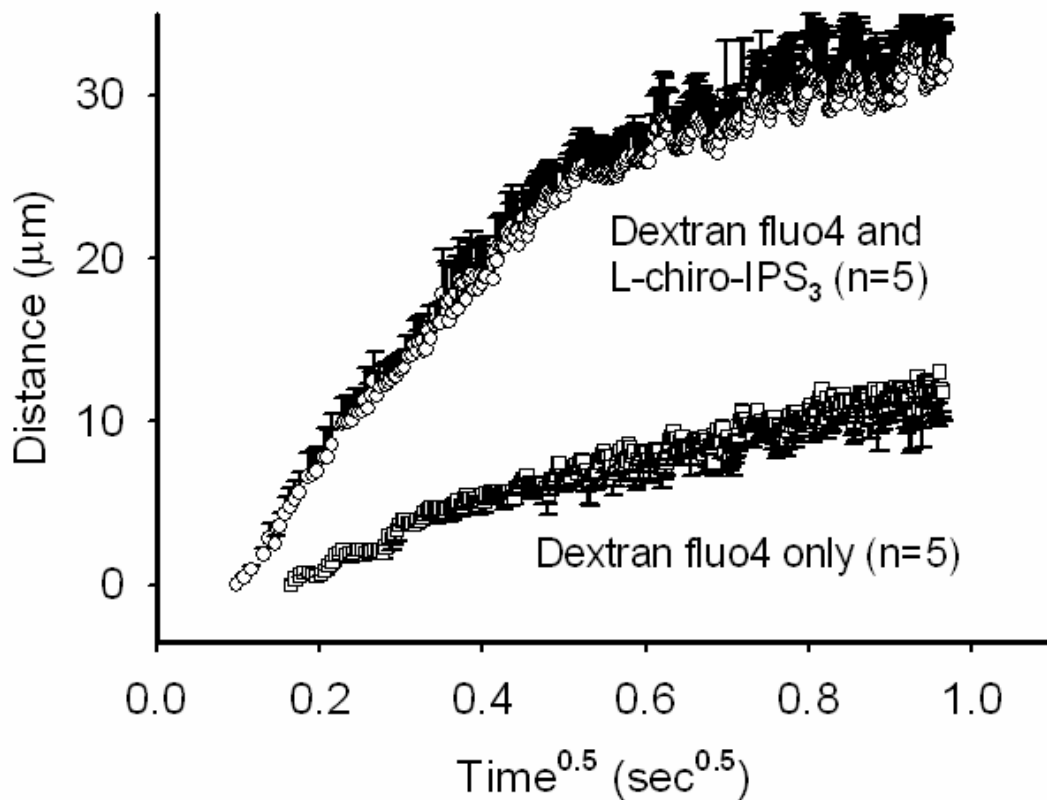


Figure 10. L-chiro-Ins(1,4,6)PS₃ prolonged the duration of the initial spread but didn't alter the speed of the later spread. After 30-40 injections of Dextran fluo4 (5mM) with L-chiro-Ins(1,4,6)PS₃ (500 μM) (open circles) or 30~40 injections of 5mM Dextran fluo4 (open squares) into *Limulus* ventral photoreceptors, the spread of light-induced Ca²⁺ signals were then obtained as described in methods.

Thus L-chiro-Ins(1,4,6)PS₃, which might be expected to prolong the lifetime of Ins(1,4,5)P₃, also prolongs the duration of the initial phase of spread and its speed. The speed of the later phase of spread remains unchanged. This is consistent with the participation of the diffusion of IP₃ in the initial spread of the light-induced Ca²⁺

signal. The later phase of spread is not affected, consistent with it being due to the much slower diffusion of buffered calcium ions alone.

The diffusion of both IP₃ molecules and Ca²⁺ ions is sufficient to explain the speed and duration of the rapid phase of spread.

The above results indicate both the diffusion of Ca²⁺ ions and IP₃ molecules are necessary for the initial spread. Therefore the initial spread might be determined by a diffusion-reaction-diffusion process: As the light-induced IP₃ diffuses, it will release Ca²⁺ ions from intracellular stores once a threshold concentration is reached. The released Ca²⁺ ions then diffuse to the interior of the cell. To test whether this model is sufficient for the initial spread, several parameters in the model of IP₃ diffusion were modified to generate a model that includes diffusion of Ca²⁺ ions released by IP₃. Firstly, after [IP₃] reaches threshold Ca²⁺ ions are released after a delay of 17 ms (Ukhanov et al., 1995). Since the peak light-induced Ca²⁺ signal is as high as 300 μM and Ca²⁺ ions will diffuse freely at these concentrations (Allbritton, 1992), Ca²⁺ ions were assumed to diffuse freely through the cytoplasm (D=217 μm²/s, see Chapter 3 for details). All the other assumptions and parameters are the same as those in the model of IP₃ diffusion (see methods for details).

We calculated the expected speed of the ‘wave’ front of the Ca²⁺ signal using a criteria [Ca]_i of 2 μM, with a threshold [IP₃] for Ca²⁺ release of approximately 0.1~1 μM, the corresponding predicted V values, will fall within the range of 62 ~ 69

$\mu\text{m/s}^{0.5}$. This agrees well with experimental data measured by Dextran fluo4 ($67 \pm 8 \mu\text{m/s}^{0.5}$, $n=9$). Similarly, the predicted V values, measured by half maximum fluorescence, falls within the range of $26 \sim 33 \mu\text{m/s}^{0.5}$. This also agrees with results from Fluo-5N measurements. Therefore, diffusion of IP_3 molecules followed by the release and diffusion of Ca^{2+} ions at high concentration is sufficient enough to predict the observed V of the initial spread.

In summary, in response to a light stimulus, IP_3 molecules are continuously produced from the rhabdomeral membrane until depletion of PIP_2 molecules or end of stimulus. As IP_3 molecules diffuse into the interior of the cell with a D of $74 \mu\text{m}^2/\text{s}$, they will bind to IP_3Rs on the ER membrane. If the $[\text{IP}_3]$ exceeds a threshold of $0.1 \sim 1 \mu\text{M}$, IP_3Rs will open after a delay of 17 ms and release Ca^{2+} with a rate of 4.34 mM/s . The released Ca^{2+} will spread into the interior of the cell with a D of $217 \mu\text{m}^2/\text{s}$. At the beginning, the spread of IP_3 signal precedes that of the Ca^{2+} signal due to its earlier start. Later, because of its higher D value, the fast traveling IP_3 -induced Ca^{2+} signal will bypass that of the IP_3 signal and lead the spread of the Ca^{2+} signal (Fig 11).

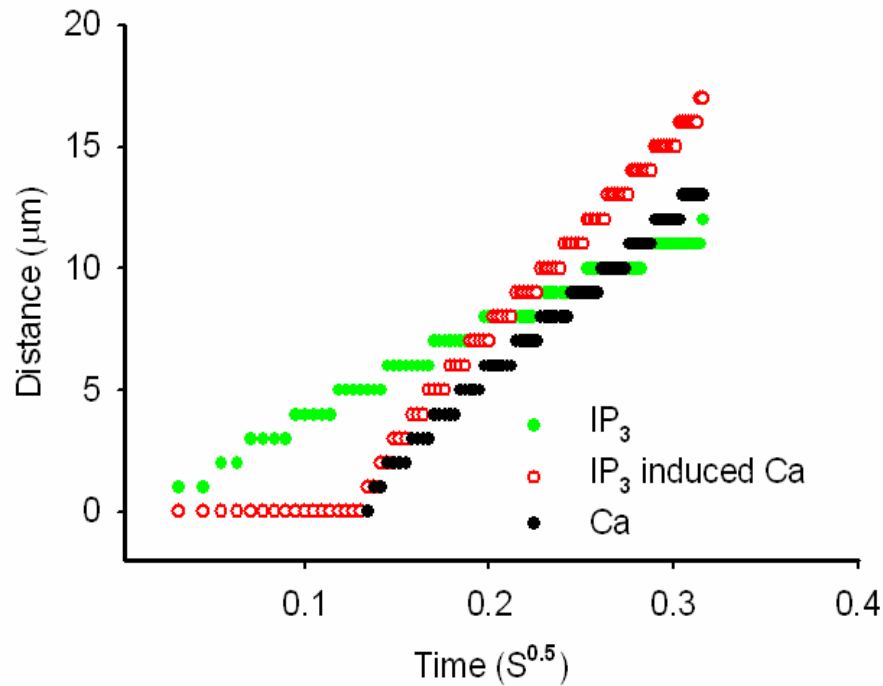


Figure 11. The diffusion of IP₃ and IP₃-induced Ca²⁺ ions speeds up the spreading of Ca²⁺ signal. Two simulations were represented in this figure. The first simulation is one example from the model IP₃-induced Ca²⁺ signal: IP₃ molecules are produced with a constant speed (13.2 mM/s), and they are hydrolyzed with a time constant of 50ms. As IP₃ molecules diffuse into the interior of the cell, if [IP₃] is equal to or above 0.2 μM (green dotted curve), Ca²⁺ ions will be released with a rate of 4.34 mM/s. The released Ca²⁺ ions then diffuse with a D value of 217 μm²/s (red circles). The criteria [Ca]_i used to describe the V of spread is 2 μM. The V of threshold [IP₃] and [Ca]_i is 36 and 66 μm/s^{0.5} respectively. The second simulation is the diffusion of free Ca²⁺ ions from the outmost shell of the model cell (black dots). The delay and release kinetics of Ca²⁺ ions are the same as those in the outmost shell of the first model. There is no Ca²⁺ release in shells other than the outmost one, and the criteria [Ca]_i used to describe its V of spread is also 2 μM.

Discussion

The light induced Ca^{2+} release was directly shown to originate at the rhabdomeral membrane of the R lobe. Consistent with its role in mediating light responses, the Ca^{2+} signal at its origin rises to its peak with a similar time course to that of the light-induced depolarization. The initial fast spread of the light induced Ca^{2+} signal from originating locations is a diffusion driven process, since its amplitude decreased as it spread into the cell. Moreover, the distance over which the fluorescence exceeds a criterion value is better fit by a square root rather than a linear function of the time elapsed after the initiation of the signal (Fig. 5D).

Simulations indicate this fast spread can not be explained by the simple diffusion of Ca^{2+} or that of IP_3 , thus the diffusion of both molecules are necessary for the fast spread. The contribution of the diffusion Ca^{2+} ions to the initial spread can be shown by effects of varying its apparent D values. Under normal conditions, the peak $[\text{Ca}]_i$ in response to an intense flash is approximately 300 μM . This is probably high enough to saturate endogenous Ca^{2+} buffers and enable Ca^{2+} ions to diffuse freely ($D=217 \mu\text{m}^2/\text{s}$, see chapter 3, Allbritton, 1992). Minimizing the diffusion of Ca^{2+} ions by buffering the Ca^{2+} signal through the injection of excess slow moving Ca^{2+} buffer, Dextran-fluo4, can slow down the fast initial spread.

The additional contribution of IP_3 diffusion to the fast phase is indicated by three lines of evidence. Firstly, excess Dextran fluo4 failed to eliminate the existence or

duration of the fast initial spread. Secondly, the reduced speed of the fast phase in the presence of excess Dextran fluo4 may be explained by a model of simple diffusion of IP_3 from the rhabdomeral membrane to activate high-affinity receptors in the R-lobe cytoplasm. Thirdly, prolonging the life span of IP_3 through L-chiro-I(1,4,6)PS₃ injections can increase the duration of the initial fast spread. Therefore, the diffusion of IP_3 also contributes to the initial fast spread. Simulations indicate that diffusion of IP_3 and Ca^{2+} released by IP_3 is sufficiently rapid to determine the initial fast spread of the intense light induced Ca^{2+} signal.

The spread range of excitation induced absorption of one single photon or dim light might be determined by the diffusion of IP_3 molecules only

After single photon excitation, how far can the threshold $[IP_3]$ spread? Calcium signals following single photons have not so far been measured in *Limulus* ventral photoreceptors. For a dim flash, delivering 50 effective photons the peak amplitude for the light-induced elevation of $[Ca]_i$ has been measured as 5 μM . The peak amplitude of a single photon calcium signal might therefore be reasonably expected to be $<1 \mu M$ (Payne and Demas, 2000). At this concentration, Ca^{2+} ions should be well buffered (Allbritton, 1992) and thus IP_3 ($D = 74 \mu m^2/s$) will lead the spread of the Ca^{2+} signal. Assuming all possibly available IP_3 molecules in one microvillus are produced simultaneously as a point source and that the same range of threshold $[IP_3]$ is assumed to induce Ca^{2+} release as those of our model (0.1~1 μM), a simple calculation of IP_3 diffusion predicts the radius of the excitation induced by absorption

of one photon as $1 \sim 2.2 \mu\text{m}$. According to results in chapter 2 and earlier measurements by Brown and Coles (1979), saturation of the photocurrent starts to occur when the number of effective photons exceeds approximately 200. Assuming the R lobe is a half sphere with a radius of $30 \mu\text{m}$, then 200 effective photons corresponds to a mean distance between photoisomerizations on the surface of the R-lobe of approximately $2 \mu\text{m}$. At this density, therefore, we predict that significant overlap of $[\text{IP}_3]$ generated by neighboring photoisomerisations will occur so as to mediate competition for calcium release sites.

Both the diffusion of IP_3 molecules and that of Ca^{2+} ions participate in the spreading of light induced excitation.

When the intensity of the light stimulus is high, more Ca^{2+} ions are released, and saturation of the endogenous Ca^{2+} buffers occurs. Thus Ca^{2+} ions will diffuse freely ($D=217 \mu\text{m}^2/\text{s}$, see chapter 3) inside the photoreceptors (Allbritton, 1992). Therefore, the fast traveling IP_3 induced Ca^{2+} ions lead the spread of the Ca^{2+} signal and the following excitation. This faster diffusion of Ca^{2+} ions may lead to the acceleration of the onset of the light response observed with increasing flash intensity by Payne and Fein (1986) and Grzywacz et al. (1988).

Ca^{2+} waves might not be appropriate for the spreading of the light induced Ca^{2+} signal

In response to a strong stimulus, global Ca^{2+} signals are generated in many kinds of cells. These usually propagate across the cell in the form of regenerative waves (Berridge, 1997; Bootman et al., 2001). However, the *Limulus* ventral photoreceptor seems to rely on diffusion alone. The reason for this difference may lie in the special needs of photoreceptor function. First, as a sensory receptor, one primary function is to detect the amplitude of the stimulus. Amplitude is coded as a graded increase in the number of channels activated. This is not a function that is well served by a regenerative calcium wave. Once a threshold is reached, a propagating regenerative Ca^{2+} wave will yield no information about light intensity, and therefore it is not helpful as an intensity detector. Second, Ca^{2+} waves are usually slow (Berridge and Irvine, 1989; Jaffe FL, 1991) and required for Ca^{2+} signals that travel long distances (Berridge MJ, 1997; Bootman et al., 2001), while the light induced Ca^{2+} signals only needs to travel a couple of microns (see above sections). For these short distances, our simulation results indicate the diffusion of IP_3 molecules is fast enough.

The functional significance of the large peak $[\text{Ca}]_i$

The peak amplitude of the light induced Ca^{2+} signal is $300 \pm 55 \mu\text{M}$ ($n = 7$; Fig. 3A).

What is the possible role of this unusually high $[\text{Ca}]_i$?

Since Ca^{2+} mediates excitation, a high $[\text{Ca}]_i$ might be needed to excite the photoreceptor. When excess Ca^{2+} buffer, Dextran fluo4, is injected into the cytoplasm, the dim light induced light response is greatly inhibited (Fig. 6). Similarly,

other manipulations that inhibit $[Ca]_i$ increase, including depletion of Ca^{2+} stores, inhibition of Ca^{2+} release and injection of the Ca^{2+} buffers, greatly reduce the amplitude of light induced current (see introduction for details). A high $[Ca]_i$ might not be a requirement for the 2-APB-insensitive (DAG and Ca^{2+} -mediated) component of the phototransduction pathway, but it might be necessary to excite the 2-APB-sensitive (Ca^{2+} -mediated) component (see Discussion, Chapter 2).

Secondly, a high $[Ca]_i$ might be necessary for rapid light adaptation of the cell. Higher $[Ca]_i$ can decrease the sensitivity of the cell to light more effectively (Lisman and Brown, 1975, Levy and Fein, 1985, see introduction for details), allowing the cell to release less Ca^{2+} in response to subsequent illumination and to recover faster.

Thirdly, a high $[Ca]_i$ might be needed for the fast spread of Ca^{2+} signals across the R-lobe. A direct result of high $[Ca]_i$ is the saturation of the endogenous Ca^{2+} buffers, thus Ca^{2+} ions will diffuse freely inside the photoreceptors (Allbritton, 1992). An increased spread of the light induced Ca^{2+} signal along the plasma membrane might allow more channels to be activated by Ca^{2+} during single photon responses, The consequence of the rapid spread of the Ca^{2+} signal into the interior of the cell is unknown.

General discussion – are there two parallel photo-transduction cascades?

To get a better understanding of the photo-transduction cascade, the light induced Ca^{2+} release was studied with the help of an IP_3 receptor inhibitor, 2-APB. Although 2-APB was not a specific blocker of IP_3 induced Ca^{2+} release, the complexity of its inhibitory effect on the light induced current at various light intensities may indicate the existence of two parallel photo-transduction cascades.

Currently, there are two proposed mechanisms for the light induced current in *Limulus* ventral photoreceptors. One uses DAG-activated TRPC channels, although a simultaneous small Ca^{2+} increase may also be required to activate this pathway (Bandyopadhyay and Payne, 2004). The other proposed pathway is Ca^{2+} -mediated. Although the events downstream of Ca^{2+} release in the second pathway are not very clear, there is some evidence that Ca^{2+} -mediated activation of guanylyl cyclase produces cGMP so as to open cGMP gated channels on the plasma membrane (Bacigalupo et al., 1991; Chen et al., 2001, Garger, et al., 2001, 2004). My results indicate that these two proposed mechanisms might co-exist in the same photoreceptor.

A DAG-Ca²⁺ mediated TRPC channels might serve as the light- and 2-APB-insensitive pathway.

What are the expected features of the DAG-Ca²⁺ pathway? Firstly, the DAG branch has fewer steps of amplification during the signal transduction cascade. This would be expected to result in a lower gain that makes it less suitable for detecting dim stimuli. Secondly, the diffusion of DAG in the plasma membrane is expected to be slower than that of IP₃ molecules and Ca²⁺ ions in the cytoplasm. The effect of DAG is therefore most likely confined to a small area within or adjacent to the excited microvillus. Thirdly, inward current induced in *Limulus* ventral photoreceptors by the DAG analog, OAG, appears to require a simultaneous increase of [Ca²⁺]_i in the micro-molar range (6~8 μM, Bandyopadhyay and Payne, 2004). Such relatively small Ca²⁺ signals are believed to be local signals that spread slowly (Allbritton et al., 1992). The simultaneous requirement for two diffusible messengers from two different mediums and locations may further restrict the area that could be activated by a single photon via the DAG- Ca²⁺ pathway.

The above three characteristics restrict the number of channels that could be activated by one effective photon. The DAG-Ca²⁺ pathway therefore would be expected to have a low gain, suitable for detecting high light intensities. If only a few channels surrounding a microvillus, carrying 1-3pA each, open in response to a single photon, the current through this pathway will be a very small fraction of the observed 1-2nA single-photon events (Johnson et al., 1991; Bacigalupo et al., 1991).

The second and third feature of the DAG- Ca^{2+} branch predicts a restricted area of excitation induced by one single photon. If some DAG mediated channels are located adjacent to open IP_3Rs , then according to Fein (2003), the relatively low $[\text{Ca}^{2+}]_i$ necessary to open the channel may make the pathway resistance to store depletion, exogenous calcium buffers or 2-APB.

Experimental observations are consistent with the above two predictions.

First, the light induced current in the presence of 2-APB begins to saturate when more than 10^5 effective photons are absorbed (Chapter 2; Fig. 10), in the same range as the total number of microvilli found in a typical ventral photoreceptor ($6 \cdot 10^5$, Brown and Coles, 1979). This is consistent with excitation from neighboring photon hits only overlapping when neighboring microvilli are excited and so it is consistent with a limited spread of excitation beyond a microvillus. Second, if the maximal current (~ 517 nA) in the presence of 2-APB is divided by the total number of effective photons, then the current passing through one single microvillus may be estimated as approximately 1 pA. This value is similar to the amplitude of current that passes through one single light activated channel (~ 1 or 3 pA, Bacigalupo et al., 1991). Therefore, it is possible that only one DAG mediated channel is associated with one microvillus. Under these conditions one effective photon would induce a current of approximately 1 pA through the proposed DAG- Ca^{2+} -sensitive channel associated with a microvillus and therefore single photon events will become negligible.

Therefore, as predicted by our DAG-Ca²⁺ hypothesis, the gain of this DAG-Ca²⁺ branch is very low.

Therefore, this DAG-Ca²⁺ pathway, mediated by TRPC channels, might be the light- and 2-APB-insensitive component of the light response in *Limulus* ventral photoreceptors.

An IP₃-Ca²⁺-cGMP pathway might be the 2-APB and light sensitive pathway.

Unlike the DAG-Ca²⁺ pathway, the IP₃-Ca²⁺ branch is expected to have the following features. Firstly, unlike DAG, the fast spread of IP₃ molecules and Ca²⁺ ions in the cytoplasm (see chapter 3.) makes it possible to activate many ion channels on the plasma membrane. Secondly, this pathway has more steps of signal transduction. This enables higher amplification of the signal, thus making it suitable for sensing dim stimuli.

Both of the above two features would predict high gain and a large area activated by one effective photon. Experimental evidence is consistent with these predictions. Firstly, the 2-APB-sensitive single-photon gain of approximately 1nA/effective photon is 1000 higher than that of the DAG-Ca²⁺ branch. Secondly, we predict from our diffusion measurements that one effective photon could activate an area with a radius of 2 μm if all of the IP₃ within a microvillus were hydrolyzed (See chapter 4, first paragraph on page 120). If we assume the R lobe is a half sphere with a radius of 30 μm and it has the estimated average number of microvilli ($6 \cdot 10^5$, Brown and

Coles, 1979), then the spread of the single photon excitation mediated by Ca^{2+} would activate 1333 microvilli on average. Therefore, in response to a single effective photon, both the gain and the excitation area mediated by the $\text{IP}_3\text{-Ca}^{2+}$ branch is 1000 times larger than those mediated by DAG-Ca^{2+} branch. Since the single channel conductance of light induced channels is similar (10 & 40 ps, Bacigalupo et al., 1991) and DAG mediated channels may be localized within microvilli, this suggests that Ca^{2+} mediated channels, most likely cGMP gated channels, might also be localized within microvilli.

The fact that Ca^{2+} release is located upstream of this signal transduction cascade makes this approach more sensitive to fluctuations in $[\text{Ca}^{2+}]_i$. Therefore, as observed, the inhibition by 2-APB on IP_3 -induced Ca^{2+} release, store depletion, or introduction of exogenous Ca^{2+} buffers, have a significant effect on channel opening.

Therefore, this $\text{IP}_3\text{-Ca}^{2+}$ branch, perhaps mediating the activation of cGMP channels, might be the light and 2-APB sensitive pathway component of the light response in *Limulus* ventral photoreceptors.

This two-branch hypothesis can be easily tested by the testing the effect of genetic or pharmacological manipulations of TRPC channels. Since there are no specific TRPC channel inhibitors available and the long life span of *Limulus* makes mutation of channel proteins not applicable, one possible approach is to reduce the expression of channel proteins using the interference RNA technique (RNAi). TRPC RNAi can be

injected into the photoreceptors and suppress the expression of TRPC channels. If the two-pathway hypothesis is correct, then a decrease in the expression level of TRPC channels will not affect the amplitude of single photon events, but current induced by intense light would be significantly reduced. Current induced by IP₃ injection would also not be predicted to be affected by reducing TRPC expression. On the contrary, the current induced by injection of OAG and Ca²⁺ in the μM range would be significantly reduced. If all these above predictions are proven to be true, then there do exist two signal transduction cascades in *Limulus* ventral photoreceptors: a DAG-TRPC branch and a Ca²⁺ mediated pathway. Then this will be the first known photoreceptor that that has two photo-transduction cascades

If further experimental evidence proves that cGMP gated channels are the final activation step of the Ca²⁺ mediated pathway, then the ventral photoreceptor of *Limulus* has a light sensitive cGMP pathway and a light insensitive TRPC branch. The first one is common for vertebrates while the latter is used mostly by invertebrates (See chapter 1 for details). Therefore, the *Limulus* ventral photoreceptor could provide some hints about the evolution of photoreceptors. It is possible that both of these two cascades existed in ancestor photoreceptors. During evolution, different eye structure and signal transduction cascades of photoreceptors evolved according to the environment and animal behavior. *Limulus* ventral photoreceptors keep both these two mechanisms to survive in habitats with large luminance variations: the ocean floor (darker environments) and open sand (brighter circumstances).

Signal transduction complexes in microvilli bridged by IP₃ receptors in the cytoplasm?

For *Drosophila*, a flying diurnal insect, higher amplification and better light sensitivity are not necessary. Instead, quick light responses are needed. The photoreceptors of *Drosophila* have evolved at least two strategies to meet this need: all machinery required for a single photon response is packed into a single microvillus and the machinery for photo-transduction is believed to form a complex (Hardie and Raghu, 2001). These two arrangements reduce messenger loss caused by diffusion and speed up the light response by shorting the diffusion distance between steps of photo-transduction. Therefore, the light response in *Drosophila* photoreceptors is fast and efficient.

For the slow moving, nocturnal *Limulus*, a fast light response is not necessary. On the contrary, higher amplification or light sensitivity is required to enable *Limulus* to survive in the dark. Besides adopting larger photoreceptors and longer microvilli to collect photons more efficiently, the ventral photoreceptors of *Limulus* also use IP₃, a faster diffusible messenger, and a cascade with more amplifying stages to fulfill this need. IP₃ molecules and Ca²⁺ ions travel further so as to excite more light-sensitive channels. As a result, the delay and the amount of messenger loss become significant. Our simulation results indicate that the diffusion of all possibly available IP₃ molecules from one microvillus itself is enough to explain the experimentally observed spread of the light induced excitation. Therefore, it is likely that the

microvilli in *Limulus* ventral photoreceptors serve as discrete reservoirs of IP₃ molecules: all the machineries required to generate IP₃ molecules are localized within the microvilli (chapter 1), so that high enough [IP₃] can be achieved beneath the plasma membrane of photoreceptors.

However, although more time is needed both for IP₃ molecules to travel further and for those steps that lead to the opening of channels after Ca²⁺ release, the light induced current follows the first detectable Ca²⁺ release within only a few milliseconds (Ukhanov, et al., 1995, chapter 4). This indicates that the machinery downstream of Ca²⁺ must be really close to each other, or a multi-molecular complex is formed. This is consistent with previous reports about the close vicinity between ER and that of the plasma membrane of photoreceptors (Clark et al., 1969; Calman and Chamberlain, 1982; Feng J et al., 1994) and our finding that Ca²⁺ release originates at the rhabdomeral membrane. The close spatial-temporal relationship between Ca²⁺ release and light activated channels indicates that the photo-transduction machinery downstream of Ca²⁺ might be packed together, localized beneath or on the plasma membrane. The upstream components, by contrast, are confined within microvilli, just like those in *Drosophila*. By this arrangement, *Limulus* ventral photoreceptors can get enough gain to sense dim light, and at the same time, time delays and messenger dilution are minimized downstream.

REFERENCE

- Acharya, J.K., Jalink, K., Hardy, R.W., Hartenstein, V., Zuker, C.S. InsP₃ receptor is essential for growth and differentiation but not for vision in *Drosophila*. *Neuron* 1997; 18: 881-887.
- Allbritton NL, Meyer T, Stryer L. Range of messenger action of calcium ion and inositol 1,4,5-trisphosphate. *Science*. 1992, 258(5089):1812-5
- Arrio-Dupont M, Cribier S, Foucault G, Devaux PF, d'Albis A. Diffusion of fluorescently labeled macromolecules in cultured muscle cells. *Biophys J*. 1996; 70(5):2327-32.
- Atri A, Amundson J, Clapham D, Sneyd J. A single-pool model for intracellular calcium oscillations and waves in the *Xenopus laevis* oocyte. *Biophys J*. 1993; 65(4):1727-39
- Axelrod D, Koppel DE, Schlessinger J, Elson E, Webb WW. Mobility measurement by analysis of fluorescence photobleaching recovery kinetics. *Biophys J*. 1976; 16(9):1055-69
- Bacigalupo J, Johnson EC, Vergara C, Lisman JE. Light-dependent channels from excised patches of *Limulus* ventral photoreceptors are opened by cGMP. *PNAS*. 1991; 88(18):7938-42
- Baimbridge KG, Celio MR, Rogers JH. Calcium-binding proteins in the nervous system. *Trends Neurosci*. 1992; 15(8):303-8.
- Bandyopadhyay BC, Payne R. Variants of TRP ion channel mRNA present in horseshoe crab ventral eye and brain. *J Neurochem*. 2004; 91(4):825-35
- Battelle BA, Dabdoub A, Malone MA, Andrews AW, Cacciatore C, Calman BG, Smith WC, Payne R. Immunocytochemical localization of opsin, visual arrestin, myosin III, and calmodulin in *Limulus* lateral eye reticular cells and ventral photoreceptors. *J Comp Neurol*. 2001; 435(2):211-25.
- Baylor DA, Lamb TD, Yau KW. The membrane current of single rod outer segments. *J Physiol*. 1979; 288:589-611.
- Baylor SM, Hollingworth S. Fura-2 calcium transients in frog skeletal muscle fibres. *J Physiol*. 1988, 403:151-92. Erratum in: *J Physiol (Lond)* 1988; 407:616.
- Berridge MJ. Inositol trisphosphate and calcium signaling. *Ann N Y Acad Sci*. 1995; 766:31-43.

- Berridge MJ. Elementary and global aspects of calcium signalling. *J Physiol.* 1997; 499: 291-306
- Blatter LA, Wier WG. Intracellular diffusion, binding, and compartmentalization of the fluorescent calcium indicators indo-1 and fura-2. *Biophys J.* 1990; 58(6):1491-9.
- Bloomquist BT, Shortridge RD, Schneuwly S, Perdew M, Montell C, Steller H, Rubin G, Pak WL. Isolation of a putative phospholipase C gene of *Drosophila*, *norpA*, and its role in phototransduction. *Cell* 1988; 54(5): 723-33.
- Bolsover, S.R. and Brown, J.E. Calcium ion, an intracellular messenger of light adaptation, also participates in excitation of *Limulus* photoreceptors. *Journal of Physiology* 1985; 364: 381-393.
- Bootman MD, Berridge MJ. The elemental principles of calcium signaling. *Cell.* 1995; 83(5):675-8.
- Bootman MD, Lipp P, Berridge MJ. The organization and functions of local Ca^{2+} signals. *J Cell Sci.* 2001; 114(Pt 12):2213-22
- Bootman MD, Collins TJ, Mackenzie L, Roderick HL, Berridge MJ, Peppiatt CM. 2-aminoethoxydiphenyl borate (2-APB) is a reliable blocker of store-operated Ca^{2+} entry but an inconsistent inhibitor of $InsP_3$ -induced Ca^{2+} release. *FASEB J.* 2002; 16(10):1145-50.
- Braun FJ, Aziz O, Putney JW Jr. 2-aminoethoxydiphenyl borane activates a novel calcium-permeable cation channel. *Mol Pharmacol.* 2003; 63(6):1304-11.
- Brink PR, Ramanan SV. A model for the diffusion of fluorescent probes in the separate giant axon of earthworm. Axoplasmic diffusion and junctional membrane permeability. *Biophys J.* 1985; 48(2):299-309.
- Brown EB, Wu ES, Zipfel W, Webb WW. Measurement of molecular diffusion in solution by multiphoton fluorescence photobleaching recovery. *Biophys J.* 1999; 77(5):2837-49.
- Brown, J.E., Blinks, J.R. Changes in intracellular free calcium concentration during illumination of invertebrate photoreceptors. Detection with aequorin. *J. Gen. Physiol.* 1974; 64: 643-665.
- Brown JE, Coles JA. Saturation of the response to light in *Limulus* ventral photoreceptor. *J Physiol.* 1979; 296:373-92.
- Brown JE, Lisman JE. An electrogenic sodium pump in *Limulus* ventral photoreceptor cells. *J Gen Physiol.* 1972; 59(6):720-33.

- Brown JE, Rubin LJ. A direct demonstration that inositol triphosphate induces an increase in intracellular calcium in *Limulus* photoreceptors. *Biochem. Biophys. Res. Commun* 1984; 125: 1137-1142.
- Brown JE, Rubin LJ, Ghalayini AJ, Tarver AP, Irvine RF, Berridge MJ, Anderson RE. *myo*-inositol polyphosphate may be a messenger for visual excitation in *Limulus* photoreceptors. *Nature* 1984; 311: 160-162.
- Bruins HR, Overhoff J, Wolff LK. The molecular weight of vitamin A. *Biochem J.* 1931; 25(2):430-8.
- Burgoyne RD, Weiss JL. The neuronal calcium sensor family of Ca²⁺-binding proteins. *Biochem J.* 2001; 353(Pt 1):1-12. Review. Erratum in: *Biochem J* 2001; 354(Pt 3):727.
- Calman BG, Chamberlain SC. Distinct lobes of *Limulus* ventral photoreceptors. II. Structure and ultrastructure. *J Gen Physiol.* 1982; 80(6):839-62
- Chen FH, Ukhanova M, Thomas D, Afshar G, Tanda S, Battelle BA, Payne R. Molecular cloning of a putative cyclic nucleotide-gated ion channel cDNA from *Limulus polyphemus*. *J Neurochem.* 1999; 72(2):461-71.
- Chen FH, Baumann A, Payne R, Lisman JE. A cGMP-gated channel subunit in *Limulus* photoreceptors. *Vis Neurosci.* 2001; 18(4):517-26.
- Chen Y, Muller JD, Berland KM, Gratton E. Fluorescence fluctuation spectroscopy. *Methods.* 1999; 19(2):234-52.
- Chorna-Ornan I, Joel-Almagor T, Ben-Ami HC, Frechter S, Gillo B, Selinger Z, Gill DL, Minke B. A common mechanism underlies vertebrate calcium signaling and *Drosophila* phototransduction. *J. Neurosci.* 2001; 21:2622-2629.
- Chyb S, Raghu P, Hardie RC. Polyunsaturated fatty acids activate the *Drosophila* light-sensitive channels TRP and TRPL. *Nature.* 1999; 397(6716):255-9.
- Clapham DE, Runnels LW, Strubing C. The TRP ion channel family. *Nat Rev Neurosci.* 2001; 2(6):387-96
- Clark, A.W., Millecchia, R., Mauro, A. The ventral photoreceptor cells of *Limulus*. I. The microanatomy. *J. Gen. Physiol.* 1969; 54: 289-309.
- Colton CK, Zhu MX. 2-Aminoethoxydiphenyl borate as a common activator of TRPV1, TRPV2, and TRPV3 channels. *Handb Exp Pharmacol.* 2007;(179):173-87.

- Contzen K, Nagy K. Current components stimulated by different G-proteins in *Limulus* ventral photoreceptor. *Neuroreport*. 1995; 6(14):1905-8
- Contzen K, Richter K-H, Nagy K. Selective inhibition of the phospholipase C pathway does not block the other components of the light activated current in *Limulus* ventral nerve photoreceptor. *J Comp Physiol*. 1995; 177:601-610
- Corson DW, Fein A. Quantitative pressure injection of picoliter volumes into *Limulus* ventral photoreceptors. *Biophys J*. 1983; 44(3):299-304
- Crank J. The mathematics of diffusion. Oxford, Clarendon Press, 1956, 28-29; 326-327.
- Dargan SL, Schwaller B, Parker I. Spatiotemporal patterning of IP₃-mediated Ca²⁺ signals in *Xenopus* oocytes by Ca²⁺-binding proteins. *J Physiol*. 2004; 556(Pt 2):447-61
- Dargan SL, Parker I. Buffer kinetics shape the spatiotemporal patterns of IP₃-evoked Ca²⁺ signals. *J Physiol*. 2003; 553(Pt 3):775-88
- Deckert A, Stieve H. Electrogenic Na⁺-Ca²⁺ exchanger, the link between intra- and extracellular calcium in the *Limulus* ventral photoreceptor. *J Physiol*. 1991; 433:467-82
- Deckert A, Nagy K, Helrich CS, Stieve H. Three components in the light-induced current of the *Limulus* ventral photoreceptor. *J Physiol*. 1992;453:69-96.
- Delmas P, Wanaverbecq N, Abogadie FC, Mistry M, Brown DA. Signaling microdomains define the specificity of receptor-mediated InsP(3) pathways in neurons. *Neuron*. 2002; 34(2):209-20.
- Digman MA, Brown CM, Sengupta P, Wiseman PW, Horwitz AR, Gratton E. Measuring fast dynamics in solutions and cells with a laser scanning microscope. *Biophys J*. 2005; 89(2):1317-27.
- Dorlochter M, Stieve H. The *Limulus* ventral photoreceptor: light response and the role of calcium in a classic preparation. *Prog Neurobiol*. 1997; 53: 451-515.
- Elson EL, Fluorescence correlation spectroscopy. I. Conceptual basis and theory. *Biopolymers*. 1974, 13: 1-27.
- Faddis, M.N., Brown, J.E. Flash photolysis of caged compounds in *Limulus* ventral photoreceptors. *J. Gen. Physiol*. 1992; 100:547-570.

- Faddis MN, Brown JE. Intracellular injection of heparin and polyamines. Effects on phototransduction in *Limulus* ventral photoreceptors. *J Gen Physiol.* 1993; 101(6): 909-31.
- Fain GL, Lisman JE. Membrane conductances of photoreceptors. *Prog Biophys Mol Biol.* 1981; 37(2):91-147
- Fein A. Inositol 1,4,5-trisphosphate-induced calcium release is necessary for generating the entire light response of *Limulus* ventral photoreceptors. *J Gen Physiol.* 2003;121(5):441-9.
- Fein A, DeVoe RD. Adaptation in the ventral eye of *Limulus* is functionally independent of the photochemical cycle, membrane potential, and membrane resistance. *J Gen Physiol.* 1973; 61(3):273-89.
- Fein, A., Payne, R., Corson, D.W., Berridge, M.J., Irvine, R.F. Photoreceptor excitation and adaptation by inositol 1,4,5-trisphosphate. *Nature* 1984; 311:157-160.
- Feng JJ, Carson JH, Morgan F, Walz B, Fein A. Three-dimensional organization of endoplasmic reticulum in the ventral photoreceptors of *Limulus*. *J Comp Neurol.* 1994; 341(2):172-83
- Feng JJ, Frank TM, Fein A. Excitation of *Limulus* photoreceptors by hydrolysis-resistant analogs of cGMP and cAMP. *Brain Res.* 1991; 552(2):291-4
- Finch EA, Augustine GJ. Local calcium signalling by inositol-1,4,5-trisphosphate in Purkinje cell dendrites. *Nature.* 1998; 396(6713):753-6.
- Frank TM, Fein A. The role of the inositol phosphate cascade in visual excitation of invertebrate microvillar photoreceptors. *J Gen Physiol.* 1991; 97(4):697-723.
- Frokjaer-Jensen C, Kindt KS, Kerr RA, Suzuki H, Melnik-Martinez K, Gerstbreih B, Driscoll M, Schafer WR. Effects of voltage-gated calcium channel subunit genes on calcium influx in cultured *C. elegans* mechanosensory neurons. *J Neurobiol.* 2006; 66(10):1125-39.
- Gabso M, Neher E, Spira ME. Low mobility of the Ca²⁺ buffers in axons of cultured *Aplysia* neurons. *Neuron.* 1997; 18(3):473-81.
- Garger A, Richard EA, Lisman JE. Inhibitors of guanylate cyclase inhibit phototransduction in *Limulus* ventral photoreceptors. *Vis Neurosci.* 2001; 18(4):625-32.

- Garger AV, Richard EA, Lisman JE. The excitation cascade of *Limulus* ventral photoreceptors: guanylate cyclase as the link between InsP_3 -mediated Ca^{2+} release and the opening of cGMP-gated channels. *BMC Neurosci.* 2004; 5(1):7
- Gordienko DV, Bolton TB, Cannell MB. Variability in spontaneous subcellular calcium release in guinea-pig ileum smooth muscle cells. *J Physiol.* 1998; 507 (Pt 3):707-20.
- Haeseleer F, Imanishi Y, Sokal I, Filipek S, Palczewski K. Calcium-binding proteins: intracellular sensors from the calmodulin superfamily. *Biochem Biophys Res Commun.* 2002; 290(2):615-23.
- Haggie PM, Stanton BA, and Verkman AS. Increased Diffusional Mobility of CFTR at the Plasma Membrane after Deletion of Its C-terminal PDZ Binding Motif. *J. Biol. Chem.* 2004; 279(7): 5494-5500,
- Harary HH, Brown JE. Spatially nonuniform changes in intracellular calcium ion concentrations. *Science.* 1984; 224(4646):292-4
- Hardie RC. Phototransduction in *Drosophila melanogaster*. *J Exp Biol.* 204(Pt 20):3403-9.
- Hodgkin AL, Keynes RD. The mobility and diffusion coefficient of potassium in giant axons from Sepia. *J Physiol.* 1953; 119(4):513-28.
- Hodgkin AL, Keynes RD. Movements of labelled calcium in squid giant axons. *J Physiol.* 1957; 138(2):253-81.
- Holcman D, Korenbrot JI. Longitudinal diffusion in retinal rod and cone outer segment cytoplasm: the consequence of cell structure. *Biophys J.* 2004; 86(4):2566-82.
- Hu HZ, Gu Q, Wang C, Colton CK, Tang J, Kinoshita-Kawada M, Lee LY, Wood JD, Zhu MX. 2-aminoethoxydiphenyl borate is a common activator of TRPV1, TRPV2, and TRPV3. *J Biol Chem.* 2004; 279(34):35741-8. Epub 2004 Jun 11
- Hua SY, Liu C, Lu FM, Nohmi M, Kuba K. Modes of propagation of Ca^{2+} -induced Ca^{2+} release in bullfrog sympathetic ganglion cells. *Cell Calcium.* 2000; 27(4):195-204.
- Hubley MJ, Rosanske RC, Moerland TS. Diffusion coefficients of ATP and creatine phosphate in isolated muscle: pulsed gradient ^{31}P NMR of small biological samples. *NMR Biomed.* 1995; 8(2):72-8.
- Ito K, Miyashita Y, Kasai H. Micromolar and submicromolar Ca^{2+} spikes regulating distinct cellular functions in pancreatic acinar cells. *EMBO J.* 1997; 16(2):242-51

- Jafri MS, Keizer J. Diffusion of inositol 1,4,5-trisphosphate but not Ca^{2+} is necessary for a class of inositol 1,4,5-trisphosphate-induced Ca^{2+} waves. PNAS. 1994; 91(20):9485-9.
- Johnson EC, Bacigalupo J, Vergara C, Lisman JE. Multiple conductance states of the light-activated channel of *Limulus* ventral photoreceptors. Alteration of conductance state during light. J Gen Physiol. 1991; 97(6):1187-205.
- Khalifa M, Drolet B, Daleau P, Lefez C, Gilbert M, Plante S, O'Hara GE, Gleeton O, Hamelin BA, Turgeon J. Block of potassium currents in guinea pig ventricular myocytes and lengthening of cardiac repolarization in man by the histamine H1 receptor antagonist diphenhydramine. J Pharmacol Exp Ther. 1999; 288(2): 858-65.
- Koutalos Y, Brown RL, Karpen JW, Yau KW. Diffusion coefficient of the cyclic GMP analog 8-(fluoresceinyl)thioguanosine 3',5' cyclic monophosphate in the salamander rod outer segment. Biophys J. 1995; 69(5):2163-7.
- Kushmerick MJ, Podolsky RJ. Ionic mobility in muscle cells. Science. 1969; 166(910):1297-8.
- Lisman JE, Brown JE. The effects of intracellular iontophoretic injection of calcium and sodium ions on the light response of *Limulus* ventral photoreceptors. J Gen Physiol. 1972; 59(6):701-19.
- Lisman JE, Brown JE. Light-induced changes of sensitivity in *Limulus* ventral photoreceptors. J Gen Physiol. 1975; 66(4):473-88.
- Lisman JE, Bering H. Electrophysiological measurement of the number of rhodopsin molecules in single *Limulus* photoreceptors. J Gen Physiol. 1977; 70(5):621-33.
- Lisman JE, Fain GL, O'Day PM. Voltage-dependent conductances in *Limulus* ventral photoreceptors. J Gen Physiol. 1982; 79(2): 187-209.
- Lisman JE, Richard EA, Raghavachari S and Payne R. Simultaneous roles for Ca^{2+} in excitation and adaptation of *Limulus* ventral photoreceptors. Adv Exp Med Biol. 2002; 514:507-38.
- Levy S, Fein A. Relationship between light sensitivity and intracellular free Ca concentration in *Limulus* ventral photoreceptors. A quantitative study using Ca-selective microelectrodes. J Gen Physiol. 1985 85(6):805-41
- Luby-Phelps K, Lanni F, Taylor DL. Behavior of a fluorescent analogue of calmodulin in living 3T3 cells. J Cell Biol. 1985; 101(4):1245-56.

- Luby-Phelps K, Taylor DL, Lanni F. Probing the structure of cytoplasm. *J Cell Biol.* 1986; 102(6):2015-22.
- Luby-Phelps K, Hori M, Phelps JM, Won D. Ca(2+)-regulated dynamic compartmentalization of calmodulin in living smooth muscle cells. *J Biol Chem.* 1995; 270(37):21532-8.
- Luby-Phelps K. Cytoarchitecture and physical properties of cytoplasm: volume, viscosity, diffusion, intracellular surface area. *Int Rev Cytol.* 2000; 192:189-221.
- Lukacs GL, Haggie P, Seksek O, Lechardeur D, Freedman N, Verkman AS. Size-dependent DNA mobility in cytoplasm and nucleus. *J Biol Chem.* 2000; 275(3):1625-9.
- Ma, H.T., Patterson, R.L., van Rossum, D.B., Birnbaumer, L., Mikoshiba, K. and Gill, D.L. Requirement of the inositol trisphosphate receptor for activation of store-operated Ca²⁺ channels. *Science (Wash DC).* 2000; 287: 1647-1651.
- Ma HT, Venkatachalam K, Li HS, Montell C, Kurosaki T, Patterson RL, Gill DL. Assessment of the role of the inositol 1,4,5-trisphosphate receptor in the activation of transient receptor potential channels and store-operated Ca²⁺ entry channels. *J Biol Chem.* 2001; 276: 18888-18896.
- Ma HT, Venkatachalam K, Parys JB, Gill DL Modification of Store-operated Channel Coupling and Inositol Trisphosphate Receptor Function by 2-Aminoethoxydiphenyl Borate in DT40 Lymphocytes. *J Biol Chem.* 2002; 277: 6915-6922.
- Martin VV, Beierlein M, Morgan JL, Rothe A, Gee KR. Novel fluo-4 analogs for fluorescent calcium measurements. *Cell Calcium.* 2004; 36(6):509-14.
- Maruyama, T., Kanaji, T., Nakade, S., Kanno, T. and Mikoshiba, K. 2APB, 2-aminoethoxydiphenyl borate, a membrane-penetrable modulator of Ins (1,4,5)P₃-induced Ca²⁺ release. *J Biochem (Tokyo).* 1997; 122: 498-505.
- Mathie A, Woollorton JR, Watkins CS. Voltage-activated potassium channels in mammalian neurons and their block by novel pharmacological agents. *Gen Pharmacol.* 1998; 30(1):13-24.
- McDonough SI, Cseresnyes Z, Schneider MF. Origin sites of calcium release and calcium oscillations in frog sympathetic neurons. *J Neurosci.* 2000; 20(24):9059-70
- Millecchia R, Bradbury J, Mauro A. Simple photoreceptors in *Limulus polyphemus*. *Science.* 1966 154(753):1199-201

- Millecchia R, Mauro A. The ventral photoreceptor cells of *Limulus*. II. The basic photoresponse. *J Gen Physiol*. 1969; 54(3):310-30.
- Millecchia R, Mauro A. The ventral photoreceptor cells of *Limulus*. 3. A voltage-clamp study. *J Gen Physiol*. 1969 54(3):331-51.
- Miura M, Boyden PA, ter Keurs HE. Ca^{2+} waves during triggered propagated contractions in intact trabeculae. *Am J Physiol*. 1998; 274(1 Pt 2):H266-76.
- Moccia F, Berra-Romani R, Baruffi S, Spaggiari S, Signorelli S, Castelli L, Magistretti J, Taglietti V, Tanzi F. Ca^{2+} uptake by the endoplasmic reticulum Ca^{2+} -ATPase in rat microvascular endothelial cells. *Biochem J*. 2002; 364(Pt 1):235-44
- Mogami H, Tepikin AV, Petersen OH. Termination of cytosolic Ca^{2+} signals: Ca^{2+} reuptake into intracellular stores is regulated by the free Ca^{2+} concentration in the store lumen. *EMBO J*. 1998; 17(2):435-42
- Montell C, Rubin GM. Molecular characterization of the *Drosophila* trp locus: a putative integral membrane protein required for phototransduction. *Neuron*. 1989; 2(4):1313-23.
- Morikawa H, Khodakhah K, Williams JT. Two intracellular pathways mediate metabotropic glutamate receptor-induced Ca^{2+} mobilization in dopamine neurons. *J Neurosci*. 2003; 23(1):149-57.
- Nagy K. Cyclic nucleotides and inositol trisphosphate activate different components of the receptor current in *Limulus* ventral nerve photoreceptors. *Neurosci Lett*. 1993; 152(1-2):1-4.
- Nasi E, Gomez, M, Payne R. Phototransduction mechanisms in microvillar and ciliary photoreceptors of invertebrates. In: Stavenga DG, de Grip WJ, Pugh EN, Jr., eds. *Molecular mechanism in visual transduction*. New York: Elsevier Science, 2000; 389-448.
- Neher E. Vesicle pools and Ca microdomains: New tools for understanding their roles in neurotransmitter release. *Neuron*. 1998; 20: 389-399
- Oberwinkler J, Stavenga DG. Calcium transients in the rhabdomeres of dark- and light-adapted fly photoreceptor cells. *J Neurosci*. 2000; 20(5):1701-9
- Oberwinkler J, Stavenga DG. Calcium imaging demonstrates colocalization of calcium influx and extrusion in fly photoreceptors. *Proc Natl Acad Sci U S A*. 2000; 97(15):8578-83.

- O'Day PM, Gray-Keller MP. Evidence for electrogenic Na⁺/ Ca²⁺ exchange in *Limulus* ventral photoreceptors. J Gen Physiol. 1989 93(3):473-94.
- O'Day PM, Gray-Keller MP, Lonergan M. Physiological roles of Na⁺/ Ca²⁺ exchange in *Limulus* ventral photoreceptors. J Gen Physiol. 1991 97(2):369-91.
- Orrenius S, Nicotera P. The calcium ion and cell death. J Neural Transm Suppl. 1994; 43:1-11
- Payne R, Corson DW, and Fein A. Pressure injection of calcium both excites and adapts *Limulus* ventral photoreceptors. J Gen Physiol. 1986a; 88: 107-26
- Payne R., Corson, D.W., Fein, A. and Berridge, M.J. Excitation and adaptation of *Limulus* ventral photoreceptors by inositol 1,4,5 trisphosphate result from a rise in intracellular calcium. J. Gen. Physiol. 1986b; 88: 127-142.
- Payne, R., and Demas, J. Timing of Ca²⁺ Release from Intracellular Stores and the Electrical Response of *Limulus* Ventral Photoreceptors to Dim Flashes. J. Gen. Physiol. 2000; 115: 735-747.
- Payne R, Fein A. Inositol 1,4,5 trisphosphate releases calcium from specialized sites within *Limulus* photoreceptors. J Cell Biol. 1987; 104(4):933-7
- Payne R, Flores TM, Fein A. Feedback inhibition by calcium limits the release of calcium by inositol trisphosphate in *Limulus* ventral photoreceptors. Neuron. 1990 4(4):547-55
- Payne R, Flores TM. The latency of the response of *Limulus* photoreceptors to inositol trisphosphate lacks the calcium-sensitivity of that to light. J Comp Physiol [A]. 1992 170(3):311-6
- Payne R, Ukhanov K. Latencies of calcium elevation and depolarization in *Limulus* ventral photoreceptors injected with GDP-beta S. J Photochem Photobiol B. 1996;35(1-2):91-5.
- Prakriya M, Lewis RS. Potentiation and inhibition of Ca²⁺ release-activated Ca²⁺ channels by 2-aminoethyldiphenyl borate (2-APB) occurs independently of IP₃ receptors. J Physiol. 2001; 536(Pt 1):3-19.
- Pepose JS, Lisman JE. Voltage-sensitive potassium channels in *Limulus* ventral photoreceptors. J Gen Physiol. 1978; 71(1):101-20.
- Phillips AM, Bull A, Kelly LE. Identification of a *Drosophila* gene encoding a calmodulin-binding protein with homology to the trp phototransduction gene. Neuron. 1992; 8(4):631-42.

- Popov S, Poo MM. Diffusional transport of macromolecules in developing nerve processes. *J Neurosci.* 1992; 12(1):77-85
- Postma M, Oberwinkler J, Stavenga DG. Does Ca^{2+} reach millimolar concentrations after single photon absorption in *Drosophila* photoreceptor microvilli? *Biophys J.* 1999; 77(4):1811-23
- Raghu P, Colley NJ, Weibel R, James T, Hasan G, Danin M, Selinger Z, Hardie RC. Normal phototransduction in *Drosophila* photoreceptors lacking an InsP_3 receptor gene. *Mol Cell Neurosci.* 2000; 15: 429-445.
- Safrany ST, Mills SJ, Liu C, Lampe D, Noble NJ, Nahorski SR, Potter BV. Design of potent and selective inhibitors of myo-inositol 1,4,5-trisphosphate 5-phosphatase. *Biochemistry.* 1994;33(35):10763-9.
- Seidler NW, Jona I, Vegh M, Martonosi A. Cyclopiazonic acid is a specific inhibitor of the Ca^{2+} -ATPase of sarcoplasmic reticulum. *J Biol Chem.* 1989; 264(30):17816-23
- Silver RB, Sugimori M, Lang EJ, Llinas R. Time-resolved imaging of Ca^{2+} -dependent aequorin luminescence of microdomains and QEDs in synaptic preterminals. *Biol Bull.* 1994; 187(3):293-9
- Simon SM, Llinas RR. Compartmentalization of the submembrane calcium activity during calcium influx and its significance in transmitter release. *Biophys J.* 1985. 48(3):485-98
- Stern J, Chinn K, Bacigalupo J, Lisman J. Distinct lobes of *Limulus* ventral photoreceptors. I. Functional and anatomical properties of lobes revealed by removal of glial cells. *J Gen Physiol.* 1982; 80(6):825-37
- Stieve H, Benner S. The light-induced rise in cytosolic calcium starts later than the receptor current of the *Limulus* ventral photoreceptor. *Vision Res.* 1992 32(3):403-16
- Stieve H, Reuss H, Hennig HT, Klomfass J. Single photon evoked events of the ventral nerve photoreceptor cell of *Limulus*. Facilitation, adaptation and dependence on lowered external calcium. *Z Naturforsch.* 1991; 46c:461-486
- Stieve H, Schlösser B. The light energy dependence of the *Limulus* photoreceptor current in two defined states of adaptation. *Z. Naturforsch.* 1989, 44(c): 999-1014.
- Strautman AF, Cork RJ, Robinson KR. The distribution of free calcium in transected spinal axons and its modulation by applied electrical fields. *J Neurosci.* 1990; 10(11):3564-75

- Tansey MG, Luby-Phelps S K, Kamm KE, and Stullg JT. Ca²⁺-dependent phosphorylation of myosin light chain kinase decreases the Ca²⁺ sensitivity of light chain phosphorylation within smooth muscle cells. 1994, 269(13): 9912-9920.
- Tesfai Y, Brereton HM, Barritt GJ. A diacylglycerol-activated Ca²⁺ channel in PC12 cells (an adrenal chromaffin cell line) correlates with expression of the TRP-6 (transient receptor potential) protein. *Biochem J.* 2001; 358(Pt 3): 717-26.
- Tillotson D, Nasi E, Ca²⁺ diffusion in the cytoplasm of *Aplysia* neurons: its relationship to local concentration changes. In *Calcium and Ion Channel Modulation*. 1988. Plenum Publishing Corp., NY.
- Timmerman MP, Ashley CC. Fura-2 diffusion and its use as an indicator of transient free calcium changes in single striated muscle cells. *FEBS Lett.* 1986; 209(1):1-8.
- Tinel H, Cancela JM, Mogami H, Gerasimenko JV, Gerasimenko OV, Tepikin AV, Petersen OH. Active mitochondria surrounding the pancreatic acinar granule region prevent spreading of inositol trisphosphate-evoked local cytosolic Ca(2+) signals. *EMBO J.* 1999; 18(18):4999-5008.
- Trebak M, Bird GS, McKay RR, Putney JW Jr. Comparison of human TRPC3 channels in receptor-activated and store-operated modes. Differential sensitivity to channel blockers suggests fundamental differences in channel composition. *J Biol Chem.* 2002; 277(24):21617-23. Epub 2002 Apr 9.
- Ukhanov, K., Payne, R. Light activated calcium release in *Limulus* ventral photoreceptors as revealed by laser confocal microscopy. *Cell Calcium.* 1995; 18: 301-313.
- Ukhanov KY, Flores TM, Hsiao HS, Mohapatra P, Pitts CH, Payne R. Measurement of cytosolic Ca²⁺ concentration in *Limulus* ventral photoreceptors using fluorescent dyes. *J Gen Physiol.* 1995;105(1):95-116.
- Ukhanov K, Payne R. Rapid coupling of calcium release to depolarization in *Limulus* polyphemus ventral photoreceptors as revealed by microphotolysis and confocal microscopy. *J Neurosci.* 1997 1; 17(5):1701-9
- Ukhanov K, Ukhanova M, Taylor CW, Payne R. Putative inositol 1,4,5-trisphosphate receptor localized to endoplasmic reticulum in *Limulus* photoreceptors. *Neuroscience.* 1998; 86(1):23-8

- Wang JH. Tracer-diffusion in liquid. IV. Self-diffusion of calcium ion and chloride ion in aqueous calcium chloride solutions. *J. Am. Chem.Soc.* 1953. 75:1769 – 1770.
- Wang Y, Deshpande M, Payne R. 2-Aminoethoxydiphenyl borate inhibits phototransduction and blocks voltage-gated potassium channels in *Limulus* ventral photoreceptors. *Cell Calcium.* 2002; 32(4):209-16.
- Wojcieszyn JW, Schlegel RA, Wu ES, Jacobson KA. Diffusion of injected macromolecules within the cytoplasm of living cells. *Proc Natl Acad Sci U S A.* 1981; 78(7):4407-10.
- Wu X, Babnigg G, Zagranichnaya T, Villereal ML. The role of endogenous human trp4 in regulating carbachol-induced calcium oscillations in HEK-293 cells. *J Biol Chem.* 2002, 277(16):13597-608. Epub 2002 Feb 5
- Xu SZ, Zeng F, Boulay G, Grimm C, Harteneck C, Beech DJ. Block of TRPC5 channels by 2-aminoethoxydiphenyl borate: a differential, extracellular and voltage-dependent effect. *Br J Pharmacol.* 2005; 145(4):405-14.
- Xu XZ, Chien F, Butler A, Salkoff L, Montell C. TRPgamma, a *Drosophila* TRP-related subunit, forms a regulated cation channel with TRPL. *Neuron.* 2000; 26(3):647-57.
- Yao Y, Choi J, Parker I. Quantal puffs of intracellular Ca²⁺ evoked by inositol trisphosphate in *Xenopus* oocytes. *J Physiol.* 1995; 482 (Pt 3):533-53